Photocatalytic Oxidation for the Removal of Chlorpyrifos from Aqueous Solution

A Major Qualifying Project Report

Submitted to the Faculty of

WORCESTER POLYTECHNIC INSTITUTE

In partial fulfillment of the requirement for the

Degree of Bachelor of Science

Submitted by:

Brendan Matheny

Jay Ringenbach

Project Advisors:

Professor Fred Hart, WPI

Professor John Bergendahl, WPI

Project Sponsor:

University of Nova Gorica

This report represents the work of two WPI project teams working in conjunction with one another. Consequently, report JIB 1305 contains identical sections to report FLH AAEE.

Abstract

Due to an increase in pesticide usage in agriculture worldwide, a need exists for the development of an effective pollutant removal process for pesticides in agricultural run-off water. It is advantageous for the treatment process to not require the addition of treatment chemicals, which could potentially have harmful effects on the environment. An advanced oxidation process (AOP) that utilizes titanium dioxide (TiO_2) with exposure to ultraviolet light is a possible treatment method for this application. Experiments were run using an immobilized TiO_2 catalyst in conjunction with a bench-scale batch reactor and a pilot-scale compound parabolic collector (CPC) reactor to analyze the degradation of chlorpyrifos using UV-Visible spectroscopy, HPLC, TOC, and LCMS. The fixed-film batch and CPC reactors yielded average treatment efficiencies of 80% and 89%, respectively, after 2 hours, suggesting successful degradation of chlorpyrifos using photocatalytic oxidation. The degradation of chlorpyrifos was found to follow first order kinetics. Using the data gathered during analysis, a final design for a system utilizing CPC reactors to treat chlorpyrifos from storm water runoff collected at the Nunes Farm in Newport, Rhode Island was proposed following the guidelines set forth by the Civil and Environmental Engineering Department at WPI.

Acknowledgements

We would like to take the time to thank all the individuals without whom this project would not have been possible:

Professors John Bergendahl and Frederick Hart, our advisors, for their advice, guidance, and organization while reviewing our report drafts and their overall help throughout the entirety of this project. Without them, this project would not have been a success.

The faculty from the University of Nova Gorica (UNG), our sponsor, for the help and resources provided to us throughout this project. All showed great hospitality for which we are extremely grateful.

Thank you to all the individuals who took the time to meet with us during our time working on this project to provide us with valuable advice and information:

- Urška Lavrencic Stangar – Dean of the School of Environmental Sciences, UNG
- Fernando Fresno – Research associate, Laboratory for Environmental Research (LRO), UNG. Your mentorship allowed us to move forward through the various roadblocks in this project.
- Romina Žabar – PhD assistant, LRO, UNG. Our project would not have been possible without your patient guidance.
- Marko Kete – Young researcher, LRO, UNG. Had it not been for your efforts, our HPLC analysis and TOC results would not have been possible.
- Andraž Šuligoj – Young researcher, LRO, UNG. You aided us in starting this project and without your direction we would have been at a loss.
- Mitja Martelanc – PhD assistant, LRO, UNG. Without your aid in LCMS efforts the intermediate compounds of chlorpyrifos may still be unknown.
- Alex Margiott and Samuel Naseef – Your time and dedication in CAD allowed us to accurately present our research. For this we are very grateful.

Authorship

The chemical engineering students completing this WPI Major Qualifying Project are Iliana Schulman and Dominique Throop. They worked in conjunction with Brendan Matheny and Jay Ringenbach, both civil engineering students, to complete the following research. An MQP report completed for civil engineering degree requirements can be found under the latter mentioned names. Each member contributed different skills to make this project a success. Below highlights some of the major responsibilities undertaken by each person:

Brendan Matheny is working toward completing his Civil Engineering degree with a concentration in Environmental Engineering. Brendan spent a major part of the research conducting work with Jay Ringenbach, performing CPC reactor experiments, and designing a real-world application for a treatment system utilizing CPC reactors, while also compiling Chapters 2 this report.

Jay Ringenbach is working toward completing his degree in Environmental Engineering obtaining a commission in the United States Marine Corps. Jay spent a major part of the research conducting work with Brendan Matheny, performing CPC reactor experiments, and designing a real-world application for a treatment system utilizing CPC reactors, while also compiling Chapters 3 this report.

Iliana Schulman is working toward completing her degree in Chemical Engineering. Iliana spent a major part of the research conducting work with Dominique Throop, performing the fixed-film batch reactor experiments to determine the degradation kinetics of chlorpyrifos while also compiling Chapter 1 and the Appendices of this report.

Dominique Throop is working toward completing her degree in Chemical Engineering. Dominique spent a major part of the research conducting work with Iliana Schulman, performing the fixed-film batch reactor experiments to determine the degradation kinetics of chlorpyrifos while also compiling Chapter 4 & 5 of this report.

Executive Summary

Background

Over the past decade, an increase of pesticide usage has been found in agriculture worldwide, causing escalation in immunity among pests. Consequently, multiple pesticides are being used in conjunction with one another to protect crops. Once applied, these compounds integrate into runoff water, posing a substantial threat to any life form with which they come into contact [EPA, 2012].

Remediation of pesticide-contaminated wastewater has begun to draw interest among the scientific community. Since pesticides are nearly impossible to remove using traditional biological approaches, heterogeneous photocatalysis using a semiconductor such as TiO_2 has received much attention as a sustainable application for wastewater treatment [Quiroz, 2011]. The following research explores photocatalytic oxidation in the presence of UV light in conjunction with the use of TiO_2 as a catalyst to degrade the organophosphate commonly known as chlorpyrifos, an insecticide widely used in agriculture.

Experimental Methods

A bench-scale UV-photocatalytic batch reactor and a pilot-scale compound parabolic collector (CPC) reactor, both using immobilized fixed-film coatings of titanium dioxide, were utilized to conduct experiments with the aim of determining the degradation rate of chlorpyrifos in the photocatalytic reaction. Experiments were carried out with starting concentrations of 2.0, 1.5, 1.0, and 0.5 ppm chlorpyrifos prepared in double deionized water. The fixed-film batch reactor and CPC reactor were both run for four hours during each experiment to determine the reaction kinetics of the TiO_2/UV photocatalytic reaction.

Methods of Analysis

All samples taken from these experiments were analyzed through the use of high performance liquid chromatography (HPLC) and total organic carbon (TOC). HPLC analysis of the photocatalytic reaction provided valuable data concerning the degradation of chlorpyrifos as well as showing intermediate generation and consequent degradation. TOC analysis of the photocatalytic reaction showed the degradation of the total carbon concentration over time. Using the results gathered from these two analysis methods, further samples were selected for liquid chromatography/mass spectrometry (LCMS) analysis. Specifically, samples displaying the largest area for a potential intermediate found in the HPLC chromatograms were analyzed for the identification of unknown intermediates and their chemical components.

Results

Chlorpyrifos was determined to follow a first order reaction rate, with the majority of degradation occurring within the first hour of TiO_2/UV treatment. The average treatment efficiency after four experiments in the fixed-film batch reactor was calculated to be 80%. An experimental treatment efficiency of approximately 89.17% for the first two hours of treatment in the CPC reactors was calculated using data taken from HPLC. Potential intermediates were proposed based off of data from LCMS analysis.

Conclusions

During experimentation, the majority of chlorpyrifos removal occurred as a result of adsorption onto the catalyst surface prior to photocatalytic degradation. This can likely be attributed to the fact that the catalyst film was cleaned using double deionized water under UV exposure for 30 minutes before each experiment. These conditions produce recombination sites that are completely empty prior to experimentation, therefore not representative of actual operating conditions.

TOC results showed degradation of the total carbon concentration over time, suggesting that chlorpyrifos had degraded and formed intermediates that decomposed into gaseous CO_2, which then transferred from solution. LCMS results showed the generation of intermediates including $C_9H_{11}Cl_3NO_4P$, $C_8H_{12}Cl_3O_3PS$, and $C_6H_5NO_2$. Although chlorpyrifos oxon was determined to be slightly less toxic than chlorpyrifos, the relative toxicities of the remaining intermediates were unable to be determined.

Recommendations

It is recommended that further testing be carried out on the fixed-film batch reactor and CPC reactor with more frequent sampling and temperature testing. This would serve to aid in more accurately identifying intermediates, which may be generated toward the end of the reaction. Toxicity studies should be conducted for all intermediates. Furthermore, tracking temperature changes over the course of a reaction could serve to highlight trends such as variability in reaction rate. It is also recommended that a dip coating process be utilized when coating glass slides with catalyst. This would ensure a uniform thickness of catalyst, as opposed to the variability that can result from hand brushing.

When attempting to determine actual concentrations of samples being analyzed through HPLC, a dilution series from one large quantity of reliable stock solution should be analyzed each time as well. In this manner it would be possible to overcome variability that was inherent in HPLC over time. Lastly, the CPC reactor being used should utilize construction techniques that allow for ease of operation. If the reactor were easy to operate it would be a much simpler matter to replicate experimental conditions. Aspects of the reactor design that should be changed include the use of threaded adapters as opposed to push-on fittings, braided stainless steel tubing to avoid kinks that can reduce flow, and an easily accessible filling port as well as a drainage valve.

Capstone Design Statement

As part of the Accreditation Board for Engineering and Technology (ABET) requirement, a capstone design experience must be completed by all students seeking a degree in civil or environmental engineering. The capstone design addresses realistic constraints of a project including: economics, sustainability, environmental impact, health and safety, political, and social aspects. The final report submitted to UNG and WPI addresses each of these aspects, as highlighted in Chapter 6.

Economic Impact

Economic constraints for the construction of a CPC reactor system designed to treat chlorpyrifos using titanium dioxide photocatalysis were addressed. An analysis for each stage of the treatment process was conducted, including both material and construction cost. Upon completion of the design, a proposal outlining the total cost of system implementation was presented.

Sustainability and Environmental Impact

Since chlorpyrifos is a persistent, non-biodegradable organic pesticide that is toxic to many forms of life, the degradation of chlorpyrifos from wastewater is required before release back into the environment. This design was completed with the idea in mind of reducing the hazardous impact of chlorpyrifos on the environment by utilizing photocatalytic mineralization to reduce concentrations to the lowest level possible. The positive environmental impact of removing chlorpyrifos, and other organic molecules, from water will be felt worldwide once remediation technology is capable of treating to a higher standard.

Health and Safety Concerns

Due to toxicity levels measured in the range of parts per trillion for aquatic life, chlorpyrifos cannot be safely released. At higher concentrations, chlorpyrifos also poses a significant threat to human health, most notably by acting as an acetylcholinesterase inhibitor. For these reasons, it is highly recommended that chlorpyrifos contamination be reduced to acceptable levels or eliminated altogether. Despite the fact that research has showed chlorpyrifos to be toxic to many forms of life, the U.S. Environmental protection Agency is yet to establish acceptable discharge limitations. However, the EPA has started the process of researching chlorpyrifos with the goal of providing new regulations in the near future. Currently, toxicity limits and regulations at the state level, such as those provided by California, should be observed until EPA research is concluded.

Social and Political Concerns

As previously discussed, Chlorpyrifos is persistent in the environment and has been detected in locations as remote as Antarctica. With that in mind, it is clear that a release of untreated chlorpyrifos into the environment from any point contributes to global contamination. Due to the fact that no governing agencies worldwide have federal regulations regarding chlorpyrifos, it is imperative that nations act unilaterally to establish acceptable concentration release levels.

Final Design Specifications

After the impacts and concerns for the capstone design had been explored, a final design was proposed for the Nunes Farm Vineyard. Table 6.0 below highlights the final specifications that are required to support the maximum average flow collected from storm water runoff. These calculations were completed using the heaviest flow conditions, predicted using average monthly precipitation data. In this manner, the system was designed to handle the heavy flows present during the months of March and April.

Table 6.0: Retention Pond Specifications

Surface	1550 m^2
Required Depth	1.5 m
Volume	2326.5 m^3
Flow	2160 m^3/month

Following completion of the retention pond calculations, the parameters for the CPC reactor design were then calculated using a higher than average monthly flow to determine the design specifications for a plug-flow system. Table 6.1 below summarizes these values.

Table 6.1: CPC Reactor Design Specifications

Flow Rate	47.52 m^3/d (2000 L/H)
Retention Time	2 hours
Tube Diameter	10cm
Number of Tubes	10
Height	2 m
Length	3m
Volume	235.6 L
Number of Reactors Required	17
Inclination Angle	37^o

Once both the retention pond and CPC reactors had been sized appropriately a cost analysis of the required materials was conducted. This, in combination with approximate construction cost, provided the final cost of system implementation seen in Table 6.3.

Table 6.3 – Total Cost Analysis

Unit	**Cost**
Retention Pond Lining	$2645.00
Main Collection Pond Pump (1)	$600.00
Reactors (17)	$62,736.12
Construction	$98,971.68
Total Cost	**$164,952.80**

Table of Contents

Table of Figures

Table of Tables

1.0 – Introduction

As the population of the planet continues to increase, a larger supply of water is required for society's needs, including drinking and agricultural use. Over the past decade, organic pesticide usage in agriculture worldwide has been on the rise, resulting in an increase of pollutants found in various water sources. The type of pollutants found in water sources largely depends upon the local industries. Urban and agricultural wastewaters often contain pesticides, herbicides, fungicides, insecticides (organic compounds), and PCBs as pollutants [Oblak, 2013] and these pollutants can end up in water sources.

Over the past decade, organic pesticide use in agriculture worldwide has been increasing [MSDS – 45395, 2013]. Pesticides are defined as artificially synthesized substances that are used to fight pests and improve agricultural production [Miguel, 2007]. In recent years, the variety and concentration of pesticides used in the Mediterranean region has drastically increased due to a developing immunity to pesticides [Ballesteros, 2009]. Slovenia in particular has been severely affected by chemical pollution from organic pesticides and fungicides used in vineyards [Ambrožič, 2008]. The presence of these hazardous substances must be eliminated to sustain reusable water for the general population.

Due to an increased threat of pollution, remediation of pesticide-contaminated wastewaters has drawn interest among the scientific community. There exists a need for the development of an effective pollutant removal process that does not require the addition of treatment chemicals, which could potentially have other harmful effects on the environment. Since traditional biological treatment is not a feasible option due to the effect of pesticides on microorganisms, biological treatment is generally impractical. However, advanced oxidation processes (AOPs) allow for the breakdown of bio recalcitrant compounds into intermediates and in some cases produce even complete mineralization if properly executed. Titanium dioxide irradiated with ultraviolet light (TiO_2/UV) is an advanced oxidation process that has not yet been fully explored for the purpose of water and wastewater treatment. The use of TiO_2/UV treatment was evaluated in this project specifically for the removal of chlorpyrifos from water.

2.0 – Background

2.1 – Previous Pesticide Research in Slovenia

From 2001-2009, the Agricultural Institute of Slovenia (AIS) collected data regarding Plant Protection Products (PPP). PPPs are generally considered to be any chemical, (pesticides, herbicides, fungicides, plants growth regulators or otherwise) that is used to kill, repel, or control pest, influence the life cycle of plants, or destroy weeds. Eight locations around the country were monitored to better understand how to develop environmentally friendly PPPs that must reach the standards set by the Slovenian national government. The AIS study found that 28.6% of the grape samples from Slovenian vineyards exceeded the set level of PPPs [Česnik, 2011].

2.2 – Organic Pesticides

Organic pesticides in water are frequently resistant to traditional biological treatment [Ballesteros, 2009]. The complex molecular structure of organic pesticides often inhibits biological treatment processes due to the generation of dangerous, highly toxic intermediates. Although difficult to remove through a single biological process, conversion of such pollutants into biodegradable intermediates, or even their mineralization products, can be accomplished through photocatalytic pretreatment, resulting in the biodegradability of organic pesticide pollutants [Quiroz, 2011].

2.3 – Chlorpyrifos

Chlorpyrifos falls under the category of organophosphate insecticides, acaricides, and miticides [Kanmoni, 2012]. This compound "was first developed by DOW chemical company in 1965… and is applied in over 100 countries across the world. Chlorpyrifos has become the largest organophosphate insecticide worldwide in both volume and value" [World Outlook of Chlorpyrifos, 2011-2015]. Mainly used to control the populations of insects, soil grubs, rootworms, subterranean termites, foliage and soil-born insects, chlorpyrifos is employed on a variety of crops in agriculture [Cho, 2002].

Chlorpyrifos is a complex molecule containing chlorine, nitrogen, phosphorous, sulfur, oxygen, hydrogen, and carbon (shown in Figure 2.1) [Kanmoni, 2012].

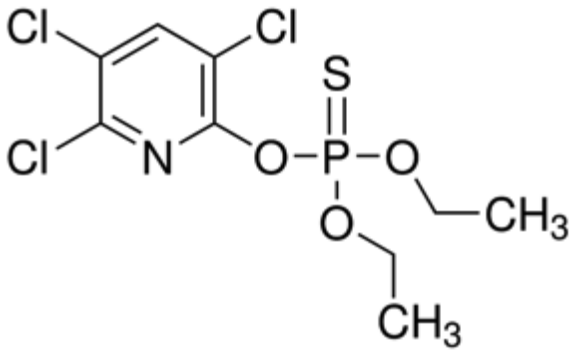

Figure 2.1: Chlorpyrifos molecular structure [Sigma-Aldrich].

Research suggests chlorpyrifos is not readily soluble in water and easily comes out of solution; however, temperatures above 63^{o}C allow chlorpyrifos to dissolve at a faster rate into solution [U. S. Department of Agriculture, 1990]. Spray drift and eroded soil particles are the primary ways that chlorpyrifos enters freshwater and saltwater ecosystems. If soil with absorbed chlorpyrifos is transported by storm water runoff, surface water may be contaminated as a result [U.S. Environmental Protection Agency, 1986].

Chlorpyrifos is highly toxic to plants and animals, and can also kill fish at concentrations as lower than a few parts per trillion [Devi, 2009]. Exposure to chlorpyrifos has been shown to

produce a variety of nerve disorders in humans. It is readily absorbed into the bloodstream through the gastrointestinal tract if ingested, through the lungs if inhaled, or through the skin if there is skin exposure [Chemical fact sheet for chlorpyrifos, 1984]. Absorption through the skin may result in systemic intoxication, or poisoning of the bodily system [Chlorpyrifos, n. d.]. Symptoms of chlorpyrifos poisoning include headaches, nausea, muscle convulsions, birth defects, and in very rare cases death [Devi, 2009]. This is due to the inhibition of the cholinesterase enzyme, which is required for proper nerve functioning [Cho, 2002]. In addition to causing inhibition of cholinesterase, acute exposure to chlorpyrifos may also cause skin irritation. Since chlorpyrifos is absorbed through the skin, contact with the pesticide should be avoided [Chemical fact sheet for chlorpyrifos, 1984]. Repeated exposures to chlorpyrifos can, without warning, causes heightened susceptibility to doses of any cholinesterase inhibitor [MSDS – 45395, 2013].

The Pesticide Incident Monitoring System reported three hundred and nineteen human exposure incidents from 1970 through 1981, most resulting from inhalation and skin exposure. Three human deaths during this study were caused by chlorpyrifos or chlorpyrifos combined with other active ingredients. Persons with respiratory ailments, recent exposures to cholinesterase inhibitors, cholinesterase impairment, or liver malfunction are at increased risk from exposure to chlorpyrifos [Guidance for re-registration of pesticides containing chlorpyrifos as the active ingredient, 1984].

2.4 – Advanced Oxidation Processes

Advanced oxidation processes (AOPs) break down organic compounds such as alcohols, aldehydes, carboxylic acids, amines, and specifically insecticides and herbicides into carbon dioxide and water with trace mineral acids. AOPs are useful in wastewater treatment due to the complete mineralization of bio-recalcitrant pollutants such as chlorpyrifos under the right conditions. AOPs are also an inexpensive alternative to more expensive chemical mineralization processes [Quiroz, 2011]. Figure 2.2 outlines many current technologies that utilize AOPs.

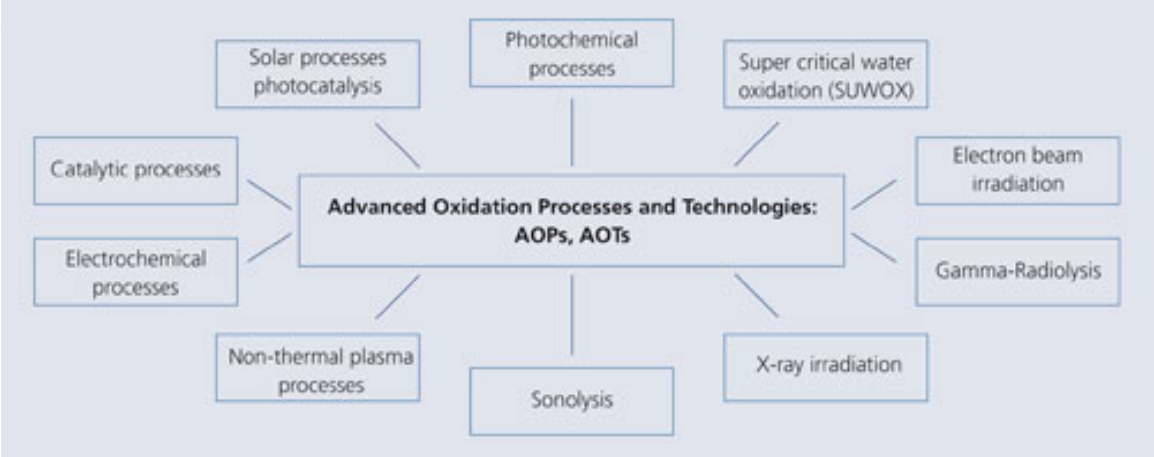

Figure 2.2: Current Advanced Oxidation Technologies [Fraunhofer IGB].

The production of free hydroxyl radicals ($OH^{\bullet}$) is a fundamental step in the advanced oxidation process due to their non-selective attack of organic pollutants [Zapata, 2009]. Hydroxyl radicals oxidize organic contaminants, making them extremely useful for wastewater treatment. Hydroxyl radicals mineralize many organic molecules while yielding CO_2 and inorganic ions as byproducts when driven to completion [Zapata, 2009]. The versatility of AOPs makes it easy to produce hydroxyl radicals by allowing specific treatment requirements to be met [Zapata, 2009].

2.5 – TiO_2 Photocatalysis

This research presents the AOP known as photocatalysis, which uses titanium dioxide (TiO_2) as a catalyst in the presence of ultraviolet radiation. Photocatalysis is defined as a change in the rate of a chemical reaction under ultraviolet, visible, or infrared radiation in the presence of a photocatalyst by absorbing light to produce a chemical transformation of the reactants [Braslavsky, 2007]. The excited state of the photocatalyst repeatedly interacts with the reactants to form reaction intermediates while regenerating itself after each cycle of interactions [Braslavsky, 2007].

Using TiO_2 as a semiconductor for photocatalytic reactions is a promising new process for wastewater treatment. Titanium dioxide is a material with numerous applications, recently because of its capacity to be photo activated by solar light [Coronado & Hernandez-Alonso, 2013]. The inert biological and chemical nature of TiO_2, as well as a resistance to chemical and photo corrosion, is a major advantage to using TiO_2 as a photo catalyst.

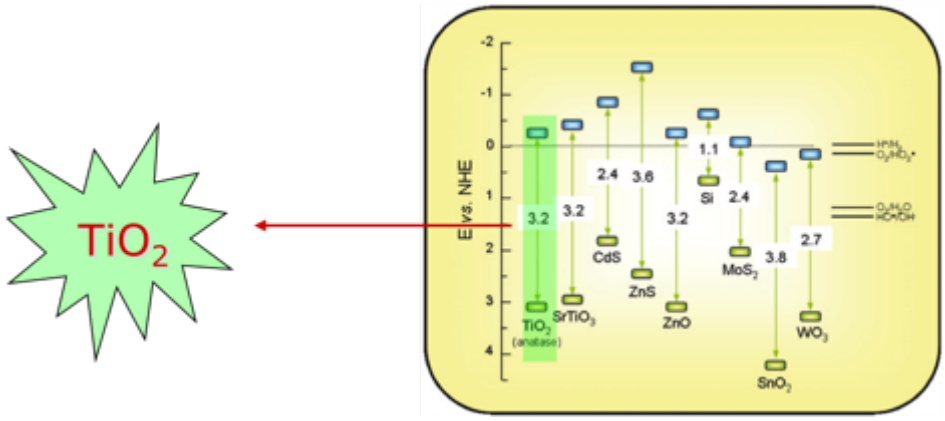

Figure 2.3: Band gap energy of titanium dioxide compared to other photocatalysts [Fresno, 2013].

Titanium dioxide has the capability to treat a wide range of organic pesticides with the appropriate radiation conditions. Photocatalysis uses TiO_2 in conjunction with UV radiation of photon wavelength less than 400 nm, since the band-gap energy of TiO_2 is 3.2 eV (Figure 2.3). This AOP is considered one of the most efficient processes for lowering the concentration of

pesticides in wastewater [Quiroz, 2011]. The reaction that occurs is an oxidation reaction that requires TiO_2 as a catalyst to produce CO_2, H_2O, and intermediates.

When atoms come together to form molecules, their atomic orbitals are shared to yield two molecular orbitals: bonding (low energy) and antibonding (high energy). These new orbitals attempt to minimize the energy of the system through valence electrons by filling only the bonding orbitals. With an increasing number of atoms, the energy gap between two adjacent molecular orbitals decreases. Therefore, in a solid with a theoretically infinite number of atoms, energy bands are formed rather than discrete orbitals. The highest occupied band in a solid is called the valence band, while the lowest unoccupied band is referred to as the conduction band. The gap of forbidden energy states between the valence and conduction bands of a solid is called the band gap. When the band gap energy (3.2 eV in the case of TiO_2) is exceeded by absorption of a photon, electrons in the valence band move across the band gap into the conduction band to create electron-hole pairs, which then initiate the photocatalytic reaction. The hole left behind in the valence band then oxidizes the organic contaminant while the excited electrons reduce oxygen in the solution. Hydroxyl radicals are generated as intermediates of this photocatalytic reaction [Chong, 2010]. Figure 2.4 below shows the process by which TiO_2 and UV light create electron hole-pairs on the catalyst surface.

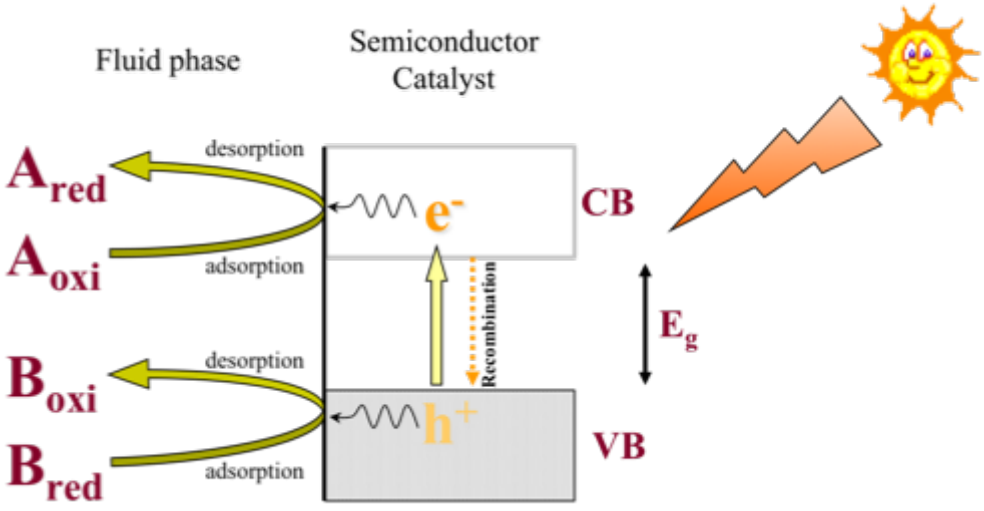

Figure 2.4: Electron hole pair production [Fresno, 2013].

Recombination is one of the main disadvantages of photocatalysis due to the waste of energy in the system. Occurring in the absence of electron acceptors/donors, recombination limits the quantum yield. Prevention of electron-hole pair recombination is therefore crucial to the photocatalytic process in order to increase efficiency of the process. Addition of external electron acceptors increases the rate of degradation, hydroxyl radical concentration, and oxidation rate of intermediates by preventing recombination. Electron acceptors, such as H_2O_2 or O_3, play an important role in the production of hydroxyl radicals [Chong, 2010]. TiO_2 has shown enhanced activity compared to other catalysts under solar radiation due to its high surface area and high capacity to adsorb water and hydroxyl groups on the catalyst surface [Devi, 2009].

2.6 – Photocatalysis Efficiency Variables

Optimizing the efficiency of TiO_2 photocatalysis requires many factors to be taken into account when considered for wastewater treatment. The semiconductor used in this study, TiO_2, plays a key role in the photocatalytic process, but many other variables can also affect the oxidation process. Among them are: catalyst composition, catalyst concentration, pesticide concentration, light wavelength, temperature, and UV intensity.

2.6.1 – Catalyst Composition

The two types of TiO_2 catalyst used in this study are P25 and PC500 (Figure 2.5). The differences in photocatalytic activity between these two types of catalyst can most likely be traced back to the difference of surface area and density of hydroxyl groups on the catalyst surface. These factors affect the adsorption behavior of the pollutant and recombination rate of electron-hole pairs. The particle size of TiO_2 is an important factor to consider since it directly affects the efficiency of the catalyst through surface area.

Figure 2.5: P25 vs. PC500 TiO_2.

P25 has a specific surface area of 50 m^2g^{-1}. PC500, on the other hand, has a specific surface area of 287m^2g^{-1}. PC500 is 100% anatase versus P25 being 75% anatase and 25% rutile by mass. While PC500 titanium dioxide has a much larger surface area than P25, the opposite is true of the crystal size. P25 has a crystal size of 21nm when compared to a 5-10 nm crystal size for PC500 [Chong, 2010].

Through past research conducted by Urh Černigoj at UNG, it was determined that the most effective mixture for research utilizing a TiO_2 small-scale slurry reactor is a 1:1 ratio of Millennium's PC500 and Degussa's P25 TiO_2. This ratio creates the best possible "balance between surface area and crystallinity… to obtain the highest photo activity" [Černigoj, 2006].

2.6.2 – Catalyst Concentration

In small-scale slurry reactors, the rate at which degradation occurs initially increases as titanium dioxide concentration increases (see Figure 2.6). At high concentrations, the degradation rate will no longer increase due to light scattering and screening from the catalyst surface. Optimum concentration values for a small-scale slurry reactor are dependent on the type of catalyst used and reactor geometry.

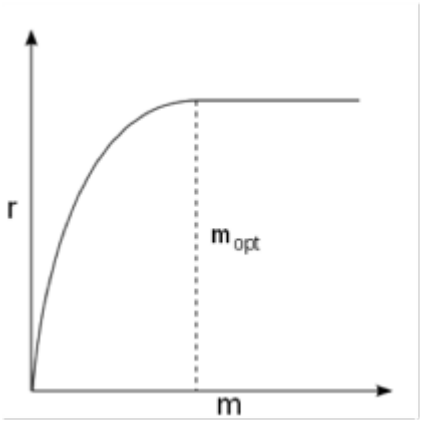

Figure 2.6: Reaction Rate vs. Catalyst Mass [Herrmann, 2010].

The optimal concentration of TiO_2 is somewhere between 1 and 3 g/L based upon past studies conducted using TiO_2/UV photocatalysis [Fogler, 1999].

In an immobilized reactor, optimal light illumination depends upon the thickness of the fixed-film. The effect light has on TiO_2 using Degussa P25 catalyst on a flat plate with ultraviolet irradiation set at 365 nm has been researched previously. The experiments showed that the maximum light absorption was reached at about 1.0 mg/cm^2. The concentration, or thickness, of titanium silicate coating on glass slides is generally measured in units of weight per area. The optimal thickness for treatment efficiency has been determined through past research to be approximately 1.0 mg/cm^2 [Cernigoj, 2007]. A larger concentration would be unnecessary once this thickness has been obtained, since the TiO_2 closest to the glass slide is no longer effective, as it is not exposed to the water being treated [Chong, 2010].

2.6.3 – Pesticide Concentration

The concentration of pollutant being treated in a photocatalytic process can significantly affect the rate of reaction. When the duration of radiation and catalyst concentration remain fixed, the concentration of hydroxyl radicals and $O_2^{\bullet}$ on the catalyst surface appears to remain constant. Therefore, not enough hydroxyl radicals are generated to participate in degradation at higher concentrations of pesticide, meaning that either UV intensity or catalyst concentration is the limiting factor [Chong, 2010].

Figure 2.7 below shows the relationship between reaction rate and pollutant concentration for any given reaction. Higher concentrations of pollutant lead to an increased reaction rate. As shown, a plateau is reached once a certain concentration is present. Since all adsorption sites are in use, additional pollutant cannot react with the catalyst surface until recombination sites are free.

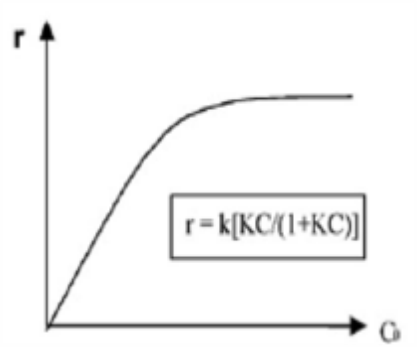

Figure 2.7: Reaction Rate vs. Pollutant Concentration [Herrmann, 2010].

2.6.4 – Wavelength

The wavelength and intensity of light radiation is a key parameter in affecting reaction rate. If the wavelength of the light source provides energy lower than the energy threshold, E_0, the desired reaction will not occur (Figure 2.8). In the case of TiO_2 it is known that a wavelength lower than 400 nm is required for a photocatalytic reaction to commence.

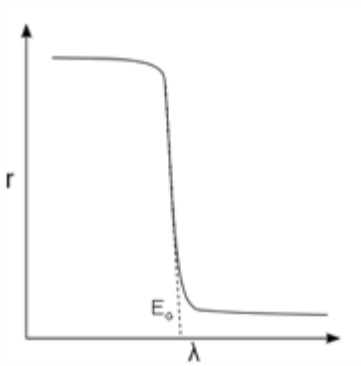

Figure 2.8: Reaction Rate vs. Wavelength [Herrmann, 2010].

While the < 400nm wavelength falls in the UV radiation range, only 3-5% of the solar spectrum is used in the oxidation process. In other words, only 4% of sunlight will be used in a given reaction with a titanium dioxide catalyst (Figure 2.9).

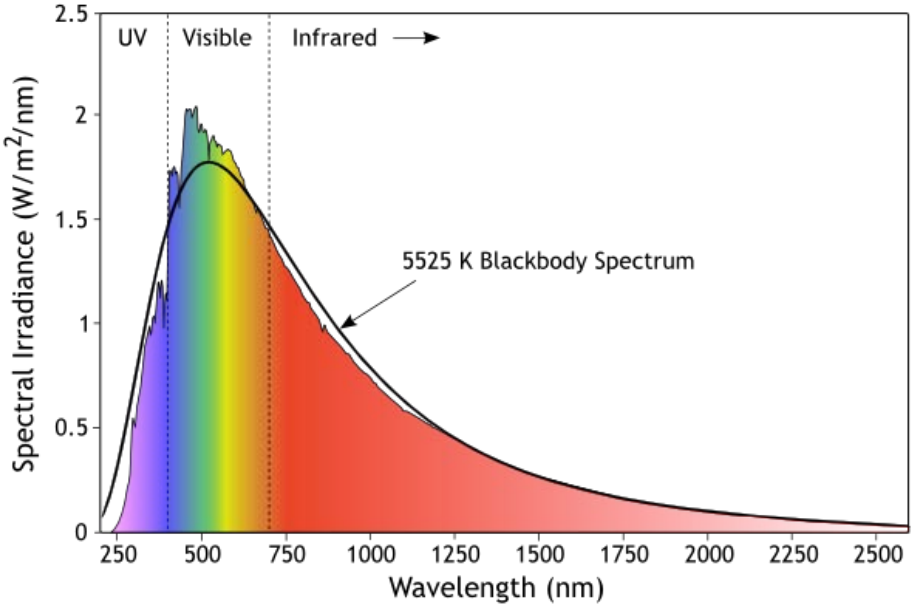

Figure 2.9: Solar radiation spectrum [Haenke, 2010].

2.6.5 – Temperature

At temperatures above 80°C, the lower adsorption of pollutant leads to decreased activity and slower reaction rates. On the other hand, lower temperatures favor adsorption, including that of reaction products, which may become inhibitors. Therefore, a temperature of about 20-50°C is recommended for this particular oxidation process, as shown in Figure 2.10 [Herrmann, 2010].

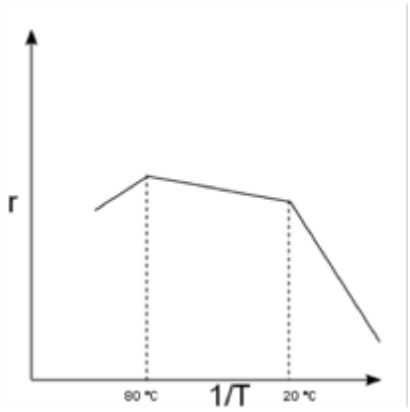

Figure 2.10: Reaction Rate vs. Temperature [Herrmann, 2010].

2.6.6 – UV Irradiation

As the intensity of UV irradiation increases, the reaction rate for the degradation of the targeted contaminants increases (Figure 2.11). Once the activation energy (3.2 eV) required to excite electrons into the next valence band of TiO_2 is achieved, the rate of degradation will no longer increase with increased UV intensity. This implies that, should the intensity required to excite electrons be exceeded, no further recombination sites will be created, causing energy to be wasted.

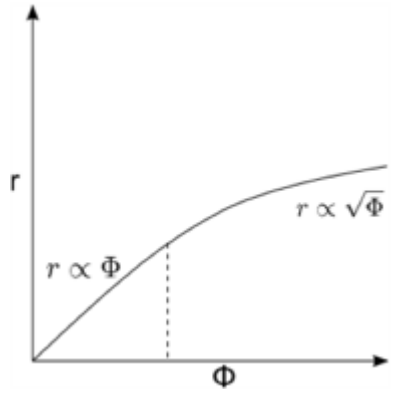

Figure 2.11: Reaction Rate vs. Irradiance [Herrmann, 2010].

2.7 – Reactor Parameters

Optimizing the efficiency of a photoreactor requires many design components be taken into account when considering heterogeneous photocatalysis for wastewater treatment. A photoreactor that accounts for variables, such as solar radiation, must be designed to efficiently degrade pollutants, specifically from vineyard runoff. Two primary reactors commonly used in solar photocatalytic processes are fixed-film batch reactors and immobilized fixed-film pilot scale compound parabolic collector (CPC) reactors, which are essential to testing various circumstances at the pilot scale level.

2.7.1 – Slurries vs. Fixed-Film Reactors

Pilot-scale reactors may be designed to utilize either small-scale slurry or immobilized fixed-film catalysts. The use of TiO_2 in suspended form is more efficient than in immobilized form. As shown in Table 2.1, each type of reactor utilizes distinct operating parameters that both come with their own set of advantages and disadvantages [Chong, 2010].

Table 2.2: Advantages and disadvantages of immobilized fixed-film and small-scale slurry reactors.

Slurry Advantages	**Slurry Disadvantages**	**Fixed-film Advantages**	**Fixed-film Disadvantages**
Greater possible TiO_2 Concentrations, allowing for increased treatment efficiency	TiO_2 recovery must occur before the release of effluent	No TiO_2 recovery required before discharge	High TiO_2 concentrations are not possible, meaning lower treatment efficiency possibilities
Faster reaction rate	High TiO_2 concentration results in opaque solutions, which can block UV irradiation	Film is self-cleaning in the presence of UV light	Slower reaction rate
Greater surface area exposure			Surface area limitations

2.7.2 – Fixed-Film Batch Reactor

The fixed-film batch reactor used in this study forces chlorpyrifos solution into contact with immobilized TiO_2. To achieve an accurate reaction, the catalyst surface must be uniformly coated. This bench-scale study must be conducted to provide information regarding the reaction kinetics before further research on reactor design can begin [Černigoj, 2006]. Figure 2.12 details a technical drawing of the process used. A 3-D model showing the specific reactor shown can be found in Figure 2.13. The pesticide infused water is added at the mixer labeled "sampling", pumped through Stream 1 into the pump, through Stream 2 into the reactor containing the immobilized catalyst and UV light source where it will be treated, and back to the mixer via Stream 3.

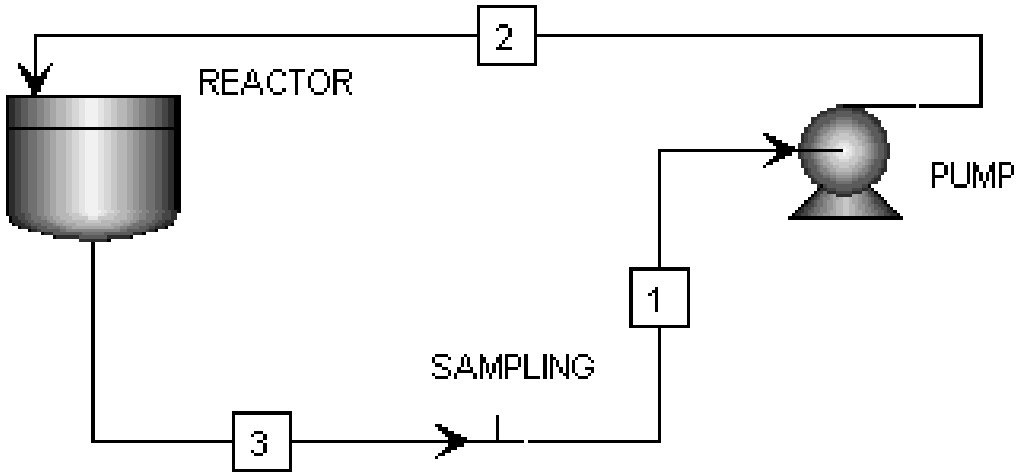

Figure 2.12: Fixed-Film batch reactor.

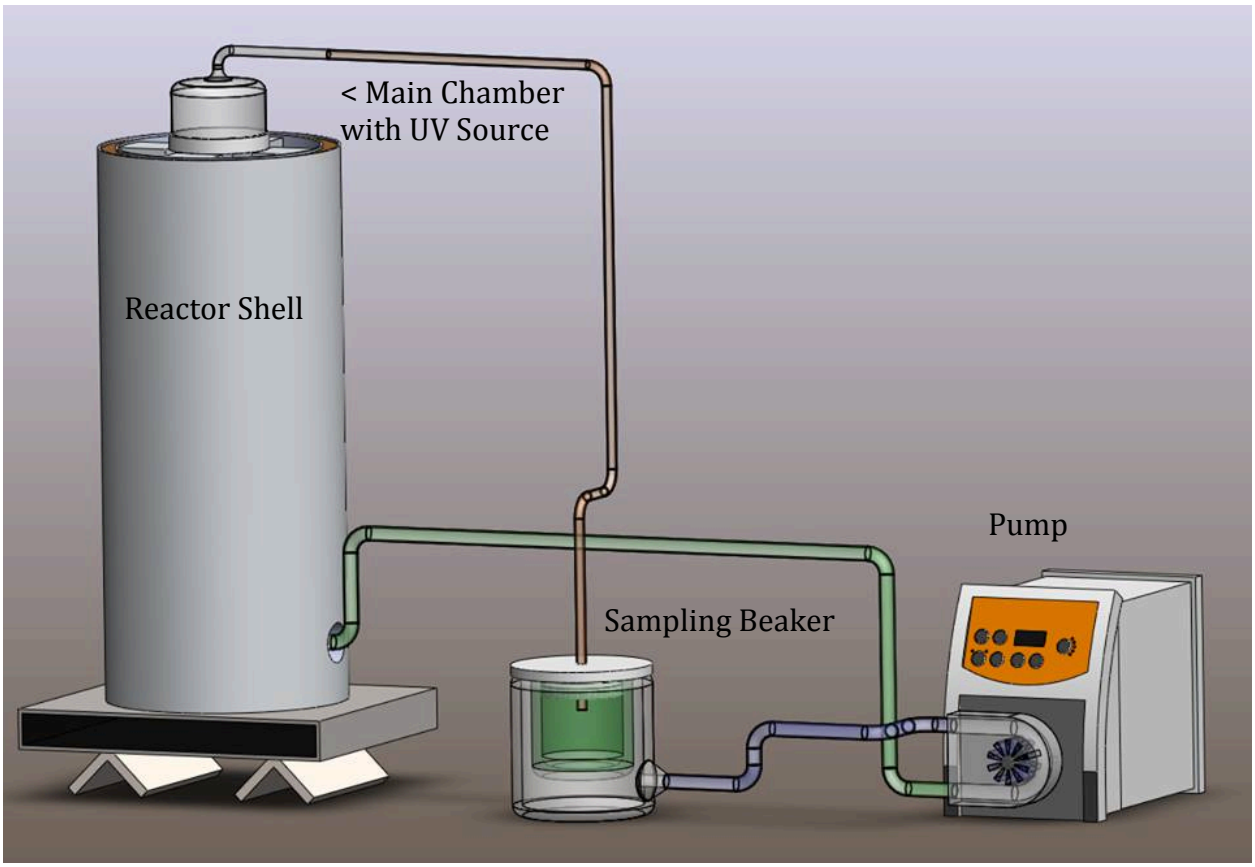

Figure 2.13: 3-D schematic of fixed-film batch reactor.

2.7.3 – Compound Parabolic Collector (CPC) Reactor

A pilot system in Almeria, Spain has provided valuable information on the reactor parameters that must be considered for this study [Compound Parabolic Collector (CPC) Photoreactors, 2013]. Figure 2.14 shows the pilot system in Almeria, Spain.

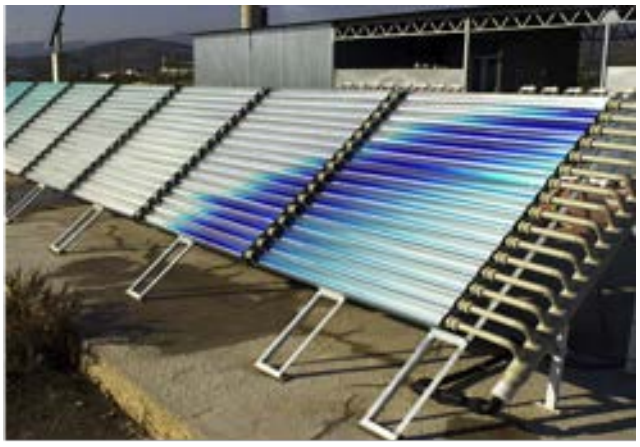

Figure 2.14: CPC reactors [Compound Parabolic Collector (CPC) Photoreactors, 2013].

CPC reactors utilize fixed-film cylinders wrapped in commercial TiO_2 that are placed throughout the reactor tubes to expose the pesticide-contaminated water to the greatest surface area possible. The diameter of piping in a CPC photoreactor is critical to both photon absorption and the hydraulics within a reactor. Steady flow ensures that a uniform residence time can be obtained, allowing for equal treatment of all water passing through a given reactor. Reactors with diameters that are small in relation to their flow rate yield higher velocities and can produce turbulent flow. As a result, efficient treatment can be difficult to carry out. Ideally, a more laminar flow rate aids in increasing treatment efficiencies. Refer to Figure 2.15 & 2.16 for a 2D diagram of the reactor used for experimentation at UNG.

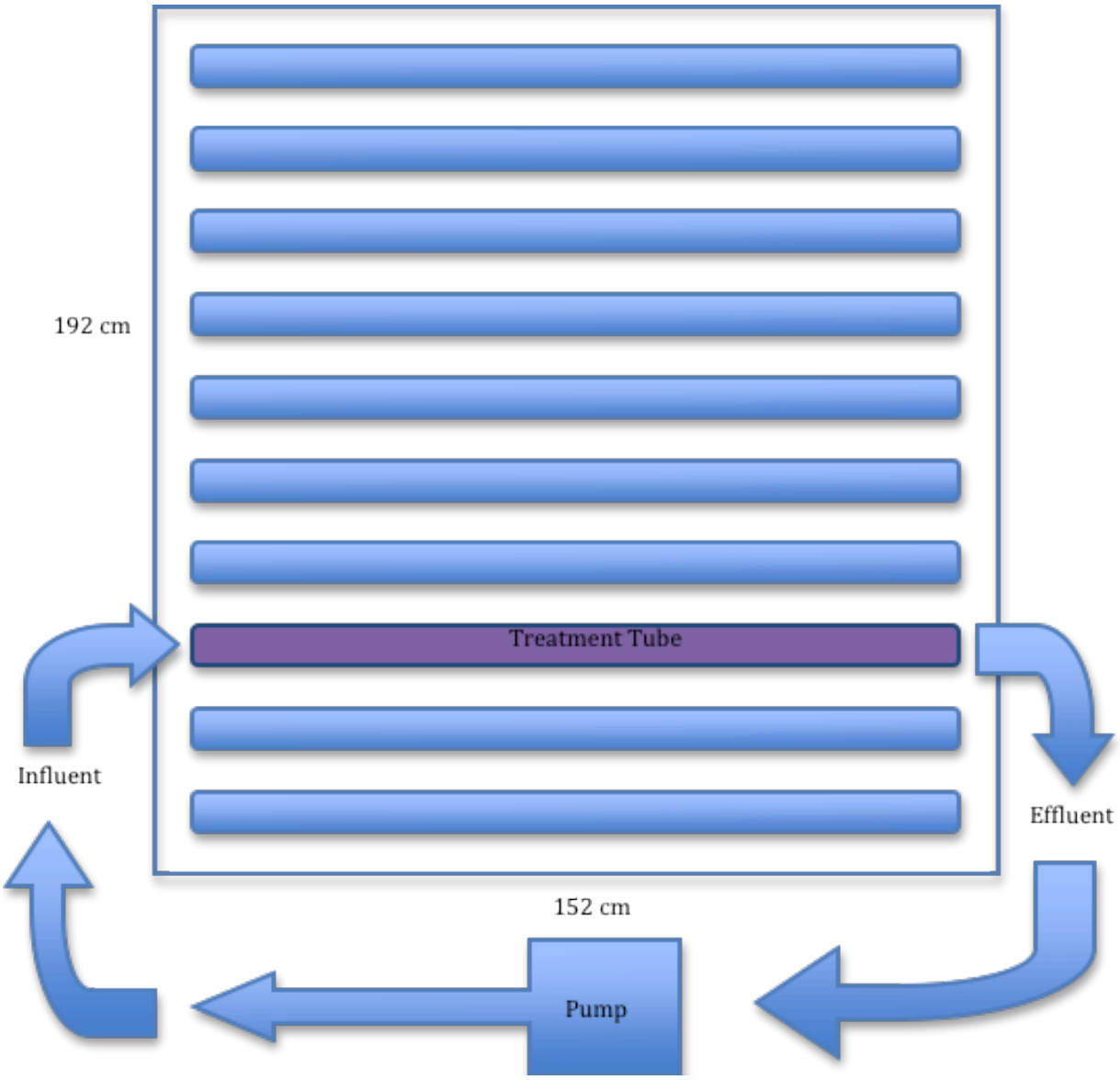

Figure 2.15: Front view of CPC reactor.

Figure 2.15 above shows the front view schematic for the CPC reactor used at UNG. As shown in the diagram, a pump circulates 5.5 L of solution through one reactor tube over the duration of an experiment. All other tubes are not used during the reaction due to an inefficient use of chemicals used to make solution. The dimensions of the reactor are approximately 1.5 m in length by 2 m in height.

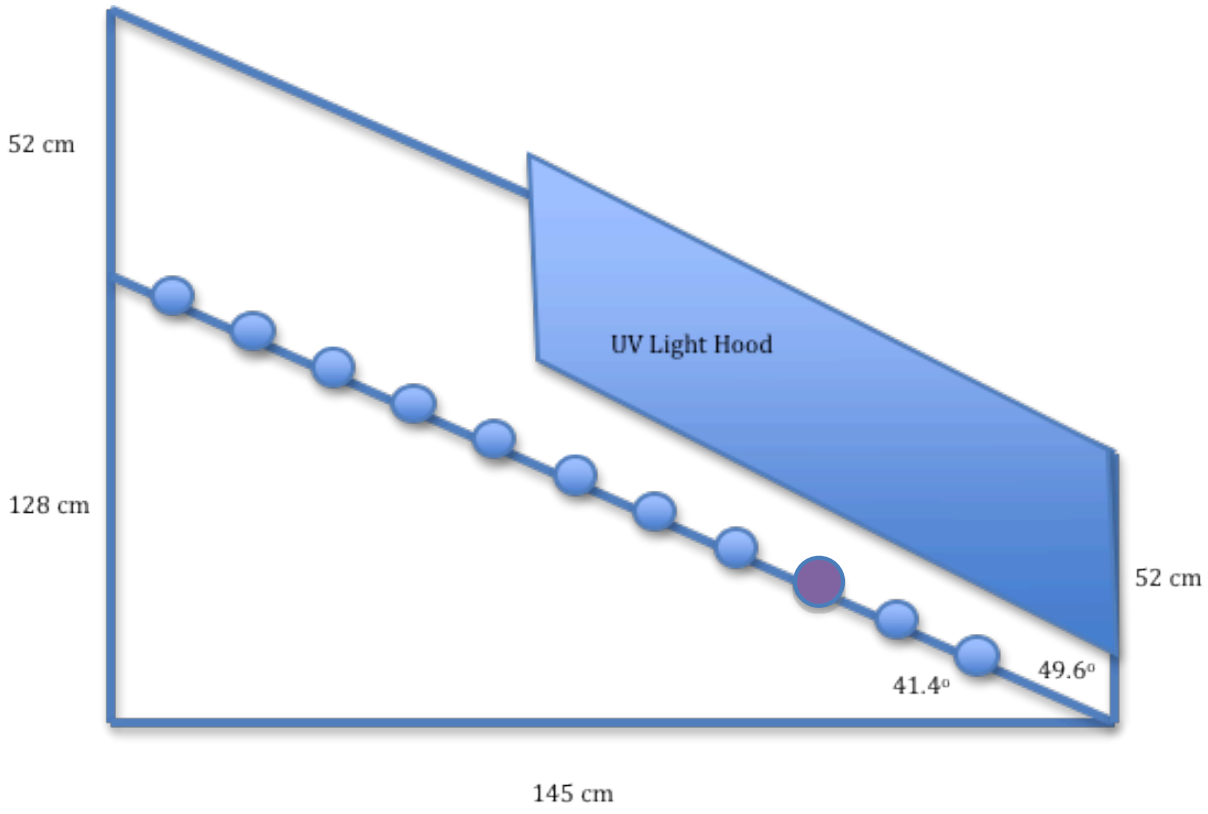

Figure 2.16: Side view of CPC reactor.

Figure 2.16 above shows the side view schematic for the CPC reactor used at UNG. As shown in the diagram, a pump circulates 5.5 L of solution through one reactor tube (third from the bottom as highlighted in Figure 2.16)) over the duration of an experiment. All other tubes were not used during the reaction due to an inefficient use of chemicals required to make solution. The UV light hood pictured only covers a small section of the reactor since only one tube was used when performing experiments. The dimensions of the reactor are approximately 1.5 m in width by 1.3 m in height.

3.0 – Methodology

This chapter details experimental procedures and analysis. The procedures presented refer only to experiments conducted with solutions of chlorpyrifos suspended in double deionized water, and do not reflect the initial stage of the project, which was conducted using chlorpyrifos suspended in a solution of 10% acetonitrile and 90% double-deionized water (refer to Appendix B). All equipment mentioned in this section is clearly documented with pictures, descriptions and model information that can be found in Appendix A.

3.1 – Chlorpyrifos Solution Preparation

Preparing a standardized solution to use in each experiment was critical to ensuring accurate, repeatable results. The following procedure was used to prepare chlorpyrifos solutions at 2 ppm in water:

1. Approximately 900 mL of double deionized water was added to a 1000 mL beaker.
2. A magnetic stir bar was added to the beaker, which was placed on a stirring plate with a heating function. The water was heated to approximately 63 °C.
3. 2 mg of chlorpyrifos were weighed and added to the beaker containing heated water.
4. Parafilm was placed over the beaker to prevent any possible pesticide volatilization or evaporation of water.
5. The solution was allowed to mix for approximately an hour after this point, or until completely homogenous (i.e. no white flecks or phase separation could be seen in the colorless, transparent solution).
6. Once the pesticide was completely dissolved, the solution was transferred to a 1000 mL volumetric flask and the final volume adjusted to 1L with double deionized water.
7. The 2 ppm solution was allowed to cool to room temperature and then used to prepare all necessary dilutions.

3.2 – UV-Visible Light Spectroscopy

To analyze the results of each experiment using High Performance Liquid Chromatography (HPLC), it was necessary to determine the wavelength at which the clearest signals from samples containing chlorpyrifos were detected. To accomplish this, a UV-visible light spectrophotometer (UV-Vis) was employed to register the adsorption spectrum of chlorpyrifos with wavelengths of 200, 230, and 290 nm considered for analysis.

Samples of chlorpyrifos solution and double deionized water were prepared and placed in quartz cuvettes, which could be used for UV-Vis analysis to determine the wavelengths associated with chlorpyrifos in the following manner:

1. Using a quartz cuvette, a blank consisting of double deionized water was analyzed by the spectrophotometer in order to zero the machine.
2. Again, using a quartz cuvette, 2 ppm chlorpyrifos solution was analyzed by UV-Vis.

Since each compound absorbs light at a certain wavelength, similar to a fingerprint, it is possible to associate a chemical with a specific absorption wavelength. Using double deionized water as a blank served to ensure that no peaks were detected due to water. In this manner the remaining peaks could be assumed to result from chlorpyrifos. The three wavelengths tested could then be clearly evaluated and the one that provided the strongest signal for chlorpyrifos would be chosen.

3.3 – Calibration Curve

A dilution series was prepared for HPLC testing to create a calibration curve. Solutions of 2.0, 1.5, 1.0, and 0.5 ppm chlorpyrifos were prepared in triplicate using double deionized water to ensure accuracy. This was accomplished by utilizing Equation 2 to find the volume of the initial solution to be added to double deionized water to dilute the solution to the desired lower concentration (C_2) as shown in Table 3.1.

$$C_1V_1 = C_2V_2 \qquad \text{[Equation 2]}$$

Where C_1 = Concentration of the initial solution

V_1 = Necessary volume of the initial solution

C_2 = Desired concentration

V_2 = Desired volume of solution.

Table 3.1: Dilution needed for each concentration of solution.

C_1 (ppm)	V_1 (mL)	C_2 (ppm)	V_2 (mL)
2.0	10.0	2.0	10.0
2.0	7.5	1.5	10.0
2.0	5.0	1.0	10.0
2.0	2.5	0.5	10.0

These four concentrations were used to create a calibration curve for chlorpyrifos in double deionized water. Using the same reagent bottle of 2 ppm solution, dilutions of 1.5, 1.0, and 0.5 ppm were made. Three HPLC vials of each were filled and analyzed to create a reliable calibration curve of concentration versus area. The area under the peak at the elution time of chlorpyrifos could then be divided by the slope of the curve to determine concentration of samples taken throughout each experiment.

3.4 – Establishing Experimental Controls

There are two processes within each experiment that may cause a decrease in the concentration of chlorpyrifos in solution. The first is adsorption onto the catalyst surface and the second is photocatalytic oxidation. As a way to distinguish between the adsorption of chlorpyrifos onto the surface of the TiO_2 catalyst and the reaction of chlorpyrifos and UV radiation with the TiO_2 catalyst, the beginning of each experiment was run in the dark.

By taking samples of chlorpyrifos solution containing suspended titanium dioxide catalyst in the absence of UV light over time, it was possible to determine when the concentration of chlorpyrifos was no longer decreasing. Once the time needed to reach this plateau had passed, meaning the catalyst surface had been saturated with chlorpyrifos, the UV light source for the experiment could be turned on and all degradation of chlorpyrifos after that time could be assumed to be a result of photocatalytic oxidation.

To determine the time required for adsorption, two experiments were run in parallel: one solution of 2 ppm chlorpyrifos containing suspended TiO_2 and one control solution of 2 ppm chlorpyrifos without TiO_2. This was performed to ensure that no outside variables were contributing to the decrease in concentration of chlorpyrifos, such as volatilization.

The total time required for complete adsorption onto the catalyst surface was determined by carrying out the following procedure:

1. Two 50 mL samples of 2 ppm chlorpyrifos were prepared.
2. One 25 mg sample of P25 TiO_2 (see Figure 3.4) was prepared and stored in an Eppendorf flip-cap tube.
3. Both samples were placed in separate 100 mL beakers and a stir bar was added to each beaker.
4. These beakers were placed on separate stir plates inside a darkness box (See Figure 3.1) and covered in aluminum foil to ensure no light exposure.

Figure 3.1: UV darkness box closed (top left), UV darkness box opened (top right), inside of UV darkness box with UV light source above stir plate (bottom).

5. One beaker was labeled as the control and the other was labeled as TiO_2. The 25 mg sample of titanium powder was added to the TiO_2 beaker. Immediately after it was mixed into the liquid, a 2 mL sample from each beaker was taken using a 5 mL syringe and injected into Eppendorf flip-cap tubes. These tubes were labeled "C" for control and "T" for titanium. (For example, T=0 min was the first sample taken. The remaining times used can be found in Table 3.2.)
6. One minute after the samples were taken, both samples were placed into the centrifuge and run for 4 minutes at 13.4 thousand rpm. (For example, T=1 min was when sample T=0 was centrifuged.)
7. As soon as the centrifuge finished, the solution inside each Eppendorf vial was drawn into a 5 mL syringe. This was done using a needle attachment on the syringe to be sure not to disturb the pellet of TiO_2 that had formed at the bottom of the vial. Likewise, the

control sample was extracted in a similar manner. (For example, T=7 min was when sample T=0 was filtered into an HPLC vial.)

8. The control sample was then injected directly into an HPLC vial labeled with the time the sample was taken from the beaker, the concentration, and that it was the control.
9. A 0.45 micron filter was placed on the end of the syringe containing the TiO_2 sample and was filtered into a similarly labeled HPLC vial stating that it contained TiO_2.

Table 3.2: Times at which both control and TiO_2 samples were taken out of the beaker, centrifugation began, and were filtered into HPLC vials in parallel.

Sample	Taken (min)	Centrifuged (min)	Filtered (min)
1	0	1	5
2	7	8	12
3	14	15	19
4	21	22	26
5	28	29	33
6	35	36	40

Once the required time for complete adsorption had been obtained, all further experiments utilized the known adsorption time. This allowed the reactors to cycle for the determined time to ensure complete adsorption before activating a UV light source.

3.5 – Small-Scale Slurry Reactor Experiments

By turning the UV light source on after complete adsorption was achieved, it was possible to distinguish between the decrease in concentration due to adsorption and the decrease in concentration due to oxidation. Since the TiO_2 slurry reacts with chlorpyrifos in a manner similar to fixed-film TiO_2, an initial rate could be approximated and used to estimate the time required for the longer experiments with batch and compound parabolic collector (CPC) fixed-film reactors. This experiment was essentially a continuation of the experiment used to determine pesticide adsorption time as discussed above in Chapter 3.4. The initial laboratory setup remained the same, as did the procedure until the previously determined time required for complete adsorption had been reached. This time was found to be T = -7 minutes, as the UV lamps needed time to warm up before conducting the experiment.

The following procedure used both a control sample containing chlorpyrifos in water and a sample of chlorpyrifos in water with the addition of TiO_2:

1. At T=-7 min, a 2 mL sample was taken from each beaker with a 5 mL syringe and injected into labeled Eppendorf flip-cap tubes.
2. The beakers were covered with aluminum foil and the UV light source was switched on, allowing the UV light to warm up without affecting the samples.
3. Steps 7-10 of Chapter 3.4 were repeated for all samples taken as shown in Table 3.2.

Table 3.3 below shows the times at which both control and experimental runs were taken from the small-scale slurry reactor, centrifugation began, and filtration into HPLC vials occurred.

Table 3.3: Small-scale slurry reactor timetable.

Sample	UV Status	Taken (min)	Centrifuged (min)	Filtered (min)
1	UV with Tinfoil Covering	-7	-6	-2
2	UV source	0	1	5
3	UV source	7	8	12
4	UV source	14	15	19
5	UV source	21	22	26
6	UV source	28	29	33
7	UV source	35	36	40
8	UV source	42	43	47

3.6 – Fixed-Film Batch Reactor

The fixed-film batch reactor pictured in Figure 3.2 was used to determine the degradation reaction kinetics of chlorpyrifos in water at initial concentrations of 2.0, 1.5, 1.0, and 0.5 ppm. The reactor consists of a polished aluminum housing which has UV lamps mounted at equal intervals around the interior. The reactor itself is a two-piece glass vessel containing six glass slides coated with catalyst, which is housed between the UV lamps. A 2D schematic of process flow can be seen in Figure 3.3.

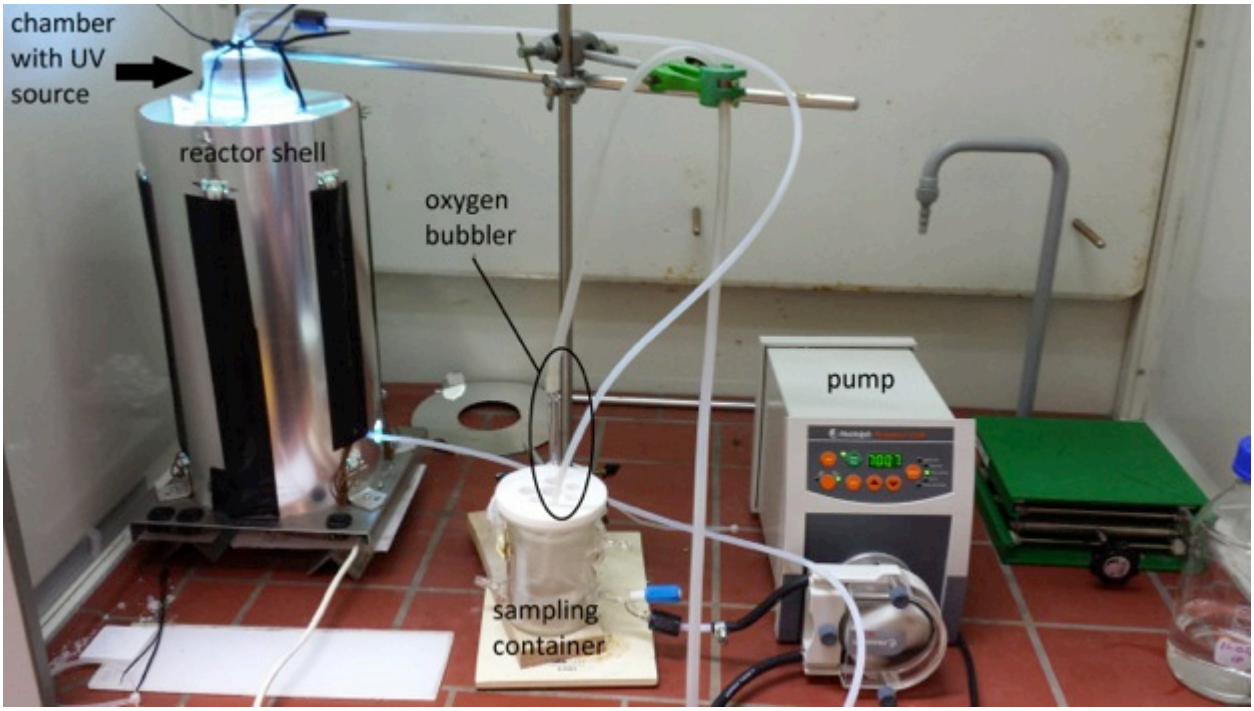

Figure 3.2: Fixed-Film batch reactor.

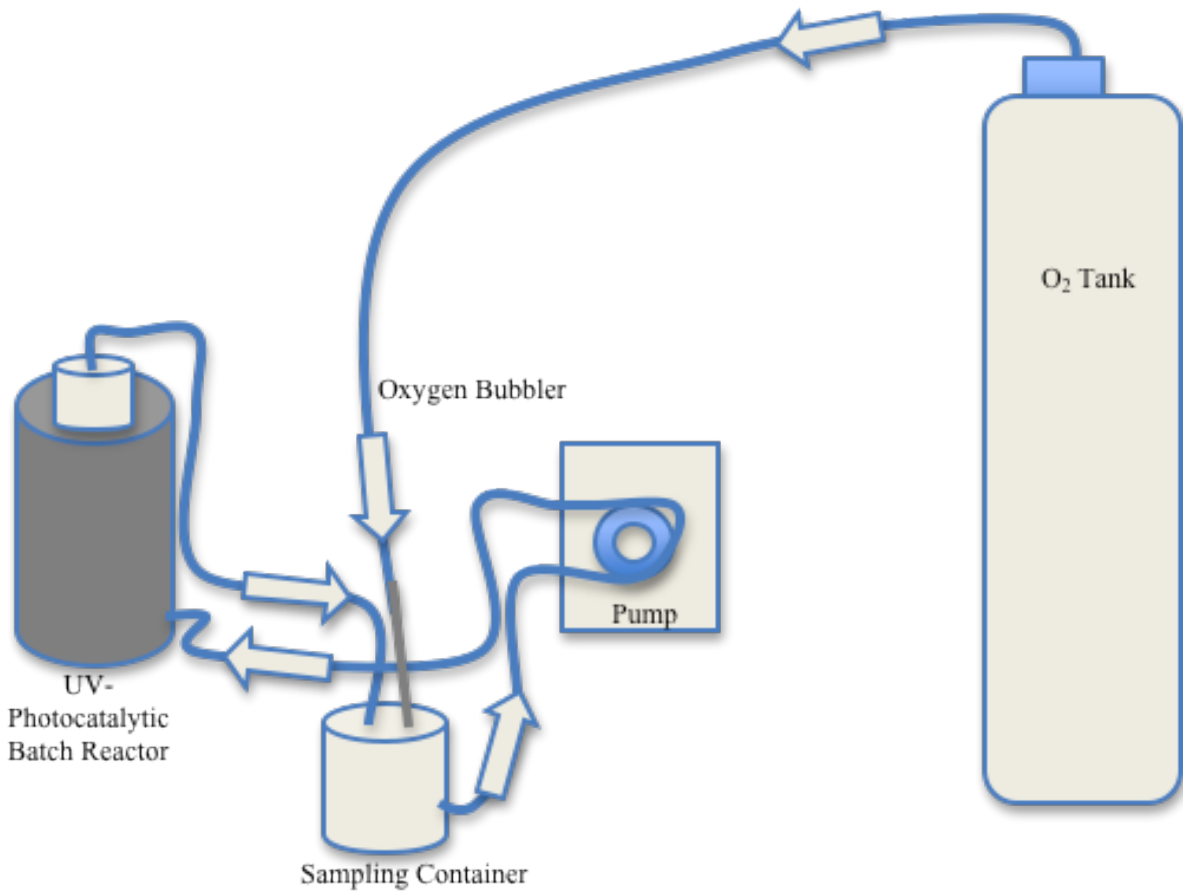

Figure 3.3: 2D schematic of fixed-film batch reactor.

3.6.1 – Fixed-Film Batch Reactor Preparation

The fixed-film batch reactor was prepared as follows:

1. Glass slides #5-12 were selected based on the mass of titanium silicate per cm^2 of surface area value being closest to 1.0 mg/cm^2.
2. The top of the glass reactor was removed, as was the top of the plastic holder (female adapter), to allow the slides to be loaded into every other slot in the cylindrical holder as shown in Figure 3.4.a.
3. Teflon tape was wrapped around the end of the slides and the holder itself to secure them.
4. The top of the holder was then replaced for additional physical support.

5. The holder was inserted into the glass chamber horizontally to avoid dropping the slides to the bottom.
6. The top of the glass reactor was reattached and wrapped with parafilm in order to prevent leakage as seen in Figure 3.4.b.
7. The reactor was carefully lowered into the metal reactor shell and secured with zip ties, utilizing the metal crossbars as shown in Figure 3.4.c. The reactor loading process is diagrammed in Figure 3.5.
8. The inlet and outlet were then connected to the pump using threaded plastic adapters.

Figure 3.4: a) Hexagonal glass slide holder b) loaded batch reactor chamber c) metal crossbars securing reactor.

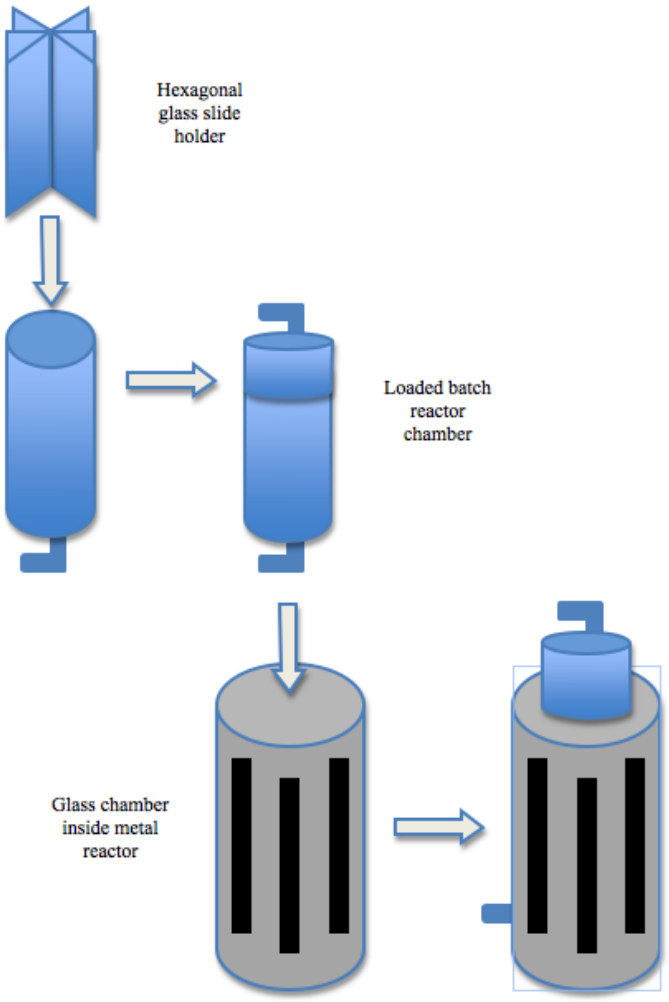

Figure 3.5: 2D schematic of hexagonal slide holder being loaded into the glass batch reactor chamber, sealing the chamber, and loading it inside the metal reactor.

3.6.2 – Flushing the Fixed-Film Batch Reactor

Once the reactor had been prepared, approximately 1.7 L of double deionized water was funneled into the sampling container until full. The positive displacement pump was set at a flow rate of 700.7 mL/min, a rotation of 156 rpm, and switched on. As soon as the sampling beaker began to drain, double deionized water was added to the sampling beaker at a rate approximately equal to the flow rate of the pump. Once the main chamber of the reactor was full and the water began to pour back into the sampling beaker, water addition ceased, the UV lights were switched on, and the system was allowed to run for a minimum of 30 minutes. This ensured that any previous contaminants on the slides or in the chamber were removed.

3.6.3 – Draining the Fixed-Film Batch Reactor

1. The pump was switched off and the outlet tube was placed into a waste container. The pump was then switched back on.
2. Once the sampling container was drained, the pump was stopped.
3. The inlet tube was removed from the sampling container and placed into the waste beaker.
4. The direction of the pump was reversed and the pump was run until the system was completely drained.

3.6.4 – Operating the Fixed-Film Batch Reactor

The process for loading the reactor with chlorpyrifos solution was similar to the process described for flushing the reactor. The solution of desired concentration was funneled into the sampling container. The glass slides previously loaded were used for all experiments, allowing the reactor chamber to remain untouched. Once the main chamber was full and solution began to pour back into sampling container, the system was allowed to run for 30 minutes in the dark to accommodate the predetermined adsorption time. A sample of the solution being loaded was taken for TOC and HPLC analysis using a 25 mL glass pipette connected to a Peleus ball and injected into a 30 mL TOC vial. After the 30-minute adsorption time elapsed, UV lights were switched on, an oxygen bubbler was placed into the sampling container, and the oxygen tank valve was opened to a pressure between 0.5-0.7 bars. Samples were taken at 0, 5, 10, 20, 30, 60, 120, 180, and 240 minutes. The system was emptied as described above and flushed with double deionized water after each experiment.

3.7 – UV Photocatalytic CPC Reactor

The compound parabolic collector (CPC) reactor shown in Figure 3.6 was used to analyze the required retention time of water contaminated with chlorpyrifos at concentrations of 2.0, 1.5, 1.0, and 0.5 ppm in double deionized water. During each experiment, samples were taken at predetermined times to be analyzed. The TiO_2 used as a catalyst in this reactor was commercial grade and had been previously embedded in a porous paper-like material.

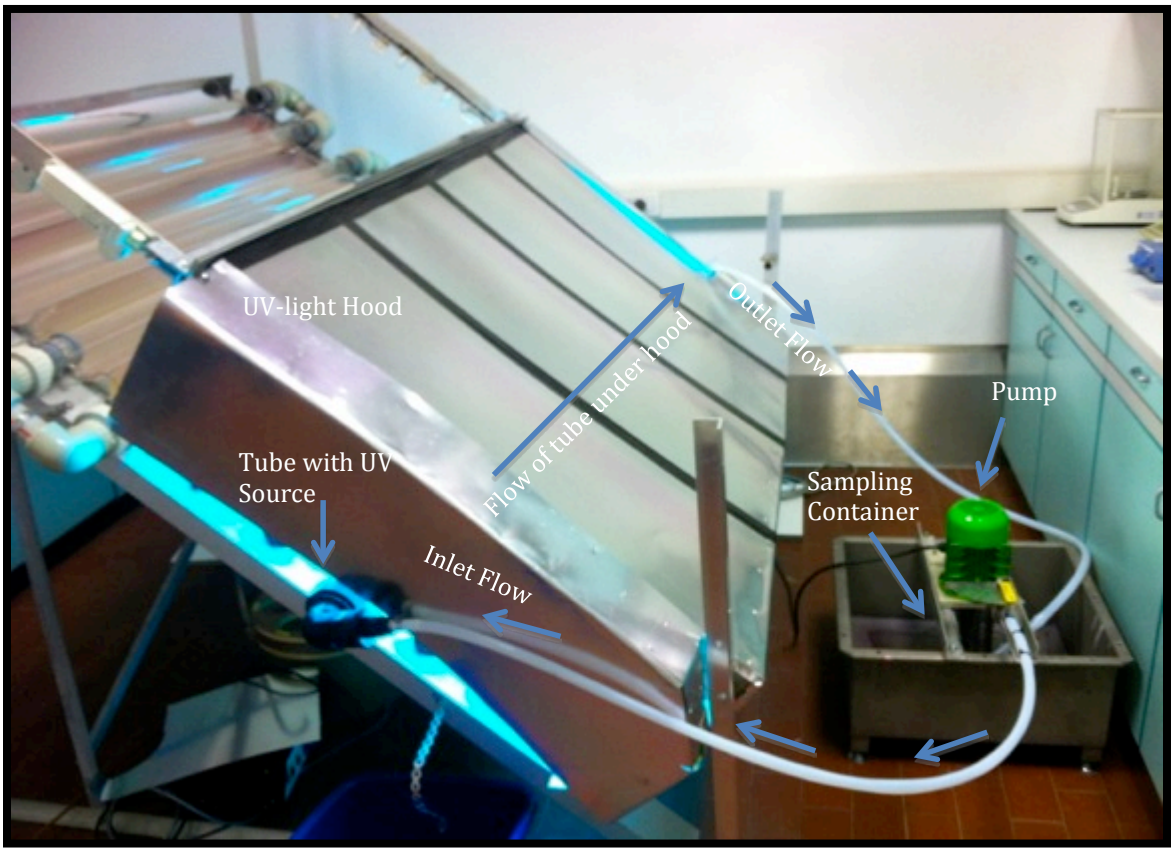

Figure 3.6: CPC reactor.

3.7.1 – CPC Catalyst Preparation

1. Four round steel holders as pictured in Figure 3.10 were set aside for wrapping in commercial grade P25 TiO_2 catalyst-embedded paper. The manufacturer of this pre-embedded paper can be found in the equipment list (Appendix A).
2. Four sheets of porous paper were cut from the roll in Figure 3.10 at lengths equal to that of the steel holders.

3. Eight sections of 10 gauge lead wire were cut at lengths approximately equal to 1.5 times the circumference of the steel holders and set aside.
4. The steel holders were each tightly wrapped by hand with the catalyst-embedded paper.
5. While one person maintained the tight wrap on the steel holders, another wrapped a piece of the precut lead wire around each end of the holder and twisted the two ends of wire together to ensure a snug fit.
6. Any excess wire was cut off with a pair of pliers and the twisted section of wire was bent down so that it was flush with the paper.
7. Steps #4-6 were repeated with each of the four holders.
8. The fitting at the end of the reactor tube in use was removed and all four steel holders wrapped in porous paper were loaded into the tube by hand.
9. The fitting at the end of the reactor tube was replaced and attached to the hose coming from the pump.

Figure 3.7: (From left to right) round steel holders, commercial grade TiO_2 catalyst embedded in porous paper, wrapped steel holders, holders being inserted into the chamber of the CPC reactor.

3.7.2 – CPC Reactor Preparation

1. The volume of the CPC reactor is approximately 5.5 L, meaning that 5.5 L of the desired sample needed to be prepared prior to each experiment.
2. With the pump valve closed, the sample solution was poured into a 2 L dish beneath the pump until the container was filled and the pump was submerged.
3. A 25 mL sample was taken from this dish to serve as a sample for time T=-30 min. This was accomplished using a 25 mL glass pipette connected to a Peleus ball.
4. The sample was then injected into a 30 mL TOC vial.
5. The pump was started and one person slowly opened the valve halfway while another poured the remainder of the sample into the 2 L dish.
6. Once the solution was flowing continuously through the reactor, the valve was opened completely and the half hour of adsorption time in the dark began.

3.7.3 – CPC Reactor Operation

1. After the adsorption time was complete, a sample at time T=0 min was taken to determine how much chlorpyrifos had been adsorbed.
2. Immediately following, the UV lights were switched on and time recorded (using a stopwatch).
3. Samples were taken in the manner described above at various time intervals.
4. After 300 minutes the UV light source and the pump were turned off.
5. The effluent line from the pump was removed from the reactor tube and placed in a waste container.
6. The pump was turned on and allowed to drain the contents of the 2 L dish into a waste container.
7. The pump was then turned off and the waste container was placed below the reactor tube.

8. The cap on the reactor tube was removed, thus allowing the waste to drain. Since the reactor is a few degrees off horizontal, draining this portion solely with the aid of gravity was possible.
9. 2 mL samples were taken from each of the TOC vials and placed into HPLC vials using a Pasteur pipette.
10. All vials were labeled appropriately and stored until the correct analysis equipment was available for use.

3.8 – Methods of Analysis

Several different methods and instruments were used to analyze the data collected from the reactors. The HPLC analysis allowed for degradation curves and intermediate generation curves to be analyzed, the TOC analysis provided data for the creation of curves depicting the removal of total organic carbon from solution, and the LCMS detailed peaks used to determine chemical compositions needed to establish the identity of intermediate molecules.

3.8.1 – HPLC Analysis Process

3.8.1.a Reaction Kinetics

The reaction rate (r) at a known concentration may be determined from experimental results. The reaction order is determined by graphing the natural log of the negative change in concentration over change in time ($-\ln(\frac{-dCa}{dt})$) versus the natural log of concentration ($\ln(Ca)$) and determining the slope of the line, α (see Equation 3). For the following experiments, chlorpyrifos was the sole reactant, referred to as species A in the following equations. Equation 3 represents the generalized rate law.

$$-r_A = k_A C_A^{\alpha} C_B^{\beta} \qquad \text{[Equation 3]}$$

Where r_A = reaction rate,

k_A = rate constant

C_A = chlorpyrifos concentration,

C_B = concentration of species B

α = reaction order of species A

β = reaction order of species B

The rate law exists to describe the relationship of these variables at specific concentrations [Folger, 2006].

Based on experimental data as well as previous research [Kanmoni, 2012], the reaction order for the degradation of chlorpyrifos could be determined. The following equation represents a first order reaction.

$$-r_A = k_A C_A \qquad \text{[Equation 4]}$$

Where k is in units of min^{-1}.

3.8.1.b Calculations

Below is the process used to find the reaction order (α) and rate constant (k) for a given concentration of chlorpyrifos in a UV-photocatalytic fixed-film reactor:

1. The changes in concentration and time from sample to sample were calculated using $C_{final} - C_{initial} = \Delta C$ and $T_{final}-T_{initial} = \Delta T$, respectively.
2. The natural log of Δconcentration/Δtime was then graphed against the natural log of concentration corresponding to this change. For example, from 20 to 30 minutes would have a Δt of 10 minutes and a ΔC of $C_{30min} - C_{20min}$. The quotient of these values would then be graphed against the natural log of C_{30min}.
3. The slope of this graph gave the reaction order (α), referred to in Equation 3.
4. The specific reaction rate, also commonly referred to as the rate constant, k, can be found through Equation 5, which also relies on the graph generated in step 3.

$$LN(k_A) = y\ intercept \qquad \text{[Equation 5]}$$

5. The integral method may also be used for first order reactions, where the rate constant can be obtained by plotting a graph of the negative natural log of final concentration divided by initial concentration $\left(-\ln\left(\frac{Ca}{Cao}\right)\right)$ versus time. The slope of the line generated is equal to the k value.

3.8.2 – TOC Analysis Method

Given the molecular formula of chlorpyrifos, $C_9H_{11}Cl_3NO_3PS$, and the known concentration of solution being prepared, it was possible to determine the theoretical total organic carbon (TOC) contained in a sample of a given volume and concentration. This value could then be used in comparison to the results produced by the TOC analyzer to determine the difference between

actual and theoretical carbon content. In this manner, it was possible to ensure that the machine was functioning properly.

Since any intermediate formed through the degradation of chlorpyrifos will contain carbon, the TOC will remain of significant value until complete mineralization is achieved. This is due to the fact that as CO_2 is generated, it will immediately volatilize and leave solution; effectively reducing the total carbon content of the sample.

By testing 2.0, 1.5, 1.0, and 0.5 ppm chlorpyrifos samples, a graph of chlorpyrifos concentration versus carbon concentration could be generated. This served as a calibration curve and aided in the analysis of chlorpyrifos mineralization.

3.8.3 – LCMS Analysis Method

Liquid chromatography/mass spectrometry (LCMS) was used to determine the composition of several intermediates formed during the degradation process of chlorpyrifos. Using HPLC results, samples from each experiment were taken at the highest peak of every intermediate that appeared and analyzed by LCMS using the same column used for HPLC analysis. Elution times that corresponded to peaks in both HPLC analysis and LCMS were used to determine areas of focus. Once the necessary peaks were determined, the mass to charge ratio (m/z) for each was used to identify possible compounds.

4.0 – Results & Discussion

Data presented in this chapter represent a portion of the research completed for this project. Additional data and analysis containing all graphs and calculations relevant to this project can be found in Appendices C & D. High Performance Liquid Chromatography (HPLC), Total Organic Carbon (TOC), and Liquid Chromatography/Mass Spectrometry (LCMS) were used to analyze photocatalytic oxidation reactions involving immobilized TiO_2 in both bench-scale fixed-film batch reactor and pilot scale compound parabolic collector (CPC) reactor. The degradation rate of chlorpyrifos and its reaction kinetics provide the information necessary to design a full-scale reactor. TOC analysis was used to determine the extent of mineralization. Similarly, LCMS analysis identified intermediate compounds that could be studied for toxicity, aiding in the determination of appropriate treatment levels.

4.1 – Analysis of UV-Visible Light Spectroscopy

UV-Visible light spectroscopy (UV-Vis) was used to determine the appropriate wavelength to analyze a sample of 2 ppm chlorpyrifos solution with HPLC. The software configuration can be seen in Figure 4.1. The HPLC analyzes each sample at wavelengths of 200, 230, and 290. As can be seen in Figure 4.2, peaks appear on UV-Vis at all three wavelengths used for HPLC analysis. Since the clearest, most defined wavelength occurred at 200 nm, this was the wavelength used to analyze all HPLC results.

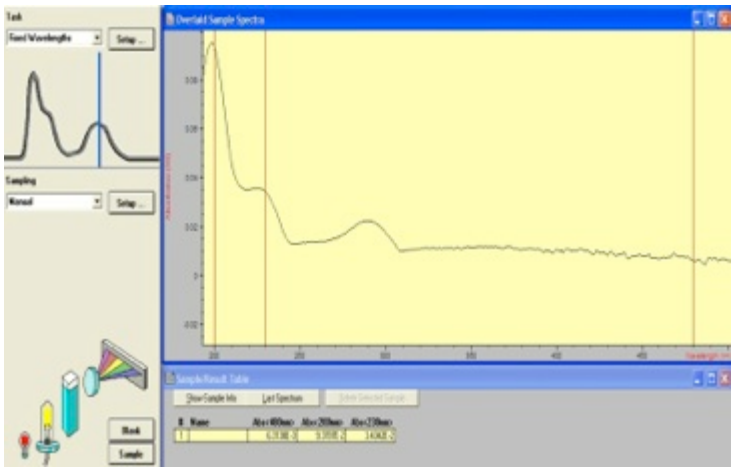

Figure 4.1: UV/Vis Spectrophotometer screen shot.

UV-Vis was also used to verify that the 0.45 micron filter used for the slurry reactor experiments (Chapter 3.5) did not interfere with the solution analysis. Injecting a sample of chlorpyrifos through the filter into a quartz cuvette and analyzing it determined that chlorpyrifos did not have an affinity for the filter material surface and remained in solvent. Analyzing one sample of filtered chlorpyrifos solution and one of unfiltered chlorpyrifos solution side by side showed that the graphs were identical, meaning the filter had no effect on the composition of chlorpyrifos in solution.

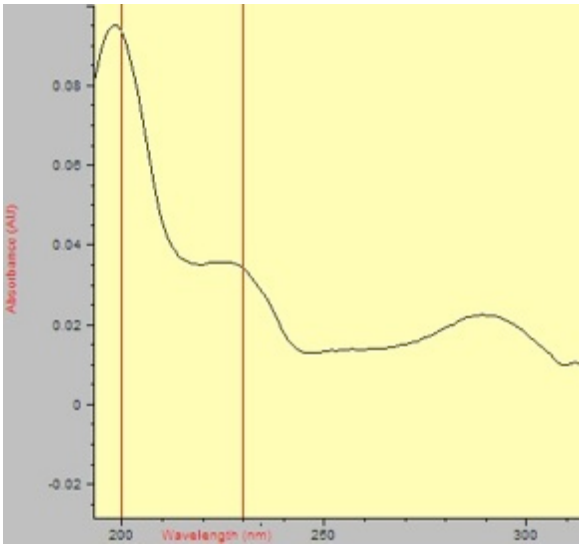

Figure 4.2: 2 ppm chlorpyrifos solution with red lines denoting wavelengths of 200 and 230 nm.

4.2 – HPLC Calibration Curve

The calibration curve shown in Figure 4.3 represents samples of chlorpyrifos at concentrations of 2.0, 1.0, 0.5, and 0 ppm (double deionized water). Analysis of 1.5 ppm samples resulted in unreliable data that was dismissed for calibration purposes.

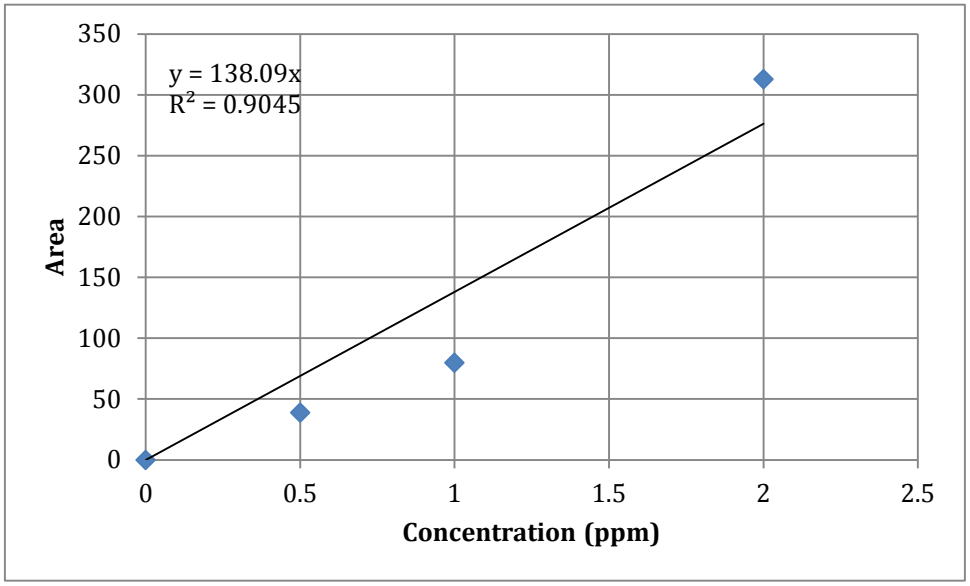

Figure 4.3: Calibration curve for solution of chlorpyrifos at concentrations of 2.0, 1.0, 0.5, and 0 ppm.

The calibration curve shown above is comprised of four points, each of which is the average of the T= -30 samples for both the batch and CPC reactors since the T=-30 samples represent starting concentrations. In this way, the degradation curve of every experiment accurately reflected the correct concentration. As shown in several experiments (such as 2.0 ppm fixed-film batch seen in Figure 4.6), the calculated concentration appears slightly higher than the target value of the prepared solution. This is likely due to the low concentration of solid chlorpyrifos that was added to double deionized water to make the initial standard solution. Due to limitations with the scale used, these low concentrations of solid chlorpyrifos may have been skewed due to sensitivity. A small error in weighing the compound could translate to a considerable percentage of error in the data.

4.3 – Experimentation Using the Slurry Batch Reactor

As previously mentioned in Chapter 3.5, a control sample of chlorpyrifos solution was run alongside an identical solution, which differed only by the addition of TiO_2 in solution. With adsorption ruled out as a variable in previous experiments, the control sample was used to determine whether or not the concentration of chlorpyrifos was changing as a result of volatilization. The experiment was run starting at T=0 in the dark until T=42 min, at which point the samples were exposed to UV light until the end of the experiment at T=84 min. As can be seen in Figure 4.4, variations exist due to human and machine error, as well as equipment limitations. Despite these variations, it can be seen that volatilization of chlorpyrifos did not occur, as the concentration remained reasonably stable, confirming that the degradation due to adsorption and photocatalysis was not influenced by volatilization.

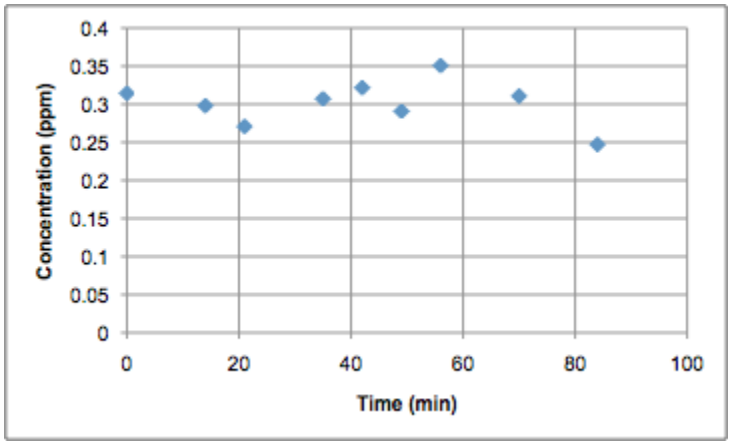

Figure 4.4: Concentration over time of control solution used in slurry reactor experiments.

The low concentrations of chlorpyrifos after 14 minutes of contact with TiO_2 without UV light were below the HPLC sensitivity range. As shown in Figure 4.5, the peak associated with chlorpyrifos drops at time T=14 min and remains constant for the remainder of the experiment.

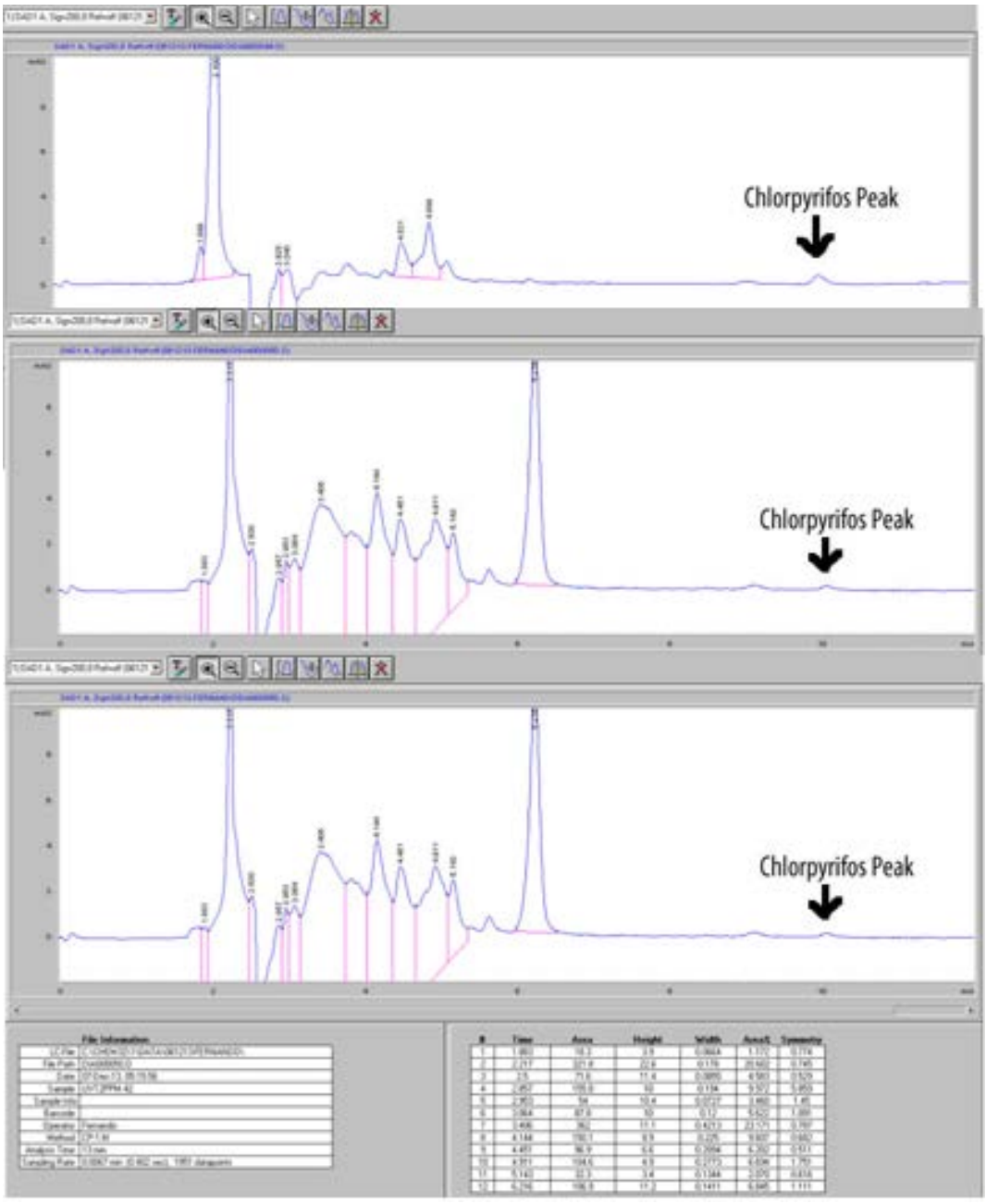

Figure 4.5: Unintegratable chlorpyrifos peaks (increasing time from top to bottom).

The purpose of this experiment was to decide upon an appropriate contact time that could be used when running the larger fixed film reactors. As a precautionary measure, additional time was added to the determined adsorption time. In this manner it was possible to ensure that the reduction in concentration of chlorpyrifos during all experiments was a result of degradation

rather than adsorption. The final time allotted for pesticide adsorption onto the catalyst surface for fixed-film reactor experiments was thirty minutes.

4.4 – Glass Slide Coating

Multiple sets of glass slides coated in titanium silicate were created using the procedure detailed in Chapter 3.6. Weight, surface area, and thickness of each slide can be found in Table 4.1. Slides 7-12 (starred in Table 4.1) were used for batch reactor experiments since they had a coating thickness closest to 1 mg/cm^2. This ensured as much surface area as possible was covered without wasting titanium silicate. Since each slide was evenly hand coated with similar dimensions and coating thicknesses, the UV light source was able to interact with the catalyst on each slide in a uniform manner.

Table 4.1: Surface area, weight, and final thickness for glass slides used in the photocatalytic batch reactor.

Slide #	Surface Area (cm^2)	Weight of 1 Coating (grams)	Weight of 2 Coatings (grams)	Weight of 3 Coatings (grams)	Final Layer (mg/cm^2)
1	150.14	0.110	0.237	0.339	2.26
2	152.29	0.109	0.229	0.340	2.24
3	150.70	0.088	0.199	0.325	2.16
4	151.83	0.114	0.209	0.323	2.13
5	151.26	0.087	0.191	0.300	1.98
6	148.44	0.119	0.241	0.309	2.08
7*	153.52	0.092	0.227	N/A	1.48
8*	152.39	0.106	0.229	N/A	1.50
9*	152.39	0.092	0.181	N/A	1.19
10*	150.70	0.121	0.256	N/A	1.70
11*	152.96	0.124	0.248	N/A	1.62
12*	151.83	0.100	0.231	N/A	1.52
13	161.36	0.167	0.3506	N/A	2.17
14	157.16	0.1002	0.2757	N/A	1.75
15	157.16	0.1718	0.3432	N/A	2.18
16	161.36	0.1339	0.295	N/A	1.83
17	161.96	0.1797	0.3403	N/A	2.10
18	161.36	0.1475	0.3353	N/A	2.08

4.5 – Fixed-Film Batch Reactor HPLC Results

The photocatalytic fixed-film batch reactor was utilized to determine the reaction kinetics of UV/TiO_2 photocatalysis, and the rate constant of the UV-exposed solution over time. In addition, the total organic carbon was recorded using TOC analysis to verify that chlorpyrifos was actually being degraded and oxidized into gaseous CO_2. Throughout the course of all fixed-film batch reactor experiments, the degradation of chlorpyrifos was determined to follow first order reaction kinetics, which allowed the use of Equation 4, as shown in Chapter 3.10.1, to solve for the reaction rate and reaction constant. Ten samples were collected from times of -30 minutes to 240 minutes. Table 4.2 shows the data collected from the experiment of the degradation of chlorpyrifos in water with a starting concentration of 2.29 ppm. As shown, the samples taken while under UV exposure after time zero were initially taken at shorter intervals to accurately capture the immediate degradation.

Table 4.2: HPLC results and concentrations.

Time (min)	Chlorpyrifos Concentration (ppm)
-30	2.29
0	1.15
5	1.04
10	0.90
20	0.77
30	0.65
60	0.39
120	0.15
180	0.06
240	n/a

The graphical representation of data presented in Table 4.2 is shown in Figure 4.6. A large decrease in the concentration of pesticide in solution was seen during the dark period from T=-30 min to T=0 min. This can be attributed to the adsorption of chlorpyrifos onto the catalyst surface. Small-scale slurry adsorption in the dark occurred after 30 minutes, meaning the time needed for full adsorption in an immobilized reactor occurs before 30 minutes due to lower concentrations of catalyst on a fixed-film surface. Following this initial adsorption, the pesticide continued to degrade exponentially with exposure to UV light. After 4.5 hours the reactor was shut down. HPLC analysis was conducted on all samples, showing that the pesticide had degraded to the levels below HPLC sensitivity after 180 minutes (shown in Figure 4.6). This suggests that the pesticide had been degraded to trace amounts within the first three hours of contact time under UV exposure.

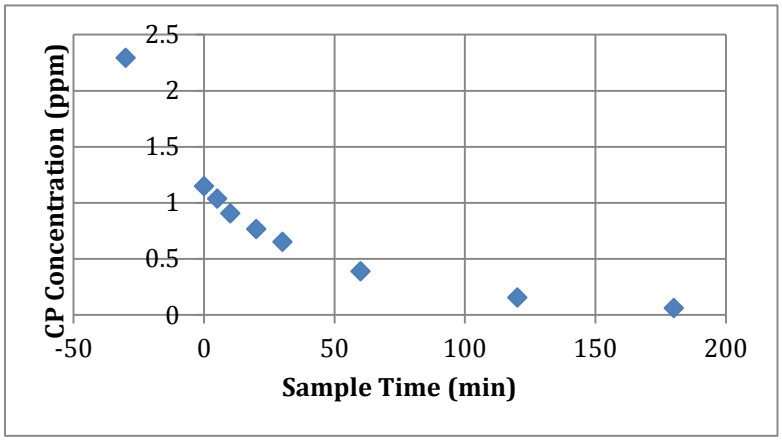

Figure 4.6: Chlorpyrifos degradation in UV-photocatalytic fixed-film batch reactor with an initial concentration of 2.29 ppm.

As discussed in methodology Section 3.10.1, raw data was used to calculate the values found in Table 4.3. This data was used to create the graphs required to determine the reaction order and reaction rate constant.

Table 4.3: Calculations and values needed to find reaction order, α, and reaction constant, k. Chlorpyrifos has been abbreviated to CP.

d[CP] (ppm)	dt (min)	LN(-d[CP]/dt)	LN([CP])	Time (min)
-1.142	30	-3.268	0.139	0
-0.113	5	-3.790	0.036	5
-0.132	5	-3.636	-0.100	10
-0.138	10	-4.286	-0.265	20
-0.116	10	-4.458	-0.429	30
-0.261	30	-4.746	-0.941	60
-0.236	60	-5.538	-1.869	120
-0.092	60	-6.481	-2.776	180

Figure 4.7, created using Table 4.3, shows the slope of the line, α, to be 0.9988, which indicates that chlorpyrifos degrades following first order reaction kinetics. Since the degradation of chlorpyrifos is first order and can be treated as an elementary reaction, a single step is required to change chlorpyrifos into its intermediate [Folger, 84]. The reaction order was of importance

when scaling up the CPC reactor for use with the pilot scale CPC reactor in the design aspect of the civil engineering project, such as the treatment of storm water runoff from vineyards and other agricultural applications as discussed in the design aspect (Chapter 5).

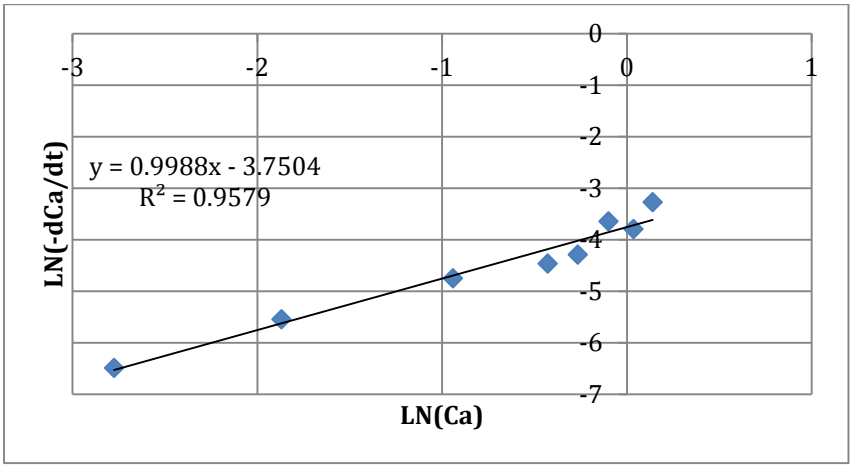

Figure 4.7: Graph depicting the slope of the line = α for batch reactor with starting concentration of 2.29 ppm.

The reaction constant was also calculated from Figure 4.7 as previously described and was found to be 0.021 min^{-1}. This was confirmed by plotting the natural log of concentration over initial concentration against the time the sample was taken. The negative slope of the line generated provided a k value of 0.016, which is reasonably close to the rate constant determined below (Figure 4.8).

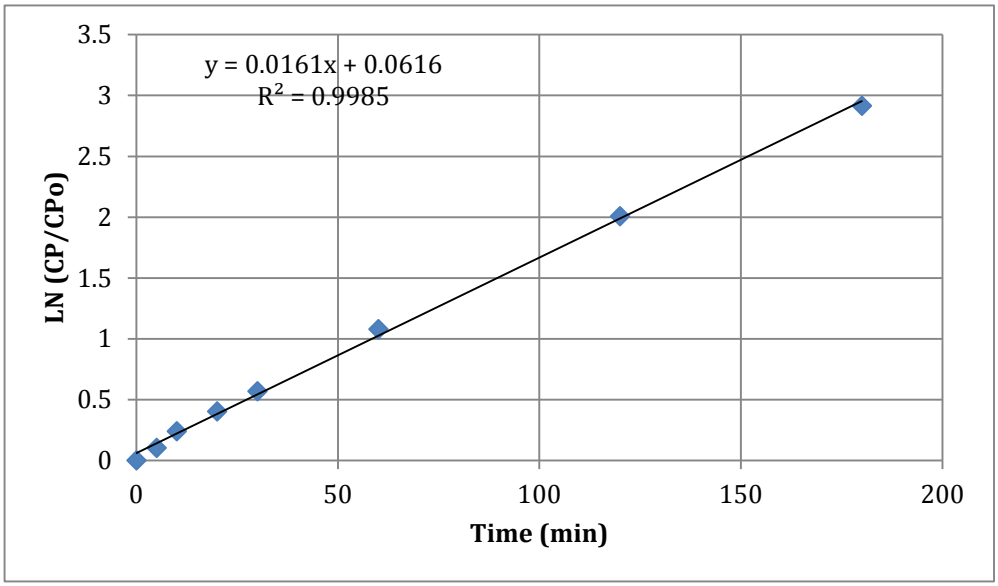

Figure 4.8: Natural log of efficiency versus time to find the value of the rate constant, k.

4.6 – CPC Reactor HPLC Results

Samples were taken at T= 0, 10, 20, 30, 60, 120, 180, and 240 minutes. After running each sample through HPLC, a degradation curve was plotted. Furthermore, intermediate generation data could also be recorded from HPLC chromatograms. The degradation curves from many of these experiments were less than ideal, but in many cases intermediate generation could clearly be seen.

The CPC samples taken during each experiment were analyzed using HPLC and compared to the calibration curve created with standard solutions. The degradation of chlorpyrifos with an approximate starting concentration of 2.24 ppm at T =-30 min (not shown for scaling purposes) can be seen in Figure 4.9. Figure 4.10 depicts the generation of an intermediate compound in terms of area under the peak seen in HPLC chromatograms. From this graph, it can be seen that an intermediate is generated during the degradation of chlorpyrifos.

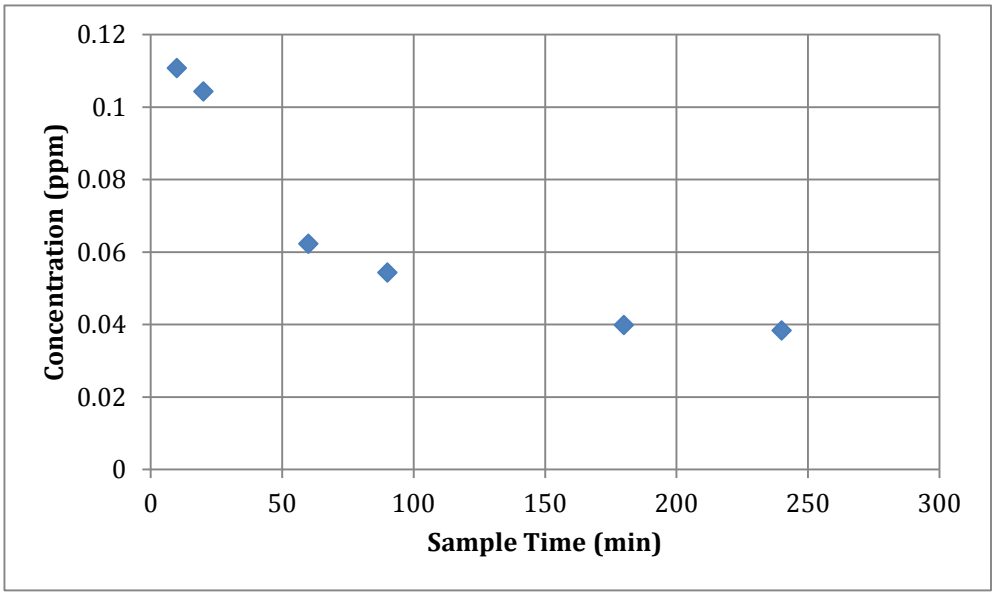

Figure 4.9: Degradation of chlorpyrifos in CPC reactor.

Figure 4.10 is of specific interest to this project because of the clear intermediate generation depicted through the logarithmic growth of the curve. Select samples from this experiment were sent for LCMS analysis to identify the compounds being generated.

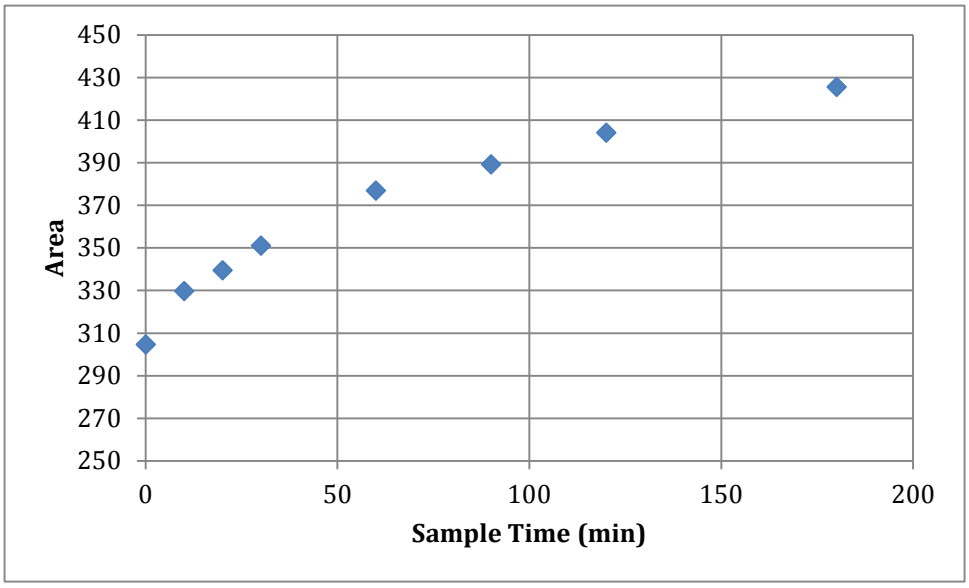

Figure 4.10: Generation of intermediate during chlorpyrifos degradation in CPC reactor.

4.7 – TOC Results

Total organic carbon was analyzed for each experimental run using samples at various times. The analysis method used to interpret the data is referenced in Section 3.10.2. Figure 4.11 displays the data from the batch reactor experiment that had a starting concentration of 0.25 ppm.

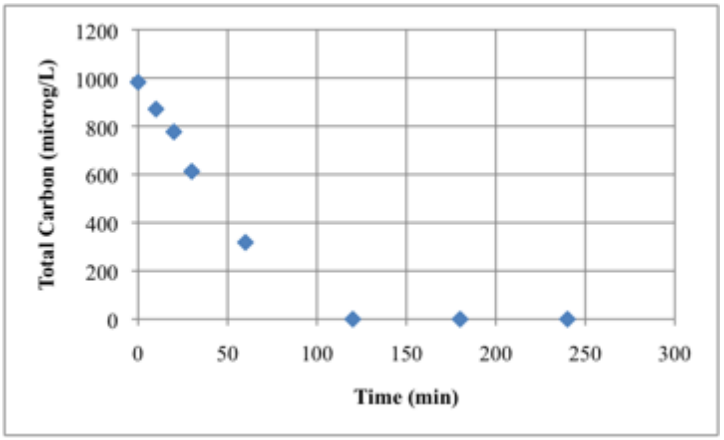

Figure 4.11: TOC over time from UV-photocatalytic fixed-film batch reactor.

As shown, the total organic carbon was 1000 µg/L at time zero and reduced to 0 µg/L after 120 minutes. This analysis aided in affirming that chlorpyrifos was degraded using TiO_2/UV oxidation since the chlorpyrifos in the sample had degraded to the point where CO_2 was generated in gaseous phase and left solution. Raw data from all TOC analysis can be found in Appendix D. It should be noted that the cleaning procedures used had the potential to contribute to the contamination of samples due to high sensitivity of the TOC equipment, which may account for the less than ideal data generated in the TOC analysis.

Given the molecular formula of chlorpyrifos and the known concentration of solution being prepared, it was possible to determine the theoretical total organic carbon contained in a sample of a given volume. Due to time constraints involved with using TOC analysis, the number of samples was severely limited. As a result, a theoretical calibration curve was utilized to ensure that all samples from reactors could be run. Using the calibration curve of theoretical

carbon at given concentrations of chlorpyrifos, the theoretical TOC values were calculated for each sample from the equation of the line in Figure 4.12.

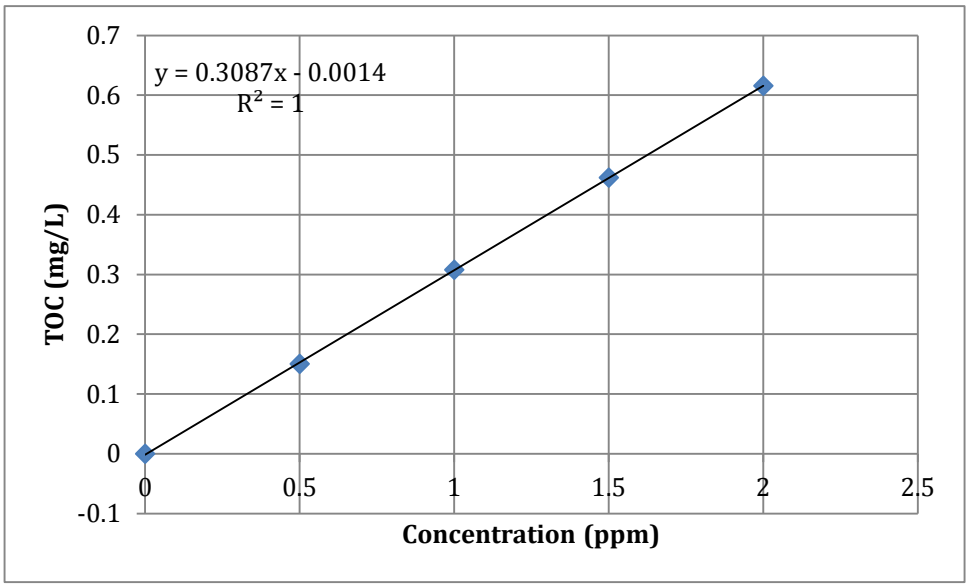

Figure 4.12: Theoretical TOC of chlorpyrifos samples.

These theoretical values could then be compared to actual TOC readings (Figure 4.13). For scaling purposes, the actual TOC reading at T=-30 minutes was omitted. The difference between the final two points can be attributed to carbon lost from complete mineralization of intermediate compounds.

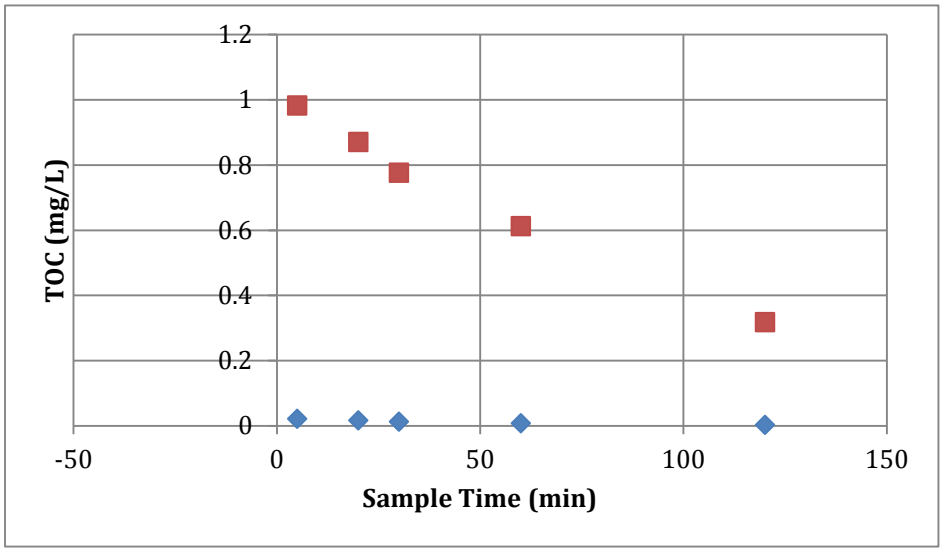

Figure 4.13: Theoretical TOC (red squares) versus actual TOC (blue diamonds).

The values of the points at T=120 minutes are 0.32 mg/L actual and 0.0031 mg/L theoretical. The difference between the two points is 0.3169 mg/L. Since the initial concentration of the solution was 0.25 mg/L, it is impossible for over 100% of the carbon to mineralize. The raw data itself revealed impossibly high numbers, showing a 1 ppm concentration of carbon in 0.5 ppm chlorpyrifos solution, suggesting contamination of samples from the glassware.

4.8 – LCMS Results

Liquid chromatography/mass spectroscopy (LCMS) results revealed the composition of several intermediates formed during the degradation process of chlorpyrifos. Using HPLC results, samples from each experiment were taken at the highest peak of every intermediate that appeared. This led to a total of twelve samples used for analysis with LCMS (see Table 4.4); two samples yielded readable results. Due to the low concentrations used in experimentation, it was difficult for the analyzer to detect many of the samples.

Table 4.4: Samples from each experiment analyzed by LCMS identifiable by the type of reactor, the starting concentration, and the time at which the sample was taken. Samples 5 and 12, highlighted, produced useable results.

Vial #	Starting Concentration	Reactor	Sample Time
1	0.5	Batch	30
2	1.0	Batch	-30
3	1.0	Batch	240
4	1.5	Batch	120
5	0.5	CPC	285
6	1.0	CPC	10
7	1.0	CPC	300
8	1.5	CPC	20
9	2.0	CPC	240
10	2.0	Batch	0
11	2.0	Slurry	42
12	2.0	CPC	180

Samples five and twelve (highlighted in grey above) produced mass spectra shown in Figure 4.14 and Figure 4.15, respectively. The highlighted areas shown were magnified and analyzed on the basis of intensity versus mass to charge ratio (m/z) as can be seen in Figure 4.16, which represents the first highlighted area in Figure 4.14. All other mass spectra can be found in Appendix G. Peaks appearing at elution times found in both HPLC and LCMS analysis were the major area of focus to identify intermediates. Chlorpyrifos did not appear in LCMS analysis, as it had degraded past the point of detection in the samples chosen.

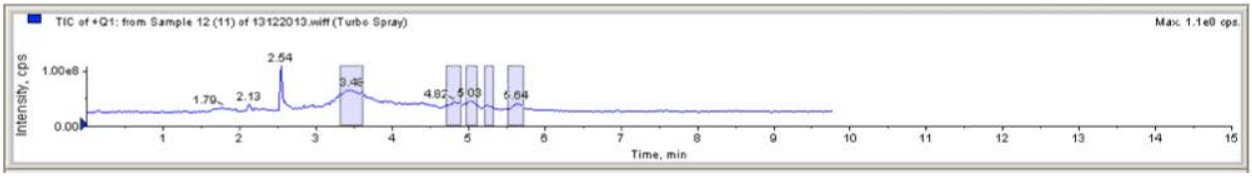

Figure 4.14: Mass spectrogram of 2 ppm slurry reactor at t=42 min.

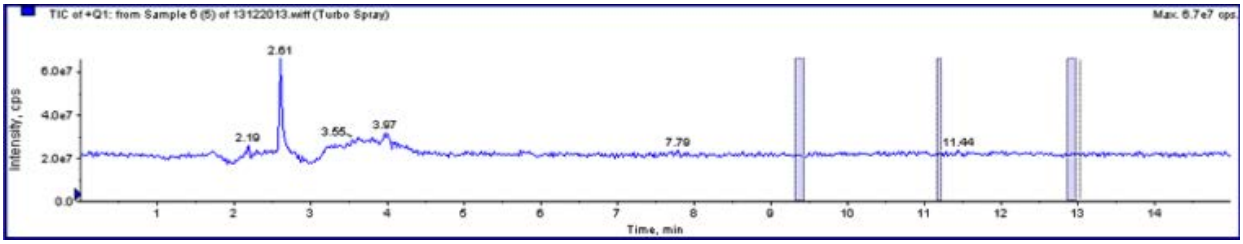

Figure 4.15: Mass spectrogram of 0.5 ppm CPC reactor at t= 285 min.

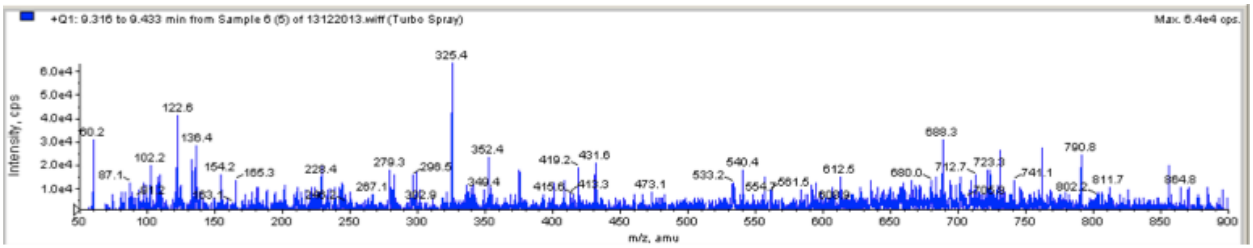

Figure 4.16: Elution times 9.316-9.433 min from Figure 4.15

Viable intermediate compounds could be formed by modifying the structure of chlorpyrifos using basic organic chemistry principles, since the molecular weight is approximately equal to the m/z value. Some viable pathways that organophosphates follow can be found from previous research presented by Konstantinou, as shown in Figure 4.17, which shows the photocatalytic degradation of organophosphates in the presence of aqueous TiO_2 suspension.

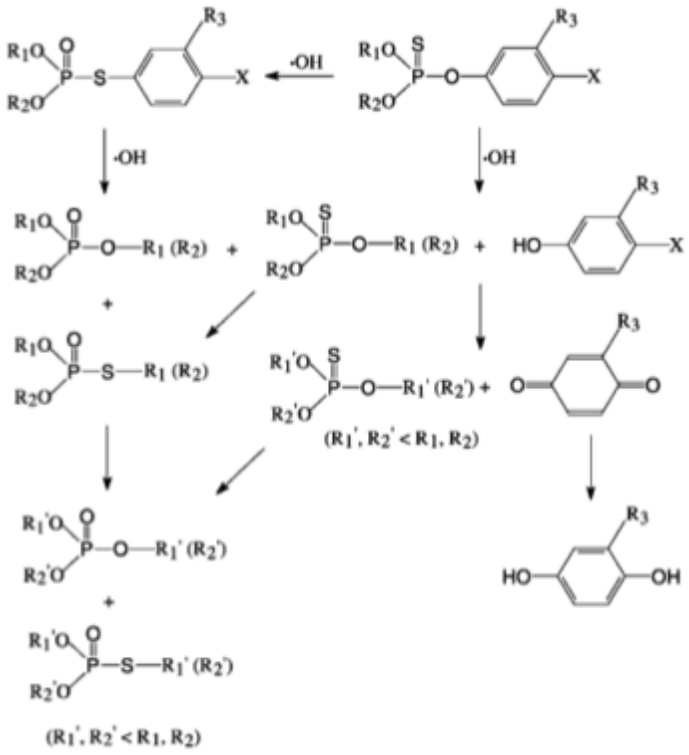

Figure 4.17: Possible reaction pathways of organophosphates in aqueous TiO_2 suspension [Konstantinou, 2002].

While several proposed intermediates follow similar pathways, the possibility of a mechanism involving ring opening exists, as can be seen in two of the proposed intermediates (Table 4.5), where nitrogen is removed.

Table 4.5: possible intermediates generated during chlorpyrifos degradation.

Elution time (min)	m/z	Formula	Possible structure	Name
4.8	199	$C_5H_2Cl_3NO$	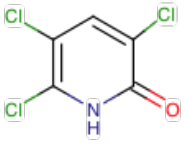	3,5,6-trichloro-1,2-dihydropyridin-2-one
4.8	339	C9H14Cl3O3PS	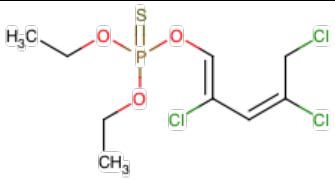	ethyl (1Z,3E)-2,4,5-trichloropenta-1,3-dien-1-yl ethoxy(sulfanylidene)phosphonite
9.3	325	C8H12Cl3O3PS	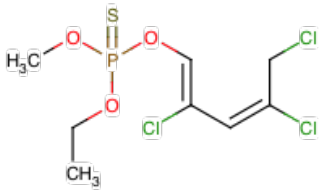	methyl (1Z,3E)-2,4,5-trichloropenta-1,3-dien-1-yl ethoxy(sulfanylidene)phosphonite
N/A	N/A	C9H11Cl3NO3PS	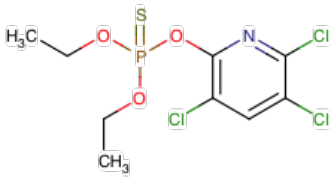	Chlorpyrifos (parent compound)
12.8	122	C6H5NO2	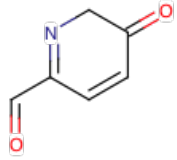	5-oxo-5,6-dihydropyridine-2-carbaldehyde
12.8	297	C9H13ClNO4PS	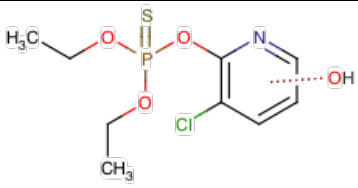	3-chloro-5-hydroxypyridin-2-yl ethyl ethoxy(sulfanylidene)phosphonite

The first two compounds were found on the same mass spectrum, due to overlapping peaks. While it was not possible to identify the correct intermediate at that point, it was much more likely that $C_5H_2Cl_3NO$ was present as opposed to $C_9H_{14}Cl_3O_3PS$, since the former represents chlorpyrifos that had been cleaved in half and the latter represents chlorpyrifos where nitrogen had been removed and the ring had been opened. This compound was present from the start of the reaction (Figure 4.18), which suggests it is formed from a photochemical reaction. Since it is not prone to photocatalytic reactions, it must be treated in a separate manner. The low starting concentration as well as toxicity studies ensuring that it is not a cholinesterase inhibitor suggests that lack of treatment is not a cause for alarm.

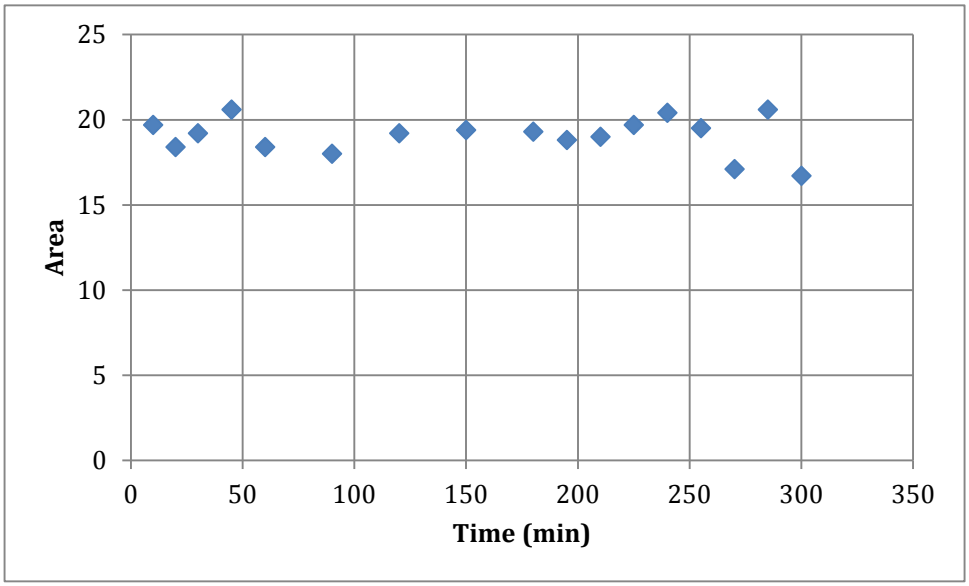

Figure 4.18: Persistence of $C_5H_2Cl_3NO$ over time.

The elution time for a given compound will not change between samples, regardless of reactor type or initial concentration of chlorpyrifos. This was verified by every experiment performed during this project, as chlorpyrifos always eluted around the same time. Likewise, intermediate generation shown in Figure 4.10 eluted between 8.9- 9.3 minutes, meaning the peak found at the time on the mass spectrogram for the CPC reactor with initial concentration of 0.5 ppm after 285 minutes in the reactor represented the same compound, proposed to be $C_8H_{12}Cl_3O_3PS$.

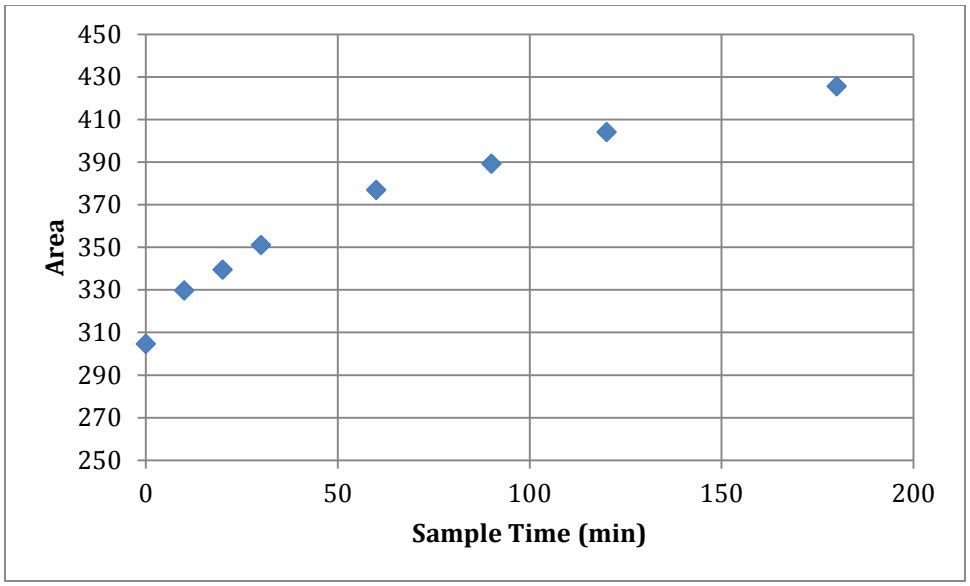

Figure 4.19 (repeated): Generation of intermediates during chlorpyrifos degradation in CPC reactor.

$C_9H_{13}ClNO_4PS$ and $C_6H_5NO_2$ were the proposed compounds found at an elution time of 12.8 min. The former is much more likely, as it again follows the known pathway for chlorpyrifos generation. The latter involves hydroxyls attacking the ring to remove chlorines. This intermediate appeared in the last thirty minutes of the 0.5 ppm CPC reactor experiment. Generation of this intermediate can be found in Figure 4.19.

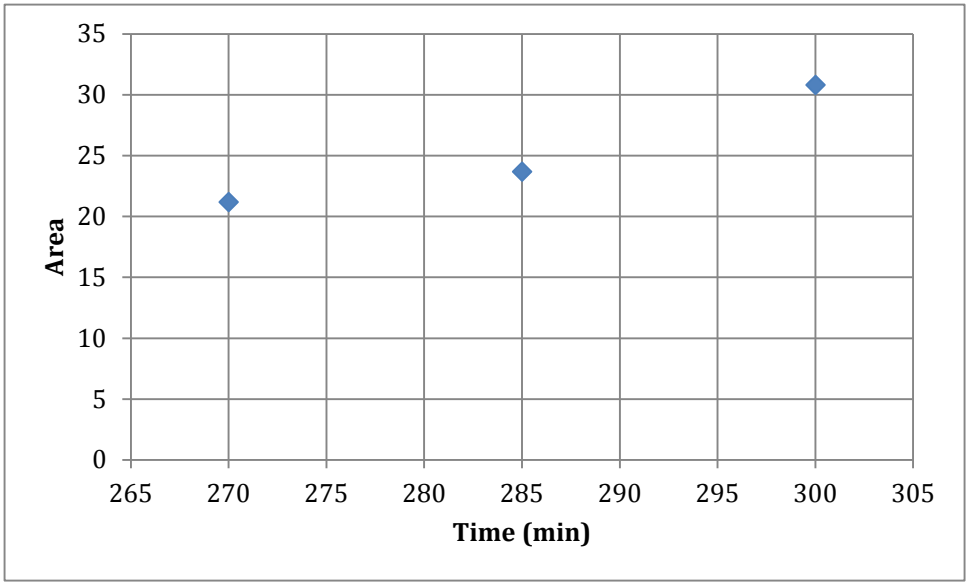

Figure 4.20: Intermediate generation.

While not found in the HPLC results, the LCMS detected a compound that was determined to be $C_9H_{11}Cl_3NO_4P$, chlorpyrifos oxon (Figure 4.20), which has a molecular weight of 334.5 g/mol. Due to the low concentration, it is understandable that it was not detected through HPLC. This compound has been proposed as both a photolytic [Kralj, 2007] and a photocatalytic [Konstantinou, 2002] reaction intermediate.

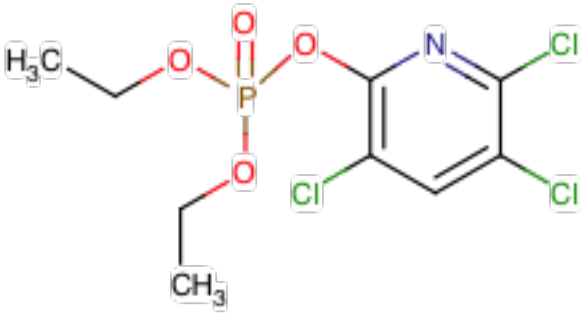

Figure 4.21: Chlorpyrifos oxon.

5.0 – Conclusions & Recommendations

The main difficulty encountered during experimentation was attempting to produce a reliable calibration curve for HPLC analysis. Without a reliable calibration curve, all results from HPLC proved difficult to analyze, hindering progress with the overall project. Initially, the calibration curve suggested that the intended 2 ppm chlorpyrifos solution was actually 5 ppm. It was found that measurements were off by a factor of 2.5, while the solubility limit of chlorpyrifos in water at room temperature and pressure is 2.0 mg/L. From these two things it was reasonable to infer that this concentration was impossible. The problem was resolved by using reliable concentrations from T=-30 min samples[1] from both the batch and CPC experiments. This provided accurate values for concentrations that could be used to create a more realistic and believable calibration curve.

HPLC results show that the majority of chlorpyrifos concentration is lost during the 30-minute darkness adsorption period, rather than during the photocatalytic reaction when ultraviolet lights were turned on. After this, however, the majority of additional chlorpyrifos degraded within two hours of treatment. The efficiency of the fixed film batch reactor during a two-hour treatment time turned out to be approximately 89% while the CPC reactor was also around 89%. Despite this fact, the fixed-film batch reactor was still preferable because it consistently produced more reliable results.

[1] T=-30 min sample time refers to a sample that was taken before any degradation or treatment had occurred.

5.1 – Glass Coating

The glass coating process was relatively simple with few places for error, but ultimately a varied coating thickness was observed. The variance in coating thickness of glass slides can be explained by both the well-used paintbrushes of varying sizes and the difference in coating technique among researchers. The following measures are recommended to minimize the variability in thickness and increase efficiency:

- A dip-coating process should be utilized to remove human error present from brush coating and ensure a uniform thickness.
- More repetition of thinner coating should be applied to increase the precision of coating thickness.

5.2 – HPLC and TOC Analysis

Many of the major hurdles faced during this project were a result of competition among different research groups for the use of analytical instrumentation. This was especially true of the HPLC. Additionally, inconsistencies from readings provided from both HPLC and TOC analyses were found at the beginning of this research. These skewed readings were a result of a lapse in regular equipment maintenance and could have been easily averted. To prevent this during future research the following suggestions should be taken into account:

- Either ensure that all testing being carried out for various research utilizes the same column or reserve the HPLC machine for the duration of a given experiment. Alternatively, all samples could be stored until the completion of research and be analyzed at one time, depending on sample stability.
- Take measures to ensure that all equipment has been calibrated and serviced before use.
- Pressure in the HPLC machine should be recorded and monitored for consistency. Tracking this data would aid in explaining fluctuations in elution times.

5.3 – LCMS Analysis

After careful evaluation of mass spectra received from LCMS analysis it was apparent that $C_5H_2Cl_3NO$ was present in solution as soon as degradation of samples containing chlorpyrifos began. It should also be noted that once formed, $C_5H_2Cl_3NO$ persisted throughout the entire treatment time. This implies that it is not treatable using UV/TiO_2 photocatalysis. Toxicity studies reveal that this compound is not an acetyl-cholinesterase inhibitor and is not a cause for alarm. A photochemical process would be needed to remove it from affected water. Chlorpyrifos-oxon was also detected in LCMS, but not HPLC due to concentrations below the HPLC detection limit. One of the more toxic possible compounds, chlorpyrifos-oxon is an acetyl-cholinesterase inhibitor. While the low concentration is promising, this compound is nearly as toxic as chlorpyrifos itself, necessitating removal in a real-world application.

Most compounds determined from LCMS did not have toxicity data readily available. To make an informed decision regarding effluent requirements for a full-scale system, further research should be conducted on the toxicity of each intermediate compound. An appropriate treatment level could then be identified to ensure toxic intermediates do not remain in effluent while simultaneously confirming that no new toxic intermediates are formed.

It is recommended that LCMS analysis conducted for samples with low concentration levels, such as the ones presented in this study, should be concentrated to ensure chemical compounds are detectable. Since the required sample volume for LCMS analysis is small, (approximately 150 μL), the concentration of samples can be achieved using a rotary evaporator or other concentration process, while still leaving ample sample volume.

5.4 – Slurry Reactor

Considering the potential environmental implications of TiO_2 suspended in discharged effluent, full-scale slurry reactors will not be a feasible option unless a TiO_2 particle recovery process follows treatment. Performing the slurry experiments was an inefficient use of time and resources as the data collected was not valuable for the batch or CPC reactor. The

concentration of catalyst in a slurry reactor is much higher than in fixed media reactors, meaning that attempting to determine reaction rate in this manner is not useful for the purposes of this study. The following recommendations should be taken into consideration when performing experiments to determine the degradation rate of chlorpyrifos:

- The reactor in use should be used to determine the specific darkness time.
- The same catalyst should be used for adsorption testing as will be used in all experiments.

5.5 – Fixed-Film Batch Reactor

HPLC results from experiments performed with varied concentrations of chlorpyrifos solution in the bench-scale fixed-film batch reactor produced exponential degradation results. Each experiment used different initial concentrations of chlorpyrifos and resulted in an average treatment efficiency of 89.3% in fewer than 4 hours. The following recommendations should be taken into consideration when performing experiments with chlorpyrifos in a bench-scale batch reactor:

- Temperature should be monitored by placing a probe in the sampling container to determine whether the difference over time is great enough to affect the reaction rate.
- Samples should be taken frequently within the 30 minute adsorption period during every experiment to find actual adsorption time and to see if that time remains the same with varied concentrations.
- Increase the number of slides in the reactor to increase the surface area of catalyst, thus accelerating the reaction. Adding slides will continue to be beneficial until adding more served to block other slides from UV exposure.
- Increase sampling frequency near the end of each experiment to better monitor the generation and degradation of intermediate compounds.

5.6 – CPC Reactor

The CPC reactor experiments failed to produce desirable results. Data collected from HPLC analysis showed that adsorption of chlorpyrifos onto the catalyst surface accounted for the greatest loss in concentration of the pesticide, with an ultimate degradation of 80.4%. With small starting concentrations of suspended chlorpyrifos in solution, it was difficult to quantify how much chlorpyrifos was actually degraded during oxidation because chlorpyrifos concentration in samples quickly dropped below the detection limit of the HPLC. Furthermore, TOC results showed a higher concentration of carbon than theoretically possible. Design of the CPC photoreactor at UNG may have contributed to the unfavorable results. The poor design of a clamp securing tubing from the pump to the photoreactor tubing led to leaks during treatment. Twice during experimentation, the tube connecting the pump to the reactor tube fell off due to the high pressure running. There was also the possibility that flow could be cut off entirely if the tubing was kinked or bent. Based on these issues the following experimental recommendations should be considered:

- Glass slides coated with titanium silicate solution produced much more favorable results for degradation and should be utilized in a CPC reactor.
- Ensure that the CPC reactor itself is easily operable. Consistency was extremely difficult due to a number of factors including:
    - Push-on fittings rather than threaded adapters,
    - An open air pump reservoir which was difficult to fill,
    - A valve used for operating the system that had no labeled flow ratings.
- All tubing used in a CPC reactor should be made of sturdy yet flexible material such as braided steel nylon tubing.
- A drainage valve should be installed at the lowest point in the system. This could be left open between flushing to ensure that the system is completely drained, as the reactor was cumbersome to clean.

5.7 – Possible Application

The pilot scale CPC reactor produced a useable efficiency, which paves the way for possible real-world applications. The civil engineering team created a full-scale reactor design which can be found in that MQP. A full-scale system would allow all runoff water from vineyards to be processed prior to being discharged to prevent pollution. This design takes into account:

- Concentration of pesticide applied
- Average rainfall
- Soil runoff
- Treatment efficiencies

5.8 – Future Research

The field of photocatalysis has the potential to rapidly expand, which will allow for the protection of natural water supplies from chemical contamination. Further research should consider:

- Using a variety of other catalysts to determine the most effective option.
- Determining methods of cheap TiO_2 slurry removal to allow use of slurry in treatment systems.
- Experimenting with additional pesticides to establish useable trends in degradation.
- Branching out from organophosphates to include a variety of plant protection products.

6.0 – Capstone Design

The research completed provided information for a real-world design utilizing CPC reactors and TiO_2 photocatalytic oxidation under solar radiation. The goal of this chapter is to present a CPC reactor design to treat storm water contaminated by chlorpyrifos, a fungicide used in many vineyards around the world. No treatment systems currently use TiO_2/UV oxidation, which means no recommended design parameters exist in literature beyond the pilot scale. Due to these constraints, it was decided that a feasibility study should be conducted to implement CPC reactors on a specific vineyard in the United States.

Newport Winery in Newport, Rhode Island was chosen as the implementation site for the CPC reactor design. "The Nunes Farm Vineyard, owned and operated by the Newport Winery is located on Aquidneck Island, one of the most desirable farming areas in the country. The micro-climate created by a combination of warm waters from the Gulf Stream to the south and moderating effects from Narragansett Bay provide a long, cool growing season ideal for developing the many complex flavors of wine" [Nunes, 2013].

The following chapter addresses key design parameters such as storm water retention requirements, temperature and precipitation forecasting, calculations for the average storm water runoff flow rate, retention pond design requirements, catalyst contact time, treatment efficiency, and CPC reactor design requirements. A cost analysis of each reactor used in the final design was conducted to determine the feasibility of using CPC reactors to treat storm water contaminated by chlorpyrifos. Conclusions and recommendations were made to determine the possibility of implementing reactors on the Nunes Farm.

All calculations pertaining to the design of this CPC reactor system can be found in Appendix J.

6.1 – About the Newport Winery

Newport Vineyards owns 50 acres of land located on Aquidneck Island, approximately 2 miles from the shore. The Nunes Farm vineyards are close enough to the water for protection against October frosts yet benefit from thermal heat off the land [Nunes, 1].

Figure 6.1: Nunes Farm

Pictured above are the Nunes Farm fields, covering an area of nearly fifteen and a half acres, or 62,650 m^2. With an elevation approximately 175 feet above sea level, the vineyard is one of the highest sites on Aquidneck Island. Grapes are harvested throughout October and early November, and winter months are spent pruning the vines for the upcoming season. The soil type is a deep, silty loam that retains enough water to resist the need for irrigation during summer months. The site also has drain tiles down every row of grapes, which collect excess water in a retention pond to the northeast [Nunes, 1].

6.2 – Temperature Forecasting

The temperature in Newport is consistent with the temperatures throughout the Northeastern United States. Winter months in the Northeast generally see temperatures that drop below freezing, meaning that agricultural production stops during this time. Therefore, it is necessary to determine the average monthly rainfall for months with an average temperature above freezing so that storm water runoff can be collected to undergo treatment via CPC reactors. From Figure 6.2 below, it can be seen that three months out of the year, (December, January, and February) have average temperatures below freezing and can therefore be discounted from this study.

Figure 6.2: Average Monthly Temperature for Newport, Rhode Island – 2012

[Average Weather for Newport RI, 2012]

6.3 – Monthly Precipitation Forecasting

In the past, the United States has been known for its abundant resources, especially its seemingly endless supplies of fresh water. In recent years, however, water resources have been strained and the possibility of longstanding droughts in many parts of the country have set in [Sawyer, 2012]. In order to combat this trend, agricultural storm water can be collected as runoff and treated in a variety of ways, including the use of advanced oxidation to degrade pollutant pesticides.

Figure 6.3: Average Monthly Precipitation for Newport, Rhode Island – 2012

[Average Weather for Newport RI, 2012]

Precipitation for Newport, RI is relatively consistent over the whole New England region. Figure 6.3 shows the average precipitation per month for the year of 2012. Excluding data from December, January, February, early March, and late November, average annual precipitation is approximately 747mm (30 inches) per year. A system capable of treating large storms with heavy rainfall is necessary as a design and safety precaution. The Rational Method was used to determine peak discharge volume of storm water runoff per month theoretically collected on the Nunes Farm.

The Rational Method is defined in Equation 6.1 below:

$$Q = C\ i\ A \qquad \text{[Equation 6.1]}$$

Where Q = Peak Discharge

C = Rational Method Runoff Coefficient (0.2-0.5)

i = Rainfall Intensity (747.35 mm/yr)

A = Drainage Area (62,650 m^2)

Due to below freezing temperatures during late November, December, January, February, and early March, the reactor design will take environmental constraints into account and not operate during these months. The storm water runoff calculations for both maximum and minimum discharge volume per month were determined as follows:

Maximum runoff: Q= (0.5)(747.35 mm/yr)(62,650m^2) = 19,838,123 L/yr

= 2962.7 L/hour

Minimum runoff: Q= (0.2)(747.35 mm/yr)(62,650m^2) = 7,935,249 L/yr

= 1185.1 L/hour

The average of the maximum and minimum volumes of storm water runoff was calculated to be 2073L/hr. The treatment capacity of the CPC rectors was designed to meet 2000L/hr, and the retention pond is to be capable of holding one month of heavy flow.

6.4 – Recommended Chlorpyrifos Dosing

According to the Villa Crop Protection Corporation, the recommended dose of Chlorpyrifos 480 EC for use in agriculture is 100g diluted with 245L of water per acre of land. That equals a concentration of 0.44 g/L of chlorpyrifos, or 26.6 mg per square meter. The most stringent guidelines regarding chlorpyrifos discharge into the environment are those set forth by the California Department of Fish and Wildlife for short-term exposure; 0.02 μg/L of chlorpyrifos in treated effluent [Siepmann and Finlayson, 2000]. The effluent produced after treatment in the CPC reactor system proposed must follow this regulation.

6.4.1 – Effluent Concentration

Unfortunately, the values listed above are not yet feasible goals for effluent concentrations. The treatment efficiency of the CPC reactor in this design will be approximately 89% over a two hour contact time, as determined experimentally. This efficiency level was further confirmed theoretically using the reaction rate constant and a retention time of two hours in the equation for a first order reaction, seen in Appendix J. Regardless of retention time, after two hours the treatment efficiency in the CPC reactor ceases to produce meaningful degradation, meaning that 89% is the maximum treatment efficiency that can be achieved using this CPC reactor configuration.

With this in mind, the average daily rainfall for RI must be compared to the amount of chlorpyrifos on the ground immediately following application. The average daily rainfall in RI is 4.8 mm per day [Weather, 2013]. Using this information, it is then possible to calculate the maximum expected concentration of chlorpyrifos in the system's treated effluent. Assuming that an equal amount of storm water and chlorpyrifos are absorbed into the soil it is then possible to determine how much chlorpyrifos is carried with storm water runoff. In this case the calculations are simplified because the maximum storm water runoff coefficient is 0.5 for the soil types identified on the Nunes Farm Vineyard, which implies that one half of the water and chlorpyrifos present are absorbed into the soil. Equation 6.2 shows the determination of chlorpyrifos concentration in storm water runoff.

$$\frac{0.0266\frac{g}{m^2}}{4.8\frac{L}{m^2}} = 0.0055\,\frac{g}{L} = 5.5\,\frac{mg}{L} \qquad \text{[Equation 6.2]}$$

Where 0.0266 = grams of chlorpyrifos per square meter of land

4.8 = Average daily rainfall per square meter of land

0.0055 = grams of chlorpyrifos per liter of runoff water

As previously discussed, the treatment efficiency of the system is 89% over two hours, meaning that the concentration of chlorpyrifos in solution can be reduced from 5.5 mg/L to 0.59 mg/L in the time span of two hours.

6.5 – Treatment System Specifications

6.5.1 – Retention Pond Specifications

The retention pond seen in the Northeast corner of Figure 6.1 collects storm water runoff from the Nunes Farm. Chapter 6.3 determined that the average rainfall for one year on Nunes farm is 747.35 mm per square meter of land. This information combined with storm water runoff calculations determined that the maximum discharge from storm water is equal to nearly 3000 L/hr or 2160 m^3 per month. If a one-month retention time in the pond is desired, then the required volume of the pond would be equal to the average monthly runoff. Since the surface area of the pond is approximately 1550 m^2 as determined through the use of Google Earth, the required depth can be obtained by finding the quotient of volume and surface area, yielding a depth of 1.4 m. Therefore, an average minimum depth of 1.5 m is recommended for the retention pond to ensure it can hold one month of runoff. This large retention time would also allow the system to be shut down for maintenance purposes, including dredging of the retention pond itself, replacement of catalyst in CPC reactors, and pump repair should failure occur. Lastly, the storm water being treated contains chlorpyrifos, a hazardous chemical that cannot leave the system until after treatment has occurred. To achieve this, a high density polyethylene liner will be put in place during initial construction to prevent any chlorpyrifos loss from the system, and consequent contamination of the surrounding environment. Table 6.0 shows the final specifications for the retention pond.

Table 6.0: Retention Pond Specifications

Surface	1550 m^2
Required Depth	1.5 m
Volume	2326.5 m^3
Flow	2160 m^3/month

6.5.2 – Hazardous Waste Disposal

This retention pond also doubles as a clarifying system, removing large colloidal particles and other debris from runoff that could cause potential damage to CPC reactors. Furthermore, this clarification system will serve to reduce turbidity, which will increase the efficiency of the photocatalytic oxidation process by allowing greater penetration of solar radiation into the CPC reactor tubes. One drawback to this system is that solids will accumulate at the bottom of the retention pond and will need to be removed from time to time during maintenance. Due to the low solubility level of chlorpyrifos in water (2ppm), it can be inferred that some of the chlorpyrifos in solution will have an affinity for suspended solids in the retention pond. That being said, the sludge accumulating at the bottom of the retention pond will be contaminated with chlorpyrifos and should be treated as hazardous waste. Soils contaminated with chlorpyrifos can be dealt with in a number of ways, including incineration, adsorption, or landfilling [ASTDR, 2011]. For further information on disposal of soils containing chlorpyrifos, refer to Appendix K. It is recommended that the retention pond be scraped annually following the harvest season to remove all accumulated solids. This will ensure that the system has already been flushed and is ready for use the following year.

6.5.3 – CPC Reactor Specifications

The CPC reactor design is the last phase of treatment before release back into the environment. It was determined from the experiments run that CPC reactors had an efficiency of approximately 89%. The CPC design proposed uses commercial grade TiO_2 imbedded in porous paper that can be easily wrapped around metal holders and inserted into each glass tube as described in chapter 3.7.1. The parameters below describe the specifications of the CPC reactor design for the Nunes Farm. All calculations supporting these values shown in Table 6.1 can be seen in Appendix J.

Table 6.1: CPC Reactor Design Specifications

Flow Rate	47.52 m^3/d (2000 L/H)
Retention Time	2 hours
Tube Diameter	10cm
Number of Tubes	10
Height	2 m
Length	3m
Volume	235.6 L
Number of Reactors Required	17
Inclination Angle	37^o

3-Dimensional View

Figure 6.4: 3D View of CPC Reactor Design

Pictured above in Figure 6.4 is the proposed CPC reactor system rendered in 3 dimensions.

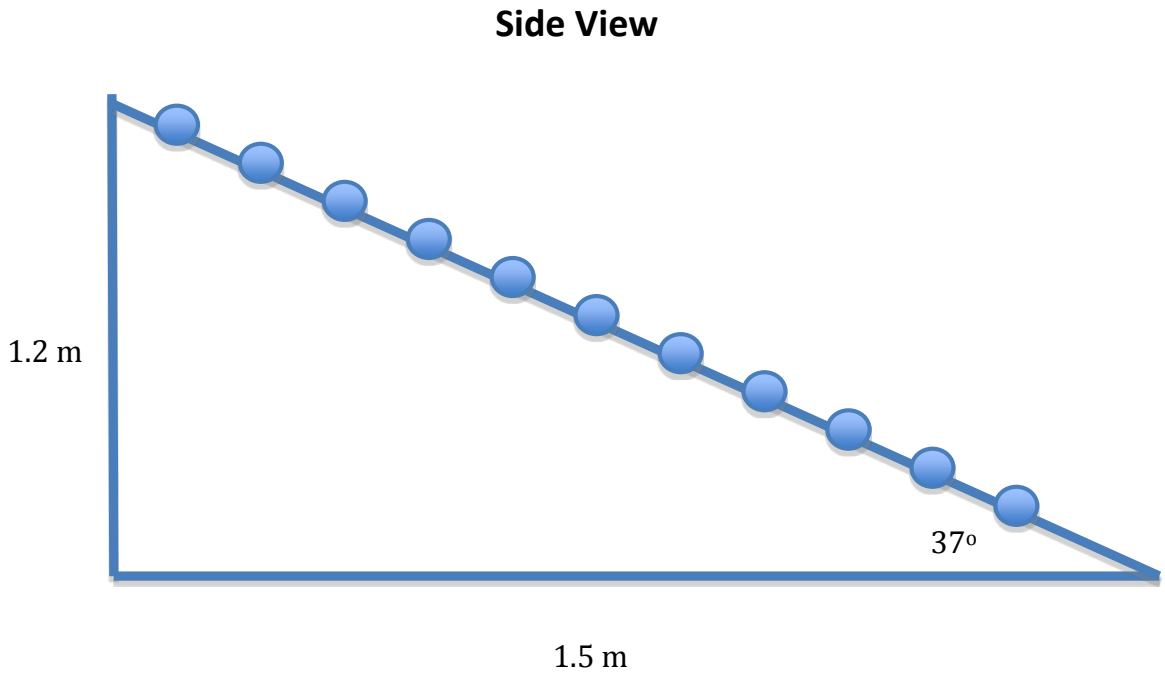

Figure 6.5: Side View of CPC Reactor Design

The CPC reactor pictured above in Figures 6.4 and 6.5 is similar to what was used to perform experiments at UNG. The only modification is that the inclination angle was changed to 37^{o}C to emulate the CPC system currently used in Almeria, Spain.

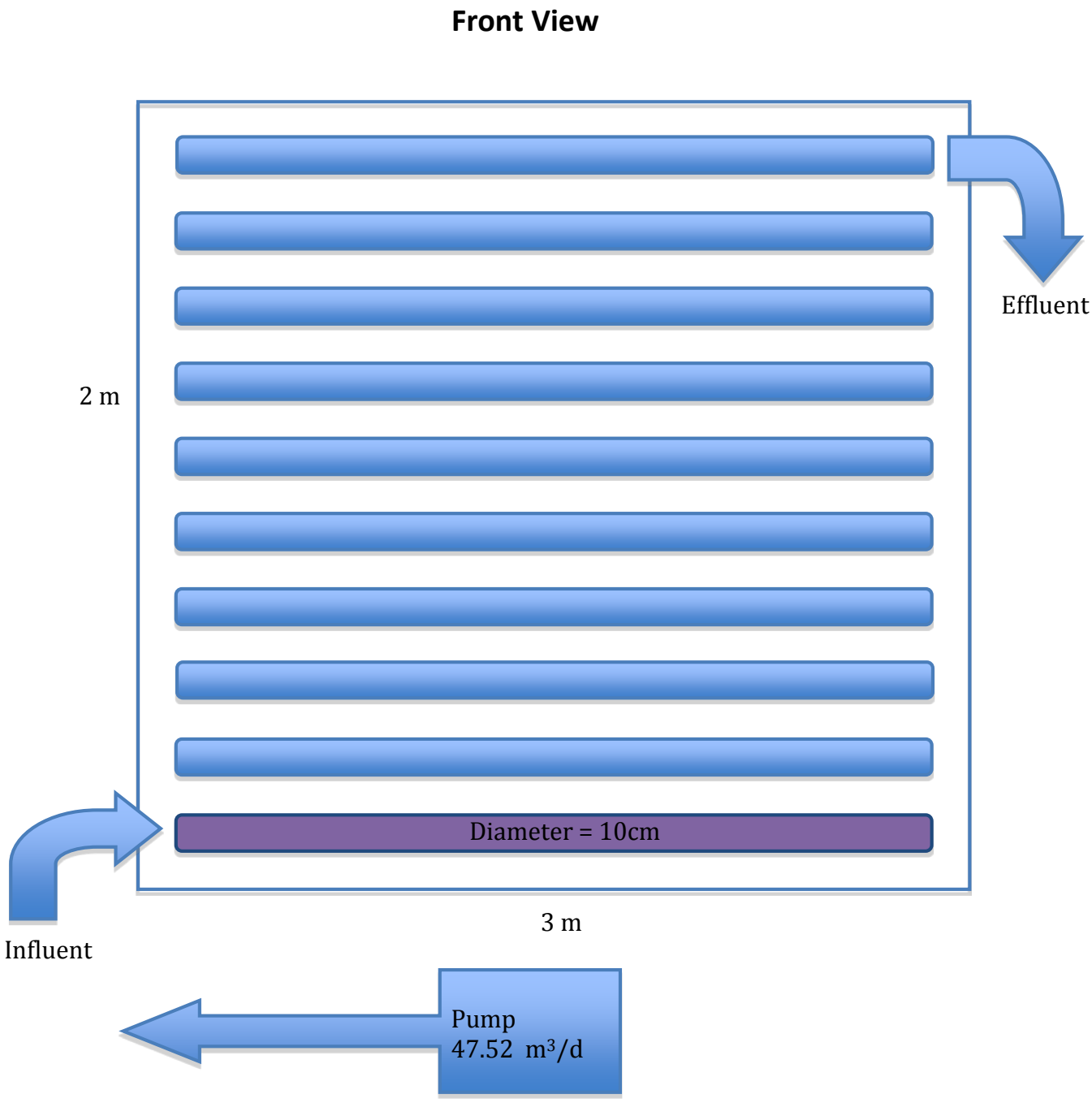

Figure 6.6: Front View of CPC Reactor Design

Figure 6.6 above shows the CPC reactor design proposed for the Nunes Farm vineyard. The pump leading into each reactor features a flow of 47.52m^3/d. A modification made to the system is a change in the tube diameter from 5cm to 10cm. The influent tube, colored in purple, receives storm water from the retention pond. The water then flows through all tubes

before leaving the top tube as effluent. The water then gets pumped into the bottom influent tube of a second CPC reactor and so on, until the water has passed through all 17 reactors and is discharged after 2 hours.

6.6 – Materials and Cost Analysis

6.6.2 – Retention Pond Materials

A high density polyethylene liner will be used in the retention pond. The price of high density polyethylene per square feet in $0.52 given the 5085 square feet required. Therefore, a total price of $2,645.00 is necessary for the lining of the retention pond [Anjon, 2014].

6.6.2 – Main Pump Requirements

The entire treatment system has a maximum flow of nearly 2000 liters per hour. An appropriately sized pump must be capable of handling this flow and more to account for a margin of safety. This pump should be submergible and capable of pumping debris (leaves, twigs, large particles, etc…). A pump meeting this description can be purchased for approximately $600 [Owiecki, 2013] at any reputable supply warehouse. It should be noted that pumps used for individual reactors would not need to be capable of handling large debris and as a result would be much cheaper.

6.6.3 – CPC Reactor Materials

Table 6.2 – CPC Reactor Cost Analysis

Material	**Price Per Unit**	**Quantity**	**Cost Per Reactor**
1” x 1” x 1/8” x 10’ Angle Iron [Depot, 2013]	$10.80	8	$86.40
1” x 1” x 1/8” x 5’ Angle Iron [Depot, 2013]	$8.64	14	$120.96
3 m x 10 mm ID borosilicate glass tubing [Science Co., 2013]	$333.00	10	$3330.00
2000 L/Hr Submersible Pump	$153.00	1	$153.00
		Total Reactor Cost	**$3690.36**

In order for this system to handle the predicted flow, ten reactors will be required. At $3690.36 per reactor (Table 6.2), the total cost of all seventeen reactors would be $62,736.12.

6.6.4 – Overall Cost of System Implementation

Assuming a water treatment industry average cost of construction to be 1.5 times the cost of materials, the total construction cost of the project can be estimated at $95,004.18, shown in Table 6.3.

Table 6.3 – Total Cost Analysis

Unit	**Cost**
Retention Pond Lining	$2645.00
Main Collection Pond Pump (1)	$600.00
Reactors (17)	$62,736.12
Construction	$98,971.68
Total Cost	**$164,952.80**

6.7 – Feasibility Discussion

The proposed CPC reactor design is intended for use on the 15-acre Nunes Farm vineyard. The total cost of implementation of the system is estimated to be $164,952.80. Featuring an 89% chlorpyrifos treatment efficiency after a two hour retention time, the efficiency of this system is backed up by the theoretical degradation kinetics of chlorpyrifos from batch reactor experiments highlighted Chapter 4.5. Complete mineralization cannot be achieved with higher contact times, as proven through experimental results also highlighted in Chapter 4.6. Although 89% removal from solution reduces initial concentrations of 5.5 mg/L down to 0.59 mg/L, this concentration is still vastly above standards set forth by the California Department of Fish and Game at 2.0 ppt. However, it is worth noting that to achieve these levels, 99.99% treatment efficiency would be required given an influent concentration of 5.5 mg/L.

Over time, there will undoubtedly be improvements to the design of CPC reactors and UV/TiO_2 photocatalytic oxidation in general. These improvements will likely yield greater treatment efficiencies and should be considered for future work. The treatment system proposed in this design is only one of many possibilities that was considered using the UV/TiO_2 oxidation process. Since greater contact time with the catalyst under UV radiation ceased to yield higher treatment efficiencies after two hours, it was unnecessary to design a system with a longer contact time. If new technologies present data that indicates a longer contact time is desirable, then it would be worthwhile to investigate the possibility of using a system that utilizes influent recycling. This type of design could serve to eliminate the need to add costly new reactors to the treatment system proposed in this report.

References

Abhijit, V. (2005). Advanced oxidation process. *Res Chem Intermed* , 33:359. Ballesteros Martín, M. M., Sánchez Pérez, J. A., Casas López, J. L., Oller, I., & Malato Rodríguez, S. (2009). Degradation of a four-pesticide mixture by combined photo-Fenton and biological oxidation. *Water Research*, 43, 653–660.

Anjon , M. (2014, January 20). *Hdpe pond and containment*. Retrieved from http://02d9421.netsolstores.com/largewatercontainment.aspx

ASTDR. Center for Disease Control, Agency for Toxic Substances and Disease Registry. (1998). *Public health statement chlorpyrifos*. Retrieved from website: http://www.atsdr.cdc.gov/ToxProfiles/tp84-c1-b.pdf

Average Weather for Newport, RI (2012). Retrieved from http://www.weather.com/weather/wxclimatology/monthly/graph/USRI0040.

Braslavsky SE (2007), Glossary of terms used in photochemistry – 3rd ed. Pure Appl. Chem. 79: 293-465.

Černigoj, U., Štangar, U. L., Trebše, P., Krašovec, U. O., & Gross, S. (2006). Photocatalytically active TiO< sub> 2</sub> thin films produced by surfactant-assisted sol–gel processing. *Thin Solid Films*, *495*(1), 327-332.

"Chlorpyrifos." PESTANAL®, *Analytical Standard*. N.p., n.d. Web. 6 Nov. 2013. Retrieved fromhttp://www.sigmaaldrich.com/catalog/product/fluka/45395?lang=en&region=US.

Cho C. M., Mulchandani A., Chen W. (2002). Bacterial cell surface display of organophosphorous hydrolase for selective screening of improved hydrolysis of organophosphate nerve agents. *Appl Environ Microbiol* , 68:2026.

Chong M. N., Jin B., Chow C. W.K., Chris S. (2010). Recent developments in photocatalytic water treatment technology: A review. *Water research*, 44: 2997-3027.

Compound parabolic collector (CPC) photoreactors. (2013). Unpublished manuscript.

Coronado JM and Hernandez-Alonso MD, " The Keys of Success: TiO_2 as a Benchmark Photocatalyst", in J.M. Coronado, F. Fresno, M.D. Hernandez-Alonso, R. Portela (Eds.), "Design of Advanced Photocatalytic Materials for Energy and Environmental Applications", Springer (London), 2013, ch. 5.

Depot, M. (2013, DECEMBER). *A36 structural steel angle*. Retrieved from http://www.metalsdepot.com/products/hrsteel2.phtml?page=angle

Devi L. G., Murthy B. N., Kumar S. G. (2009). Photocatalytic activity of V5?, Mo6? and Th4? doped polycrystalline TiO2 for the degradation of chlorpyrifos under UV/solar light. *J Mol Catal A ,* 308:174.

Fastenal. (2013, DECEMBER). *1/2" dia. grade 60 rebar*. Retrieved from http://www.fastenal.com/web/products/details/0999867

Fogler H. S. (1999). Elements of Chemical Reaction Engineering: Chapter 10: Catalysis and Catalytic Reactors. *Prentice-Hall PTR Inc*., 581–685.

Greenville, B. (2013, DECEMBER). *Greenville ready mix concrete*. Retrieved from http://www.greenvilleconcrete.net/index.html

Harada K., Hisanaga T., Tanaka K. (1987). Photocatalytic degradation of organophosphorous insecticides in

aqueous semiconductor suspensions. *New J Chem ,* 11:597.

Herman J. M. (1999). Heterogeneous photocatalysis: fundamentals and applications to the removal of various types of aqueous pollutants. *Catal Today,* 53:115.

Jacoby, Bill, Dr. "Photocatalytic Oxidation." Penn State Department of Architectural Engineering. Penn State, n.d. Web. 03 Oct. 2013.

Miguel, N., Ormad, M. P., Lanao, M., Ibarz, C., & Ovelleiro, J. L. (2007, October). Pedro Cerbuna (Chair). *Effectiveness of Advanced Oxidation Processes with O_3 and O_3+H_2O_2 in Pesticides Degradation*. IOA Conference and Exhibition, Valencia, Spain. Retrieved from http://www.chimia.it/pdf/Paper 2.04.pdf

Nunes, Paul. "Vineyard Overview." *Newport Vineyards*. N.p.. Web. 10 Dec 2013. <http://www.newportvineyards.com/overview.htm>.

Owiecki, J. (2013, DECEMBER). *Power equipment direct*. Retrieved from http://www.sumppumpsdirect.com/PHCC-Pro-Series-S3100-Sump-Pump/p6572.html.

"Photodynamic Therapy: An overview." *The Photochemistry Portal*. N.p., n.d. Web. 13 Nov. 2013. http://photochemistryportal.net/home/wp-content/uploads/2009/09/tio2_overall_schematic.png.

Quiroz M. A., Bandala E. R., Martínez-Huitle C. A. (2011). Advanced Oxidation Processes (AOPs) for Removal of Pesticides from Aqueous Media, Pesticides - Formulations, Effects, Fate, Prof. Margarita Stoytcheva (Ed.), ISBN: 978-953-307-532-7.

Sawyer, Evan. *Water Shortage in the US*. Report. 8 Feb. 2012. Print.

Science Co., I. (2013, DECEMBER). *Borosilicate clear glass tubing*. Retrieved from http://www.sciencecompany.com/Pyrex-Glass-Tubing-8mm-OD-15-inch-Pk2-P16257C2634.aspx.

Siepmann, S., and Finlayson, B., 2000, Water quality criteria for diazinon and chlorpyrifos: California Department of Fish and Game Administrative Report 00-3, 59 p.

Stoytcheva M. (Ed.), ISBN: 978-953-307-532-7, InTech, Available from: http://www.intechopen.com/books/pesticides-formulations-effects-fate/advanced-oxidation-processes-aops-forremoval-of-pesticides-from-aqueous-media

Weather, S. (2013, DECEMBER). *Historical weather: Providence Rhode Island*. Retrieved from http://weatherspark.com/history/31334/2013/Providence-Rhode-Island-United-States

Zapata A., Malato S., Sanchez-Perez J. A., Oller I., Maldonado M. I. (2010). Scale-up strategy for a combined solar photo-Fenton/biological system for remediation of pesticide-contaminated water. *Catalysis Today*, 151, 100–106.

Appendix A – Equipment

Equipment	Brand	Series
Stir Plate (for solution)	IKA RH	Basic 2
Stir Plate (for solution)	IDL GmbH & Co. KG	
Sonicator	Pio Iskra	Sonis 4
Hair Dryer	Braun	Swing 1200
Oven	Bosio	
HPLC	Agilent	1100
UV-Vis Spectrophotometer	Hewlett-Packard	8453
CPC pump	Modentic and Corp	
Batch Reactor Pump	Heidolph	Pumpdrive 5206
pH Meter	Hanna Instruments	HI 8417
Centrifuge	Eppendorf	MiniSpin
Stir Plate (for short exp.)	IKA Labortechnik	RH Basic
Stir Plate (for short exp.)	IDL GmbH & Co. KG	MEA 30
UV Bulbs	Osram Eversun	
Catalyst-embedded paper	Ahlstrom	paper BR 1048:75
TOC Analyzer	Analytikjena	Multi N/C 3100
Stir Plate (for 397T)	IKAMAG	
HPLC Column	BIA Separations	0506015R

Figure A-1: Stir plates used for short experiments.

Stir plates used for making solution: when preparing different concentrations of chlorpyrifos solution, the beakers mixed on either a IKA RH Basic 2 or a IDL GmbH & Co. KG magnetic stir plate. For this process, the heating element was used in both plates to aid in the process of making the solution.

Figure A-2: Sonicator.

Sonicator: located in a lab hood, this Pio Iskra Sonis 4 sonicator was primarily used to assist in the making of varying concentrations of chlorpyrifos solution. It was also used during the preparation of the titanium silicate solution used to coat the glass slides for the UV-photocatalytic batch reactor.

Figure A-3: Hair dryer.

Hair dryer: this Braun Swing 1200 hair dryer was used to assist in the drying process after the glass slides for the batch reactor were coated with the titanium silicate catalyst solution. This was done prior to placing the slides in the oven.

Figure A-4: Oven.

Oven: after using the hair dryer to initially start to dry the coated slides, the slides were then placed into a Bosio oven to complete the drying processing.

Figure A-5: HPLC.

HPLC: samples taken from short experiments and experiments done with both reactors were run through this Agilent 1100 high pressure liquid chromatography (HPLC) machine to determine the components of the samples and see how much, if any, of the pesticide was present in each sample.

Figure A-6: HPLC Column.

HPLC column: the column used was manufactured by BIA Separations and utilizes Kromasil as a packing material, with serial number 0506015R.

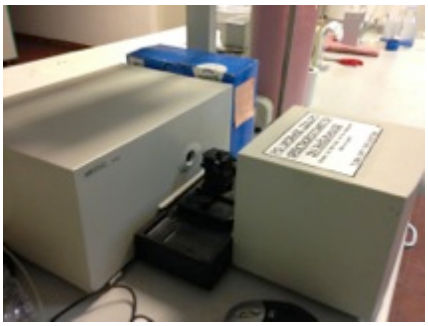

Figure A-7: UV-Vis Spectrophotometer.

UV-Vis spectrophotometer: this Hewlett-Packard 8453 UV-visible light spectrophotometer was used to decide which was the optimal wavelength to run during HPLC analysis.

Figure A-8: CPC pump.

CPC pump: the 230V pump for the CPC reactor, manufactured by Modentic and Corp, was used to pump the contaminated water through the reactor to be treated.

Figure A-9: Batch reactor pump.

Batch reactor pump: this Heidolph Pumpdrive 5206 pump was used for the bench-scale UV-photocatalytic batch reactor to pump the contaminated water through the reactor to be treated.

Figure A-10: pH meter.

pH meter: this HI 8417 pH meter, manufactured by Hanna Instruments, was used to measure the pH of the samples taken from both reactors.

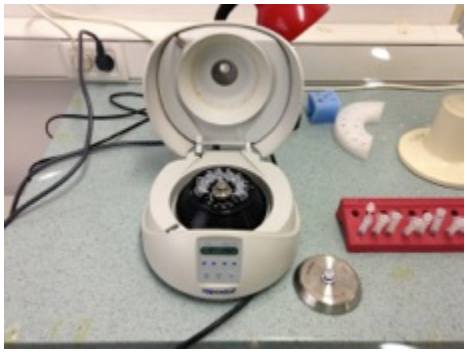

Figure A-11: Centrifuge.

Centrifuge: to assist with the filtering process during the short experiments, the samples taken were first put into this Eppendorf MiniSpin centrifuge before being filtered into HPLC vials.

Figure A-12: Stir plates used for making solution.

Stir plates used for short experiments: when performing the short experiments inside the darkness box, the two beakers of solution were each placed on magnetic stir plates. The stir plate on the left was an IKA Labortechnik RH Basic and the one on the right was a IDL GmbH & Co. KG MEA 30, both equipped with the ability to attract a magnetic stir bar to the center of the plates for optimal mixing. Each stir plate also has a heating element that operates between zero and 250 °C, however this function was not utilized for this particular experiment.

Figure A-13: UV bulbs.

UV bulbs: the Osram Eversun 100W UV bulbs were used in both reactors.

Figure A-13: Catalyst-embedded paper.

Catalyst-embedded paper: the Ahlstrom paper BR 1048:75 was wrapped around steel holders an place inside the CPC reactor chamber.

Figure A-14: TOC analyzer.

TOC analyzer: to determine the organic carbon of samples after treatment, the samples were run through an Analytikjena Multi N/C 3100 TOC analyzer.

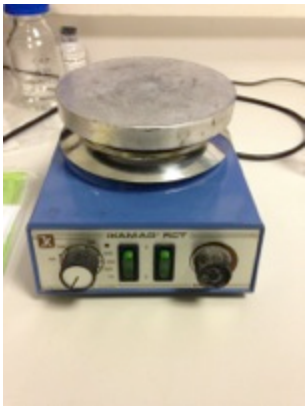

Figure A-15: Stir plate used to make 397T solution.

Stir plate used to make 397T solution: when creating the 397T solution used to coat the glass slides, the solution was mixed on a magnetic stir plate manufactured by IKAMAG.

Appendix B – Chlorpyrifos in Acetonitrile Solution

B.1 – Preparing Chlorpyrifos in Acetonitrile

1.) 100 mL of pure acetonitrile was measured in a 100 mL volumetric flask.

2.) The 100 mL of acetonitrile was added to a 1000 mL Erlenmeyer flask.

3.) Approximately 500 mL of double-deionized water was added to the 1000 mL Erlenmeyer flask. This is the solvent.

4.) 10 mg of chlorpyrifos was weighed and added to the solvent in the Erlenmeyer flask.

5.) A magnetic stir bar was added to the Erlenmeyer flask and the flask was covered with parafilm.

6.) Using a hot plate equipped with a magnetic stirrer, the solution was stirred at low heat (approximately 63 °C) for 15 minutes.

7.) The Erlenmeyer flask containing the solution was then placed in a sonicator for 15 minutes.

8.) Steps 4 and 5 were repeated alternately for approximately 3.5 hours.

9.) The solution was left on the stirring plate over night at high speed with no heat.

10.) After 16 hours of stirring, the solution appeared to be homogenous and all solids had dissolved.

11.) The solution was removed from the stirring plate and poured into a 1000 ml volumetric flask.

12.) The volumetric flask containing the solution was then filled to the 1000 mL mark using double deionized water.

This process was repeated whenever it was necessary to prepare more solution. If lower concentrations were required this solution was prepared and diluted with 10% acetonitrile solvent as necessary.

B.2 – Discussion & HPLC Results for Acetonitrile

Concentrations of chlorpyrifos higher than 2.0 mg/L at 25^{O}C are not water soluble. Originally, the HPLC's detector was in need of service and could not detect the compound at any concentration that was water soluble. Consequently, higher concentrations of chlorpyrifos at 10 ppm, 7.5 ppm, and 5 ppm were created for detection purposes. Acetonitrile was chosen to combine with double deionized water as a solvent, as it was determined that it would not interfere with the reaction and would not add additional peaks into the chromatograms. A 10% acetonitrile solution was created to ensure results as close as possible to a water- chlorpyrifos solution could be obtained (see Appendix B.1 for procedure). By running solutions with higher concentrations, it was possible to precisely measure larger amounts of solid chlorpyrifos, leading to a more accurate concentration in solution and, in turn, more precise results from the HPLC analysis. When running samples with acetonitrile solvent it could be seen that there were peaks between elution times of 2 and 4 minutes corresponding to acetonitrile contained in the solvent. This was useful later in the analysis when attempting to verify that solutions of lower concentration were actually being prepared accurately.

Once it was determined that the HPLC was in need of cleaning and had been serviced, however, the detection limit allowed for concentrations within the solubility of water. With the knowledge that the 10 ppm solution was reliable, it was easy to ensure that the 2 ppm and lower concentrations were accurate by using a simple ratio of area versus concentration. Concentrations of 2 ppm, 1.5 ppm, 1.0 ppm, and 0.5 ppm were chosen for experimentation. These lower concentrations were much closer to the actual concentration and composition of the runoff water from vineyards that would be treated, allowing for analysis of real-world scenarios.

The TOC (Total Organic Carbon) analyzer measured organic carbon and nitrogen. Since the solvent being used, acetonitrile, consists of both elements, the TOC could not accurately analyze the total organic carbon in the required samples. The samples created in double

deionized water at concentrations of 2 ppm chlorpyrifos and lower could be run through the TOC analyzer without interference from solvent.

The following table shows the results gathered from the HPLC analysis of the samples from the 10 ppm chlorpyrifos batch reactor experiment:

Table B-1: 10 ppm batch reactor experiment.

Sample Time	Elution Time	Area	Elution Time Peak A	Area
-30	9.825	1578.4	N/A	N/A
0	9.834	899.5	N/A	N/A
5	9.902	691.4	N/A	N/A
10	9.994	737.5	N/A	N/A
20	10.006	649.1	N/A	N/A
30	10.175	562.5	N/A	N/A
60	10.454	415.7	5.897	8
120	10.624	209.9	5.989	11.4
180	10.987	11.3	6.185	13.8
240	10.981	63.2	6.19	15

After analyzing these HPLC results, a graphical representation of the data was created to show concentration vs. time, displayed in the graph below:

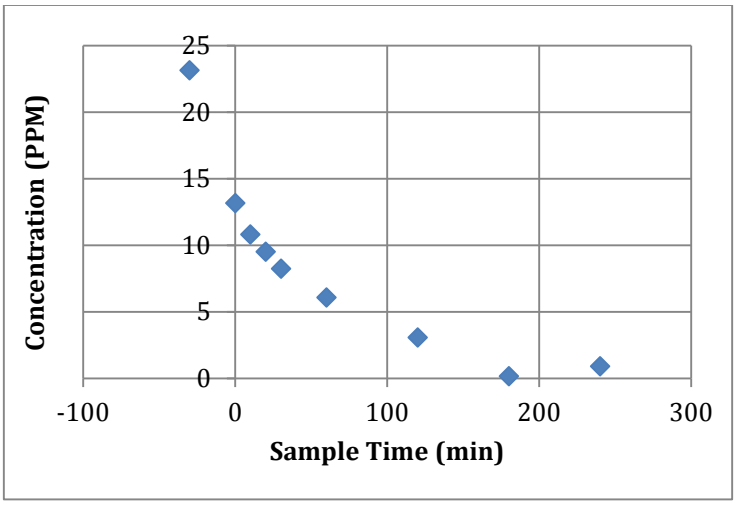

Figure B-1: 10 ppm batch reactor degradation.

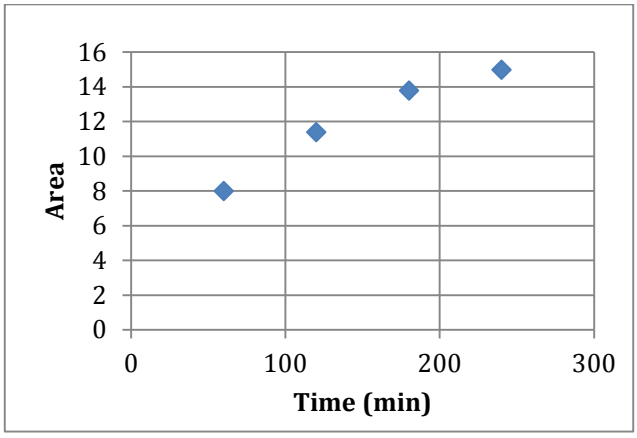

Figure-B 2: 10 ppm peak A formation.

To determine reaction order and rate constant, the raw data from this run was used to create the values displayed in the table below:

Table B-2: 10 ppm rate determining data.

Sample Time	ppm	C/C0	ln -C/C0
-30	23.1375883		
0	13.1856695	1	0
10	10.8109297	0.81989994	0.19857297
20	9.515084	0.72162312	0.32625227
30	8.24562432	0.62534742	0.46944792
60	6.09369961	0.46214564	0.77187521
120	3.07690052	0.23335186	1.45520783
180	0.16564543	0.01256253	4.37703633
240	0.9264417	0.07026126	2.65553475

The data from the table above was used to produce a graph of time vs. –ln(d[CP]) so the graph would be linear. A line of best fit was created for this graph, pictured below:

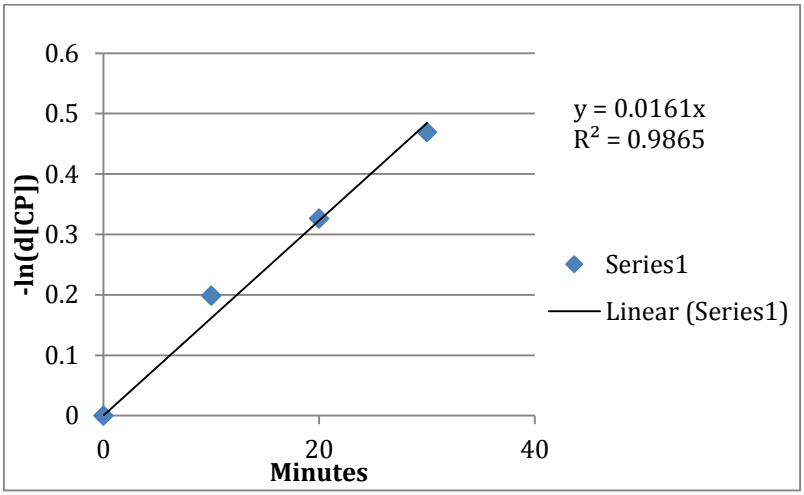

Figure B-3: 10 ppm sample time vs. -ln(d[CP]).

The following table shows the results gathered from the HPLC analysis of the samples from the 7.5 ppm chlorpyrifos batch reactor experiment:

Table B-3: 7.5 ppm batch reactor experiment.

Sample Time	Elution Time	Area	Elution Time Peak A	Area	Elution Time Peak B	Area	Elution Time Peak C	Area
-30	9.892	442	8.962	12.7				
0	9.904	333.3	8.975	29.5				
5	9.946	356.5	8.998	12.4	10.514	15.9	12.708	60.3
10	10.591	339.9	9.178	18.1			12.337	13.2
20	9.923	265.5	8.99	10.28				
30	9.902	240.6						
60	9.908	129.5						
120	9.914	60.4						
180	9.906	34.9						
240	9.89	38.9	8.958	11.9				

After analyzing these HPLC results, a graphical representation of the data was created to show concentration vs. time, displayed in the graph below:

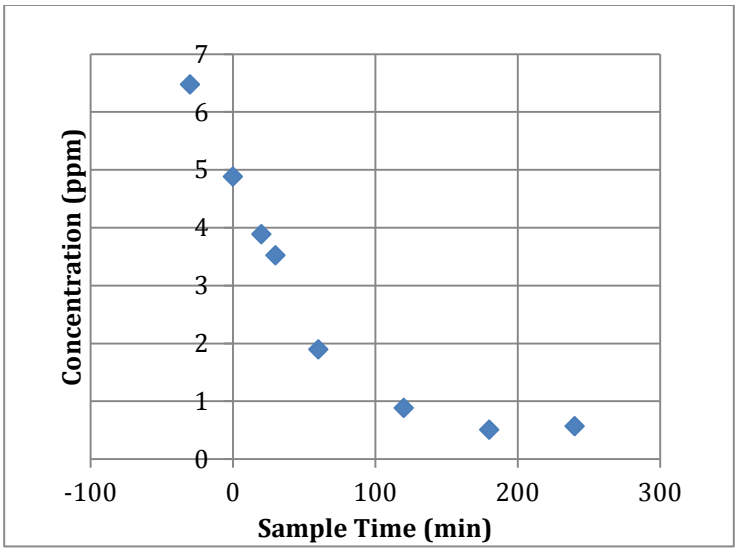

Figure B-4: 7.5 ppm batch reactor degradation.

When these samples were analyzed using the HPLC, additional peaks appeared along with the chlorpyrifos peaks. A graph of area vs. elution of these peaks is pictured below:

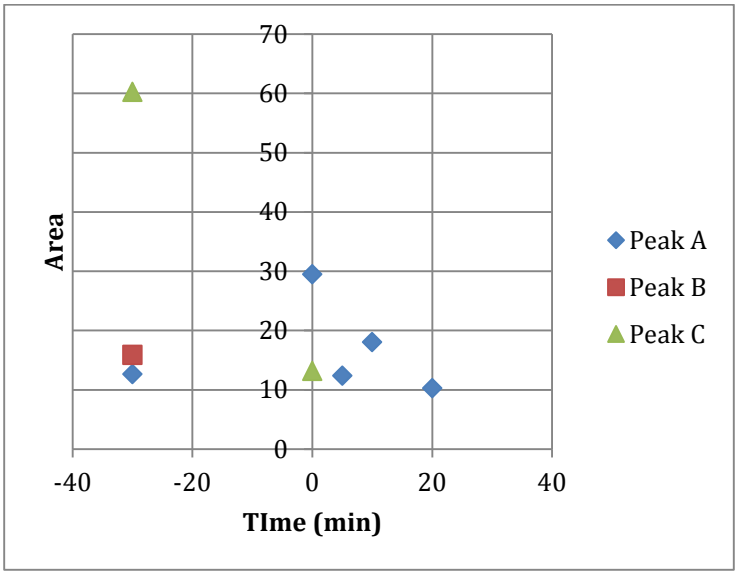

Figure B-5: 7.5 ppm peak A formation.

To determine reaction order and rate constant, the raw data from this run was used to create the values displayed in the table below:

Table B-4: 7.5 ppm rate determining data.

Sample Time	ppm	C/C0	ln (-C/C0)	r0
0	4.88580726	1	0	
20	3.89193468	0.797	0.22742814	0.05
30	3.52692838	0.722	0.32590718	0.068
60	1.89832596	0.389	0.9453621	0.149
120	0.88539682	0.181	1.70805388	0.2
180	0.51159518	0.105	2.25655616	0.219
240	0.57023073	0.117	2.14804873	0.216

The data from the table above was used to produce a graph of time vs. –ln(d[CP]) so the graph would be linear. A line of best fit was created for this graph, pictured below:

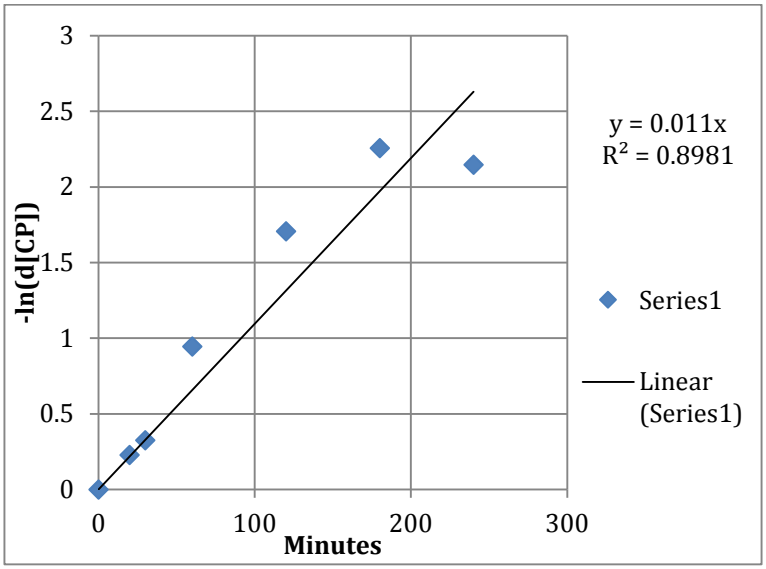

Figure B-6: 7.5 ppm sample time vs. ln(d[CP]).

The values produces in the table below were used to produce a graph to find α:

Table B-5: Data to determine alpha.

dCa	dt	ln(-dCa/dt)	ln(Ca)
-1.5934211	30	-2.935314	1.59
-0.9938726	20	-3.0018785	1.36
-0.3650063	10	-3.3104257	1.26
-1.6286024	30	-2.9134751	0.64
-1.0129291	60	-4.0814983	-0.1
-0.3738016	60	-5.0783746	-0.7

A line of best fit was created for this graph of ln(-dCa/dt) vs. ln(Ca), shown below, and the slope of this line, α, was found to be 0.9399:

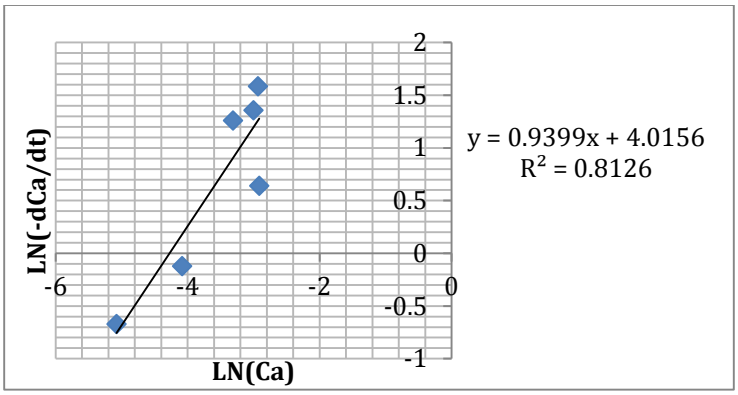

Figure B-7: Finding alpha.

Using the newly determined value of α and the negative values of dCa/dt over time, the reaction rate, k, was found and tabulated below:

Table B-6: Data to determine reaction rate.

neg. dCa/dt	time	k	
0.053114036	0	0.00217202	1
0.049693629	20	0.00297483	2
0.036500630	30	0.00419180	3
0.054286747	60	0.00221997	4
0.016882152	120	0.00035987	5
0.006230027	180	0.00013280	6
-0.000977259	240	-0.00002083	7

These k values over time were graphed below:

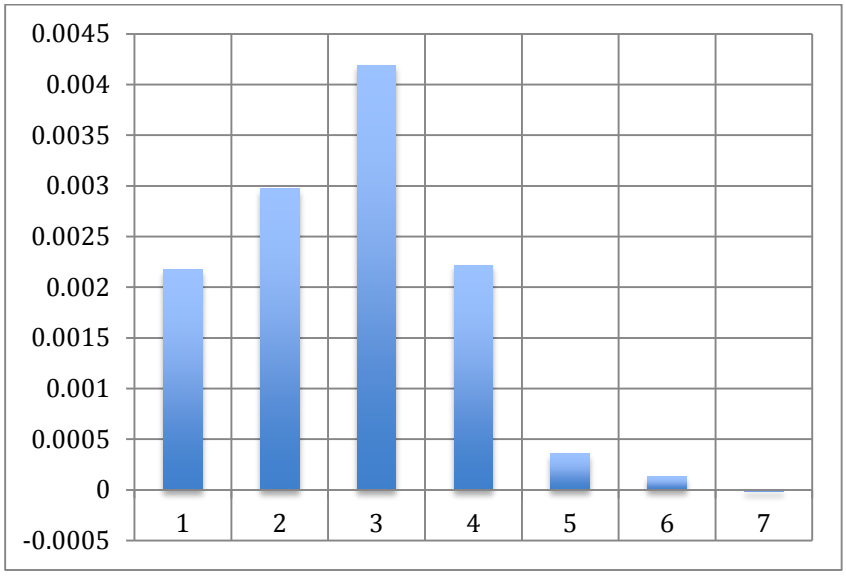

Figure B-8: Reaction rate k vs. time.

Below are the results and degradation curves obtained from the 5 ppm chlorpyrifos batch reactor experiment:

Table B-7: 5 ppm batch reactor experiment.

Sample Time	Elution Time	Area
-30	9.854	704.26
0	9.842	486.4
10	9.839	423.1
15	9.842	405.1
20	9.852	371.5
30	9.82	336.4
60	9.845	234.2
120	9.829	131.9
180	9.809	65.7
240	9.84	45.9

After analyzing these HPLC results, a graphical representation of the data was created to show concentration vs. time, displayed in the graph below:

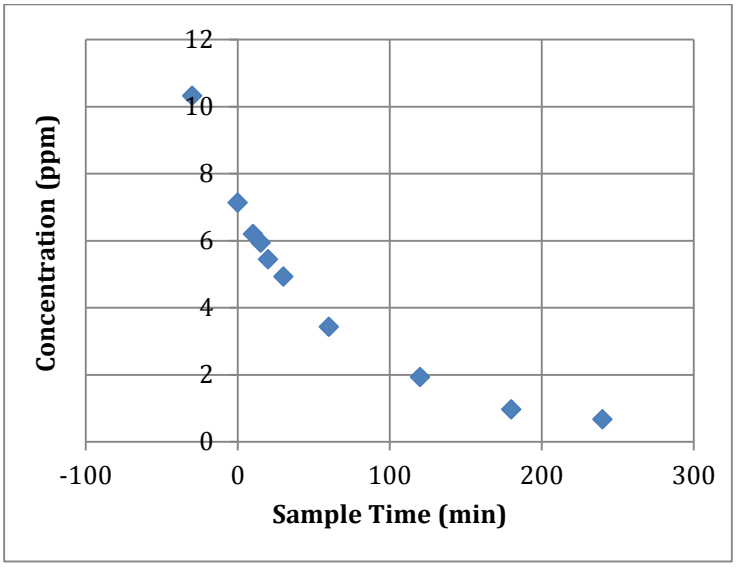

Figure B-9: 5 ppm batch reactor degradation.

The concentration of chlorpyrifos at each time interval was divided by the initial concentration and the natural logs were taken for those values. These results are tabulated below:

Table B-8: 5 ppm rate determining data.

Sample Time	ppm	C/C0	ln(C/C0)
-30	10.3236682		
0	7.13008297	1	0
10	6.20217538	0.8698602	0.13942277
15	5.9383154	0.83285362	0.18289738
20	5.44577677	0.76377467	0.26948247
30	4.93124982	0.69161184	0.3687304
60	3.4331115	0.48149671	0.73085588
120	1.93350729	0.27117599	1.30498727
180	0.96308892	0.13507401	2.00193241
240	0.67284294	0.09436678	2.36056621

A graph of sample time vs. –ln(d[CP]) is shown below:

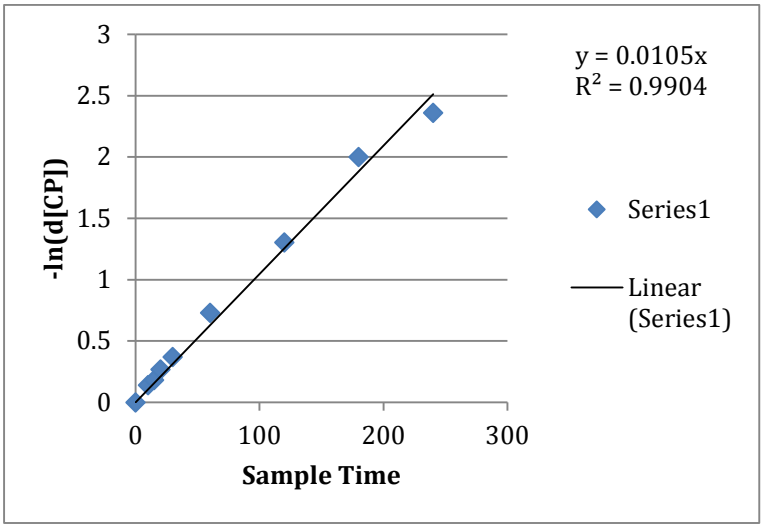

Figure B-10: 5 ppm sample time vs. -ln(d[CP]).

B.3 - TOC Analysis

The TOC (Total Organic Carbon) analyzer required samples without nitrogen, meaning all samples created with acetonitrile were incapable of analysis due to the organic nature of acetonitrile. The samples created in double deionized water at concentrations of 2 ppm chlorpyrifos and lower could be run through the TOC analyzer without interference from solvent.

Appendix C – Batch & CPC Reactor HPLC Results Run with Water

C.1 – Batch Reactor Results

The following table shows the results gathered from the HPLC analysis of the samples from the 1.5 ppm chlorpyrifos batch reactor experiment:

Table C-1: 1.5 ppm batch reactor experiment.

Sample Time	Time	Area	ppm
-30	10.157	37	0.55028407
0	10.159	24.6	0.36586454
5	10.153	20.8	0.30934888
10	10.163	16.6	0.2468842
20	10.154	12.2	0.18144502
30	10.177	11.8931	0.17688063
60	10.17	9.7	0.14426366
120	10.163	7.5	0.11154407

After analyzing these HPLC results, a graphical representation of the data was created to show concentration vs. time, displayed in the graph below:

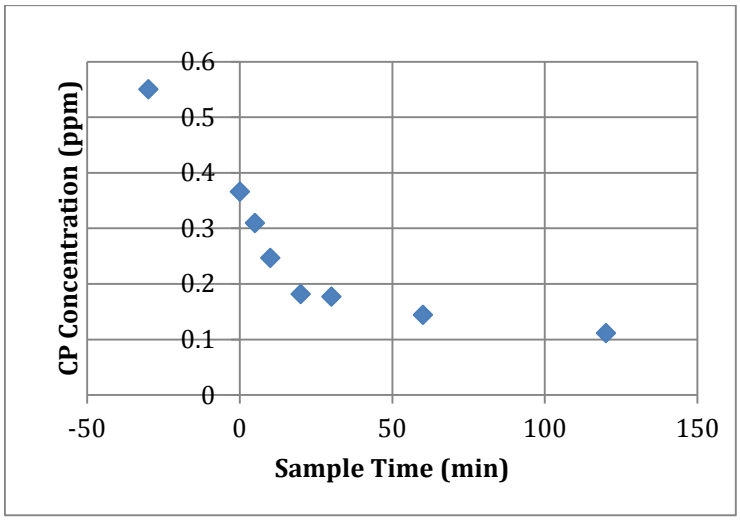

Figure C-1: 1.5 ppm batch reactor degradation.

The following table shows the results gathered from the HPLC analysis of the samples from the 1 ppm chlorpyrifos batch reactor experiment:

Table C-2: 1 ppm batch reactor experiment.

Sample Time	Elution Time	Area	ppm
-30	10.139	147.3	2.159
0	10.172	49.7	0.729
5	10.208	45.4	0.666
10	10.216	41.2	0.604
20	10.213	32.1	0.471
30	10.214	30	0.440
120	10.210	15.6	0.229
180	10.199	15.6	0.227
240	10.202	12.2	0.179

After analyzing these HPLC results, a graphical representation of the data was created to show concentration vs. time, displayed in the graph below:

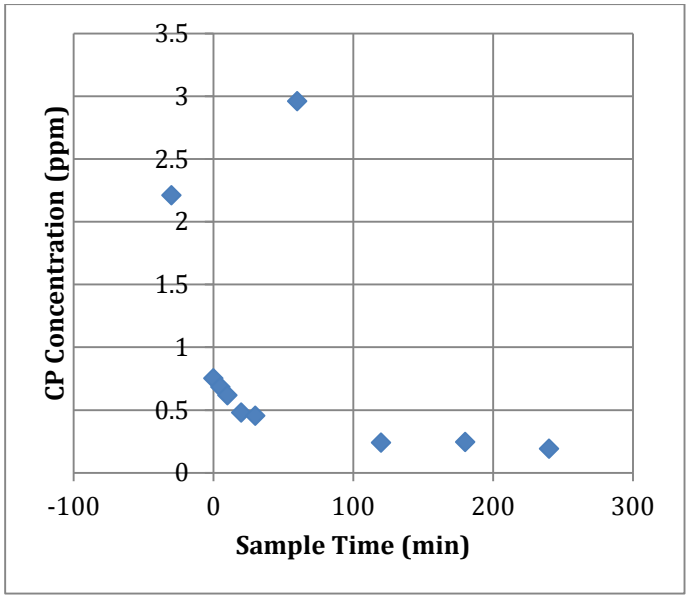

Figure C-2: 1 ppm batch reactor degradation.

The following table shows the results gathered from the HPLC analysis of the samples from the 0.5 ppm chlorpyrifos batch reactor experiment:

Table C-3: 0.5 ppm batch reactor experiment.

Sample Time	Elution Time	Area	Elution Time	Area	ppm
-30	4.813	18	10.029	34.4	0.51161546
5	4.81	18.1	10.021	10.2	0.15169993
10	4.815	13.7	10.041	9.7	0.14426366
20	4.815	18.3	10.041	9.1	0.13534014
30	4.814	18.5	10.044	6.3	0.09369702
60	4.817	13.8	10.055	4	0.05949017
120	4.816	16.1	N/A	2	0.02974508

After analyzing these HPLC results, a graphical representation of the data was created to show concentration vs. time, displayed in the graph below:

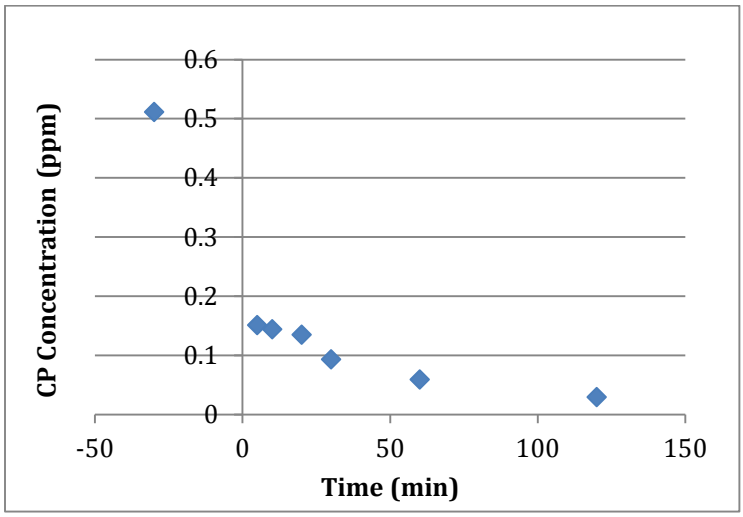

Figure C-3: 0.5 ppm batch reactor degradation.

C.2 – CPC Reactor Results

The following table shows the results gathered from the HPLC analysis of the samples from the 1.0 ppm chlorpyrifos CPC reactor experiment:

Table C-4: 1.0 ppm CPC reactor experiment.

time	elution	area
-30	10.199	12.3
0	10.208	8.3
10	10.210	10
20	10.210	8.1
30	10.191	5
60	10.203	5.4
120	N/A	N/A
180	N/A	N/A
240	10.210	N/A
300	10.225	N/A

After analyzing these HPLC results, a graphical representation of the data was created to show concentration vs. time, displayed in the graph below:

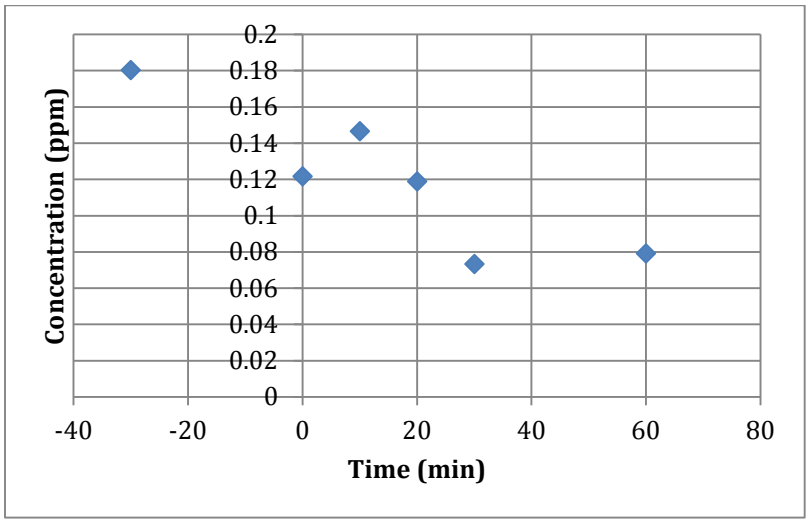

Figure C-4: 1.0 CPC reactor degradation.

The following table shows the results gathered from the HPLC analysis of the samples from the 0.5 ppm chlorpyrifos CPC reactor experiment:

Table C-5: 0.5 ppm CPC reactor experiment.

Sample Time	Elution Time	Area
-30	10.126	43.4
0	10.095	6.9
10	10.064	6.1
20	10.039	5.4
30	10.029	5.3
45	10.029	5.1
60	10.008	5.7
90	10.015	N/A
120	9.997	N/A
150	9.993	N/A
180	9.982	N/A
195	9.988	N/A
210	9.976	N/A
225	9.972	N/A
240	9.981	N/A
255	9.975	N/A
270	9.988	N/A
285	9.98	N/A
300	10.012	N/A

After analyzing these HPLC results, a graphical representation of the data was created to show concentration vs. time, displayed in the graph below:

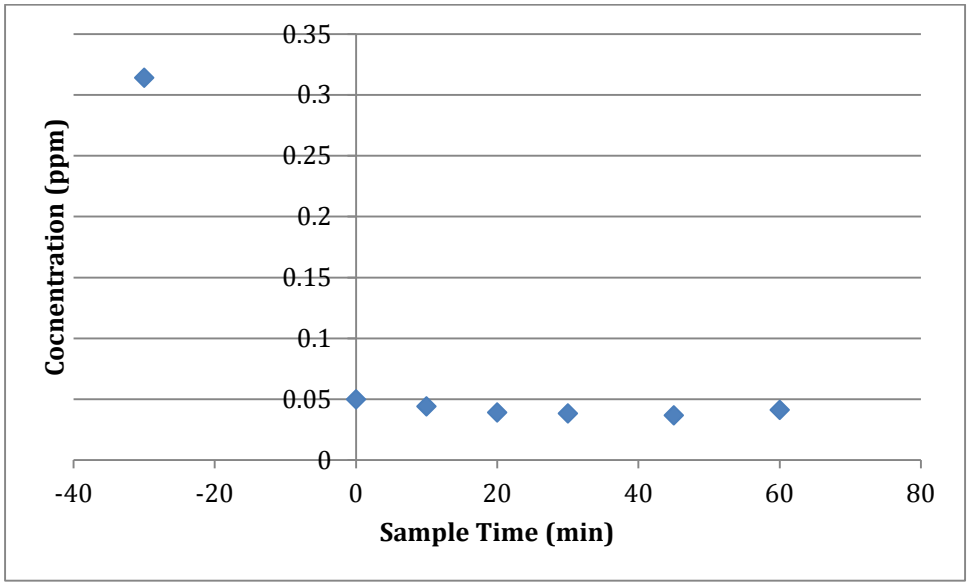

Figure C-5: 0.5 ppm CPC reactor degradation.

Appendix D – Batch Reactor and CPC Reactor TOC Results

D.1 – Batch Reactor Results

The samples taken from the batch reactor experiment underwent TOC analysis. Below are the tabulated results of the total carbon over time from the 2 ppm run:

Table D-1: 2.0 ppm batch reactor TOC results.

Sample Time	Concentration of Total Carbon c(TC) mg/L
-30	222.7
0	304
5	599.8
10	351.3
20	726.3
30	463.9
60	59.98
120	5.14
180	4.773
240	4.4

These results are represented graphically below:

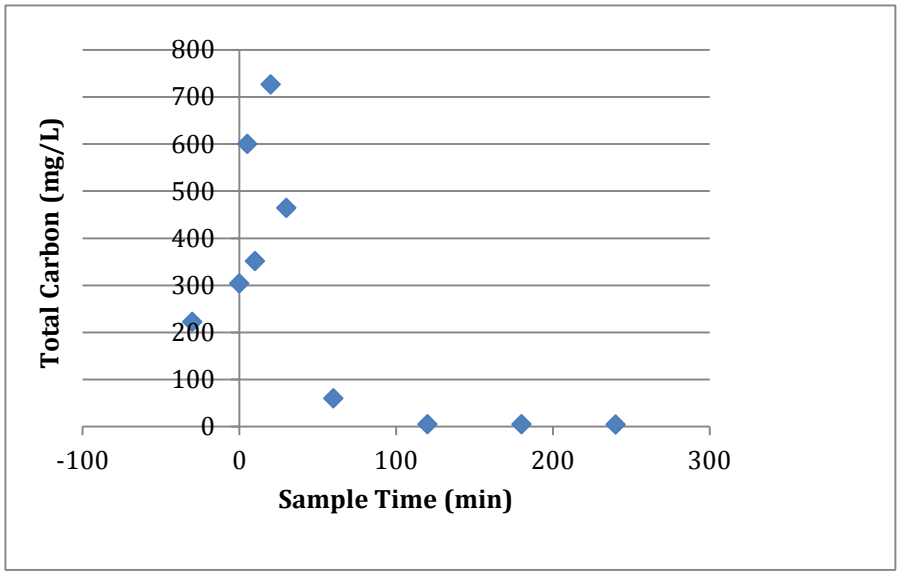

Figure D-1: 2.0 ppm Total Carbon vs. Sample Time.

The samples taken from the batch reactor experiment underwent TOC analysis. Below are the tabulated results of the total carbon over time from the 1 ppm run:

Table D-2: 1.0 ppm batch reactor TOC results.

Sample Time	Concentration of Total Carbon c(TC) mg/L
-30	4.24
0	61.26
5	54.9
10	54.88
20	54.39
30	53.83
60	52.06
120	49.25
180	44.57
240	40.26

These results are represented graphically below:

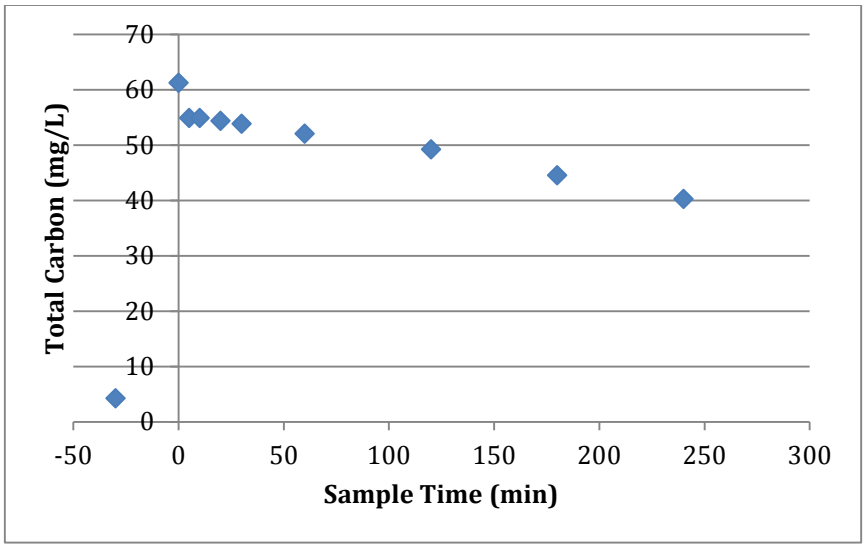

Figure D-2: 1.0 ppm Total Carbon vs. Sample Time.

D.2 – CPC Reactor Results

The samples taken from the CPC reactor experiment underwent TOC analysis. Below are the tabulated results of the total carbon over time from the 2 ppm run:

Table D-3: 2.0 ppm CPC reactor TOC results.

Sample Time	Concentration of Total Carbon c(TC) mg/L
-30	0
0	1.08
10	1.62
20	2.44
30	3.44
60	2.1
90	2.56
120	2.34
180	1.71
240	1.53

These results are represented graphically below:

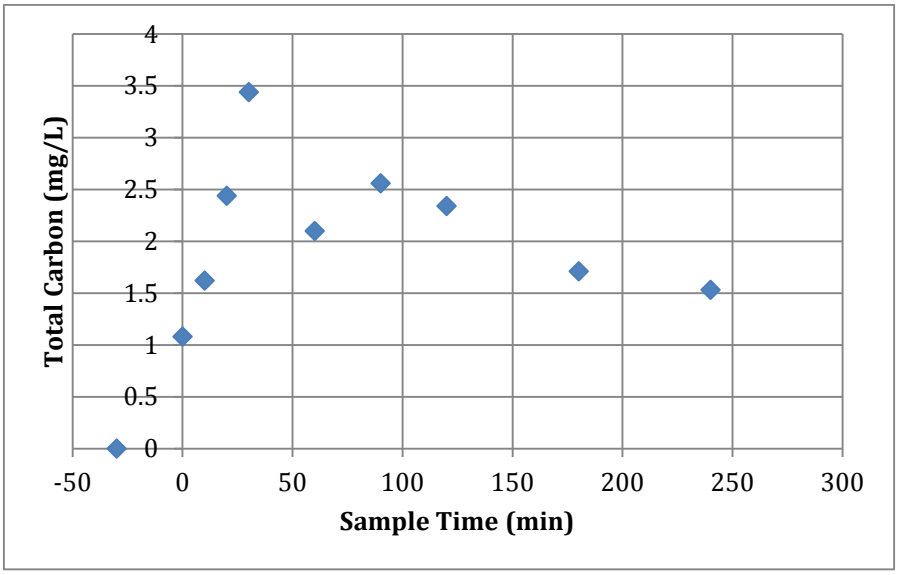

Figure D-3: 2.0 ppm Total Carbon vs. Sample Time.

The samples taken from the CPC reactor experiment underwent TOC analysis. Below are the tabulated results of the total carbon over time from the 1 ppm run:

Table D-4: 1.0 ppm CPC reactor TOC results.

Sample Time	Concentration of Total Carbon c(TC) mg/L
-30	0
0	106.3
10	0
20	0
30	0
60	0
120	161.5
180	108.3
240	503.8
300	59.42

These results are represented graphically below:

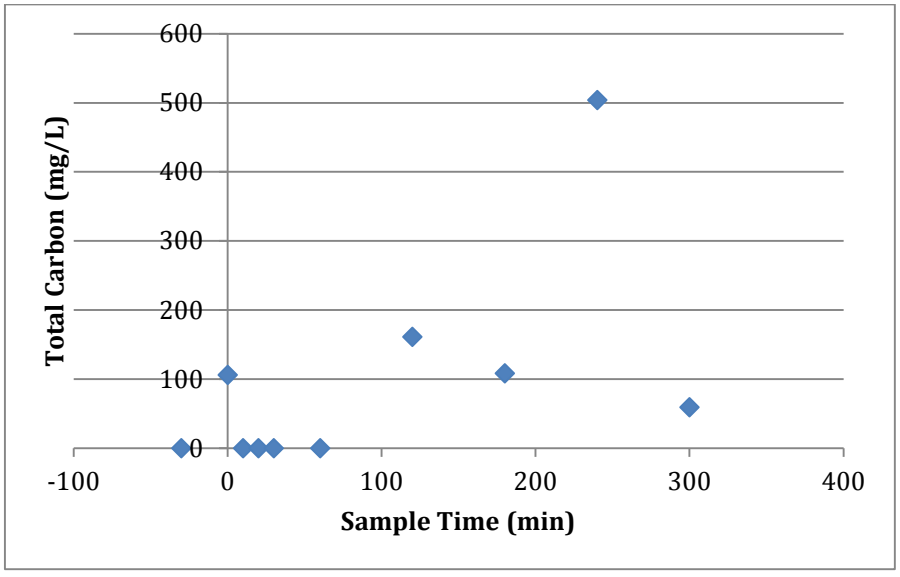

Figure D-4: 1.0 ppm Total Carbon vs. Sample Time.

The samples taken from the CPC reactor experiment underwent TOC analysis. Below are the tabulated results of the total carbon over time from the 0.5 ppm run:

Table D-5: 0.5 ppm CPC reactor TOC results.

Sample Time	Concentration of Total Carbon c(TC) mg/L
-30	0
0	41.93
10	16.06
20	0
30	0
45	0
60	0
90	0
120	0
150	0
180	0
240	0
300	0

These results are represented graphically below:

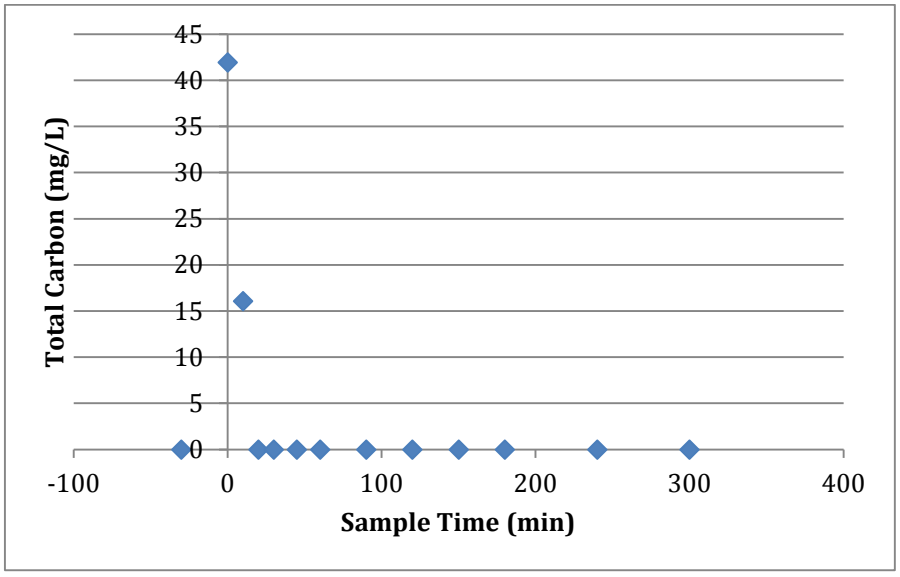

Figure D-5: 0.5 ppm Total Carbon vs. Sample Time.

Appendix E – Preparing 1F Solution

1. Add 15 mL of titanium tetraisopropoxide (TTIP) to a beaker containing absolute ethanol (1.25 mL).
2. Dissolve 1 mL of 70% perchloric acid ($HClO_4$) in 90 mL of deionized water in another beaker.
3. Add the second solution of $HClO_4$ and water drop wise to the first solution of TTIP and absolute ethanol.
4. Amorphous hydratized TiO_2 is a product of the exothermic reaction that occurred from the mixing of these two solutions.
5. Reflux the solution at 100 °C to allow for the crystallization and degradation of TiO_2 particles to occur.

Appendix F – Determination of Treatment Efficiency

F.1 - Experimental Treatment Efficiency Determination

Using concentrations of chlorpyrifos at T=0 min and T=120 min the treatment efficiency after two hours can be determined for each of the four CPC reactor experiments.

Table F: Treatment efficiency after two hours.

Experiment #	Chlorpyrifos concentration at T=0	Chlorpyrifos concentration at T=120	Treatment Efficiency
1	.05 ppm	0 ppm	1
2	.067	0 ppm	1
3	.121	0 ppm	1
4	.186	.080 ppm	.57
		Average	.8917

F.2 - Theoretical Treatment Efficiency Determination

Theoretical treatment efficiency was determined through the use of the first order reaction equation, the rate constant found for the photocatalytic degradation of chlorpyrifos using UV/TiO_2, and a retention time of two hours.

$$Eff = \frac{-1}{e^{kt}} + 1 \qquad \text{[Equation 6]}$$

Where k = Reaction rate constant

T = Retention time

$$Eff = \frac{-1}{e^{(0.02 \times 120)}} + 1 = .909$$

=90.9%

As can be clearly seen the experimental value and the theoretical value for treatment efficiency are within 2% of one another, indicating that experimental values were accurate.

Appendix G – LCMS Chromatograms

The following is a compilation of chromatograms received from LCMS analysis. Specifically contained in this appendix are the chromatograms from which intermediates were identified.

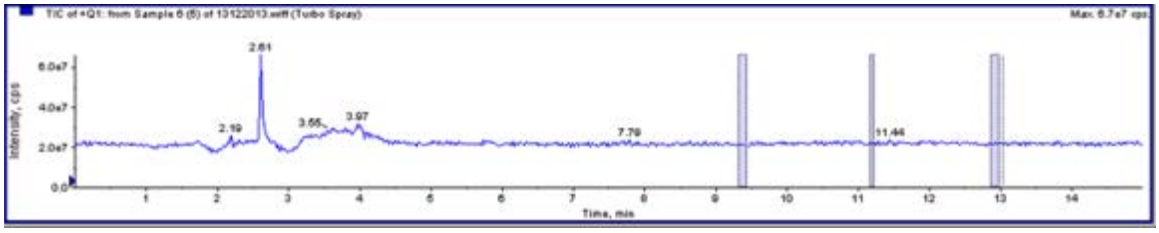

Figure G-1: Chromatogram from 0.5 ppm CPC experiment at T=285 min.

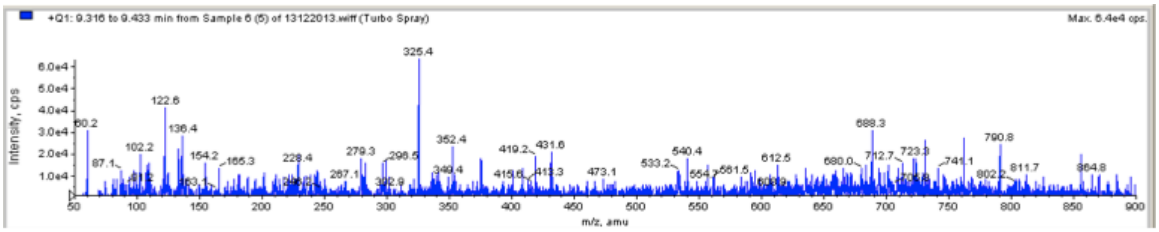

Figure G-2: Elution times 9.316-9.433 min from Figure G-1.

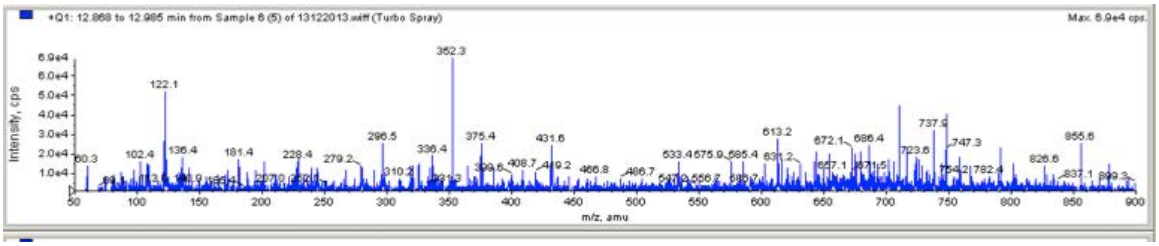

Figure G-3: Elution times 12.969 - 12.965 min From Figure G-1.

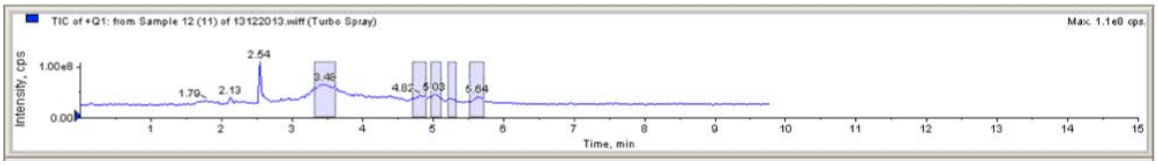

Figure G-4: Chromatogram from 2 PPM slurry experiment at T=42 min.

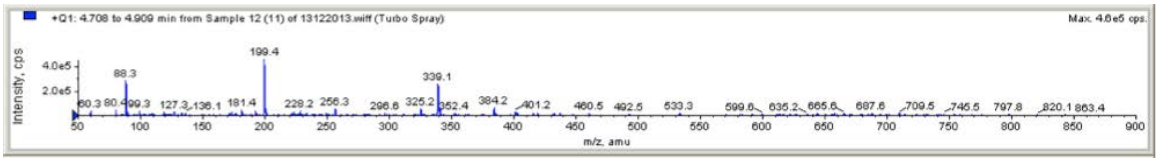

Figure G-5: Elution times 4.708 - 4.909 min from Figure G-4.

Appendix H – High Performance Liquid Chromatography (HPLC)

Each experiment containing chlorpyrifos solution was treated as described above. As it was necessary to determine the amount of chlorpyrifos remaining in solution after TiO_2/UV treatment, a high performance liquid chromatography (HPLC) instrument (model & manufacturer information found in Appendix A) was used. As samples were taken over the course of time for each experiment, aliquots were transferred to individual 2 mL HPLC vials using Pasteur pipettes. These vials were carefully labeled for organizational aid.

H.1 – HPLC Operation

The following procedure details the parameters used while operating the HPLC machine:

1. The mobile phase consisted of 80% double deionized water and 20% pure acetonitrile.
2. The pump rate of the mobile phase was 1.0 mL per minute.
3. The sample injection volume was 50 μL.
4. The run time for each sample was 13 minutes.
5. Sample vials were placed in the auto sampler portion of the machine in order of increasing sample time.
6. A blank of double deionized water was analyzed preceding each new set of samples.
7. The sequence table in the software was filled according to this order. The method used was labeled CP1 and each vial was sampled once.
8. The column was installed using two small threaded adapters, one on either end of the column, which were attached to high pressure lines between the auto sampler and the diode array detector (DAD) contained in the HPLC machine.
9. The auto sampler, the mobile phase pumps, and the DAD were all switched on using the Agilent software.
10. The lines and the column were then flushed with double deionized water at a rate of 1.0 mL per minute for 20 minutes.
11. Pressure within the column was allowed to build and become steady between 12 and 14 bars.
12. Once the pressure appeared stable the series was started.

H.2 – Analyzing HPLC Results

Results from this instrument were obtained in the form of chromatograms. The wavelengths from the diode array detector were 200.8, 230, and 290 nm. Peaks indicating the presence of a compound consistently appear at specific elution times regardless of intensity or concentration.

The peaks corresponding to chlorpyrifos were integrated using the software connected to the HPLC machine. After determining the area under a peak, the area could then be divided by the slope of the calibration curve to determine the concentration of chlorpyrifos in the sample. Once the concentrations of all samples from an experiment had been determined, these values could be plotted against the corresponding sample times. This graph effectively provided a degradation curve, which aided in determining treatment efficiency.

Appendix I – Slide Coating Procedure

Before conducting experiments with the bench scale fixed-film reactor, glass slides were brush-coated with a titanium silicate solution, known as 397T. The 397T mixture was prepared following methods developed by Andraž Šuligoj at UNG as described in the section below. The slide material chosen was critical since the material itself might have the potential to contribute byproducts to the UV/TiO_2 oxidation reaction. Glass slides were chosen to avoid the possibility of introducing unwanted ions into the solution. Sodium is the only ion that could be produced as a byproduct of the UV/TiO_2 oxidation reaction using glass slides. This effect was avoided by using temperatures below 200 °C.

I.1 – Titanium Silicate Preparation

The following procedure describes the preparation of glass slides coated with 397T solution. 397T was created using a three-step process, after which it was possible to coat the slides. The preparation of 397T solution first required mixing another formula known as 396W, also developed by Andraž Šuligoj.

The 396W solution was prepared by adding the following into a 25 mL beaker:

1. 1.86 mL tetraethyl orthosilicate, 98% (Figure I-1)
2. 1.0 mL double deionized water
3. 6.5mL HCl, 37%

A small magnetic stir bar was added to the beaker of solution on a stirring plate and mixed until homogenous (approximately 45 min).

Figure I-1: tetraethyl orthosilicate (TEOS) solution produced by Acros Organics.

Once 396W was completed, the 397T solution was prepared in a 25 mL beaker as follows:

1. 8.4 mL of 1F (a solution previously prepared by Marko Kete at UNG on July 2, 2013 - instructions found in Appendix F)
2. 2 mL Levasil 200/30% (Obermeier, Figure I-2)
3. 8 mL absolute ethanol
4. 1.2 mL 396W

This solution was placed on a stirring plate with a magnetic stir bar and mixed until homogenous (approximately 1 hour).

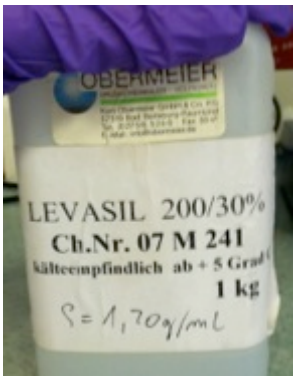

Figure I-2: Levasil.

After the 397T solution was completed, 1.6 g of PC500 TiO_2 and 1.6 g of P25 TiO_2 (see Figure I-3) were slowly added over a period of 10 minutes to ensure homogeneous mixing. Equal masses of both PC500 and P25 were used to ensure maximum surface contact area and crystallinity structure, as discussed in Chapter 2.6.1 of this report. The final titanium silicate solution was stirred for an additional 5 minutes then placed in a sonicator for 10 minutes.

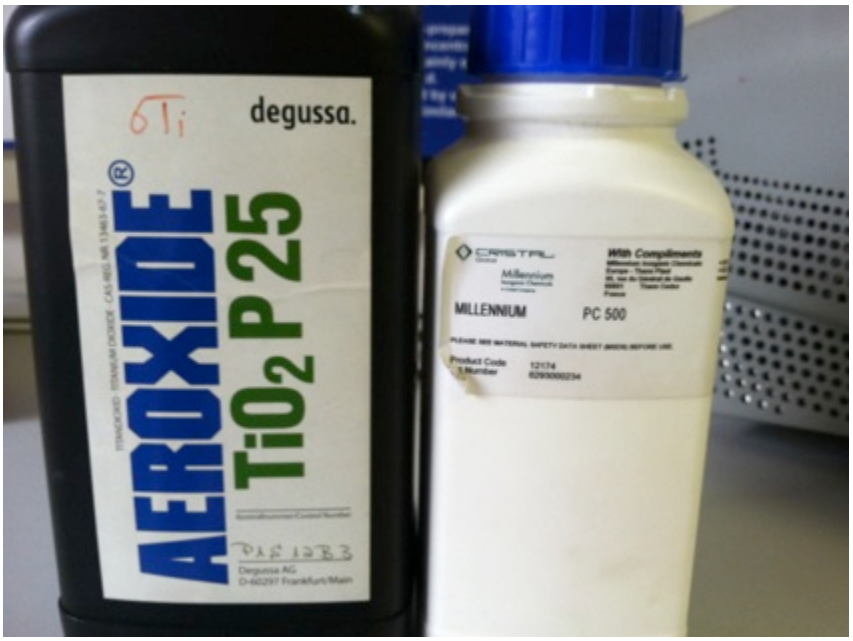

Figure I-3: P25 TiO_2 and PC500 TiO_2.

I.2 – Brush Application

When coating glass slides with the homogenous titanium silicate solution detailed above, it was necessary to ensure that each glass slide was coated with at least 1.0 mg/cm^2 of 397T. The procedure for coating the glass slides with 397T is as follows:

1. Slides were cleaned with ethanol and dried before beginning the coating process.
2. Identification numbers were etched into each glass slide by hand for easy recognition after coating.
3. Dry slides were weighed prior to coating to obtain the initial weight.
4. A small brush was dipped into the solution and used to paint each slide by hand to provide a full, even coat on all faces.
5. After each individual slide was coated they were dried with a common hair dryer and placed in an oven at 150 °C for one hour.
6. The slides were then removed from the oven and weighed.
7. The difference in weight from initial to current coat was divided by the total area of the coated slide, which effectively provided a measure of coating thickness in units of mass per area.

8. A second or third coating was added depending on whether the desired thickness of 1.0 mg/cm^2 had been achieved.

Appendix J - CPC Reactor Design Specifications

J.1 – Experimental Treatment Efficiency Determination

Using concentrations of chlorpyrifos at T=0 and T=120 min, the treatment efficiency after two hours was determined for each of the four CPC reactor experiments, as shown below in Table J-1.

Table J-1: Experimental Efficiency Determination

Experiment #	Chlorpyrifos concentration at T=0	Chlorpyrifos concentration at T=120	Treatment Efficiency
1	.05 ppm	0 ppm	1
2	.067	0 ppm	1
3	.121	0 ppm	1
4	.186	.080 ppm	.57
		Average	**.8917 = 89.2%**

J.2 – Theoretical Treatment Efficiency Determination

Theoretical treatment efficiency was determined through the use of the first order reaction equation, Equation J.1 below. The rate constant found for the photocatalytic degradation of chlorpyrifos using UV/TiO_2, was used with a retention time of two hours.

$$Eff = \frac{-1}{e^{kt}} + 1 \qquad \text{[Equation J.1]}$$

Where k = Reaction rate constant

T = Retention time

$$Eff = \frac{-1}{e^{(0.02 \times 120)}} + 1 = .909$$

Treatment Efficiency = 90.9%

As shown above, the experimental and theoretical values for treatment efficiency are within 2% of one another, indicating that the theoretical efficiency determined from the batch reactor experiments was extremely close to the experimental efficiency calculated from the pilot CPC reactor experiments. This shows that the degradation kinetics of chlorpyrifos in both reactors was similar, providing credibility to the proposed CPC reactor design specifications.

J.3 – CPC Reactor Design Parameters

Reynolds Number = 2300 (Laminar Flow)

Flow rate = Q = 2000 L/hr = 5.5 x 10^{-4} (m^3/sec)

Reactor Size = 10 tubes at 3 meters in length

Kinematic viscosity of water = 0.9 x 10^{-5} (m^2/sec)

J.3.1 – Velocity Determination Using Reynolds Number

The Reynolds Number calculation, show in Equation 5.4 below, is used to determine if a flow in a given reactor is laminar or turbulent. A turbulent flow is assigned if the Reynolds number exceeds 4000. A laminar flow is defined if the Reynolds number is 2300 or below. Therefore, a Reynolds number of 2300 was used when designing the CPC reactors.

$$R = \frac{U \times L}{V} \qquad \text{[Equation J.2]}$$

Where R= Reynolds number (2300)

U = velocity

L = Length (3m x 10 tubes)

V = Kinematic viscosity of water

$$2300 = \frac{U \times (10 \times 3)}{0.9 \times 10^{-5}}$$

Q/A = U = 0.708 (m/sec)

J.3.2 – Cross-Sectional Area Determination

Next, the known velocity and flow in the CPC reactor was used to determine the cross-sectional area of one tube using Equation 5.5:

$$U = \frac{Q}{A} \qquad \text{[Equation J.3]}$$

Where Q = Flow (m^3/sec)

A = Cross sectional area of reactor tubes (m^3)

$$0.708 m/\text{sec} = \frac{(5.5 \times 10^{-4})}{A}$$

$$A = 0.0078\ m^2$$

The cross-sectional area of the reactor tube was then used to calculate the radius of one tube using Equation 5.6:

$$A = \Pi \times R^2 \qquad \text{[Equation J.4]}$$

Where π = 3.14159

R = radius of reactor tube (m^2)

$$R = 5\ cm$$

J.3.3 – Number of Reactors Required

Also from the known velocity of 0.708 meters per second (2,548.8 meters per hour), it was possible to determine the number of reactors required, given that each reactor contains 10, 3 meter long tubes and the desired retention time is 2 hours.

$$2\ hours \times 2{,}548.8 \frac{m}{hour} = 5097.6\ m \qquad \text{[Equation J.5]}$$

$$\frac{5097.6m}{300\frac{m}{reactor}} = 16.99 \sim 17 \qquad \text{[Equation J.6]}$$

As can be seen, this system will require 17 reactors.

Appendix K – Disposal of Chlorpyrifos

Below is a direct excerpt from the Agency for Toxic Substances and Disease Registry, outlining exactly how material contaminated with chlorpyrifos should be properly disposed of as hazardous waste:

"The recommended treatment and disposal methods for chlorpyrifos are incineration, adsorption, and landfilling (IRPTC 1989). For small amounts, the recommended disposal is adsorption onto materials such as sand and burying in locations away from domestic water supplies. For the decontamination of containers, the triple rinse and drain procedure is recommended. The use of a caustic soda-methanol or caustic soda-detergent rinse solution is also effective in decontaminating the container, but the rinse solutions must be disposed of either by incineration or burial in an area away from water supplies (IRPTC 1989).

Small-scale farm operators have a pressing need for methods to dispose of unused concentrated and dilute formulated chlorpyrifos suspensions or solutions such as Rinsate. The use of solid state fermentation techniques to dispose of pesticide waste may be a viable alternative to other disposal methods that are either too expensive or technically too sophisticated. Chlorpyrifos was evaluated in bioreactors by Berry et al. (1993), who reported that chlorpyrifos levels were reduced to 0.6% (by solvent extraction) in 290 days in wheat straw/horse manure reactors, and that leachability studies showed that of the 28 µg chlorpyrifos in the soil column, only 72 ng leached.

While not strictly a disposal method, it is worth pointing out that NaOH-methanol and sodium hypochlorite can be used to degrade (but not necessarily detoxify) chlorpyrifos. For example, on exposed surfaces, the use of caustic soda-methanol or caustic soda-detergent rinse solution can also be effective in decontaminating containers used to store chlorpyrifos, but these rinse solutions must be disposed of either by incineration or proper burial (Dillon 1981). A full discussion of regulations regarding disposal of chlorpyrifos is given in Chapter 7." [ASTDR,1998]